B1. GeoPRISMS-funded Research Nuggets

Rift Initiation & Evolution

Subduction Cycles & Deformation

RIE

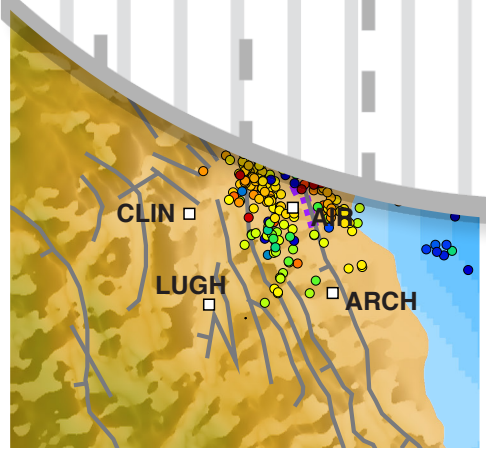

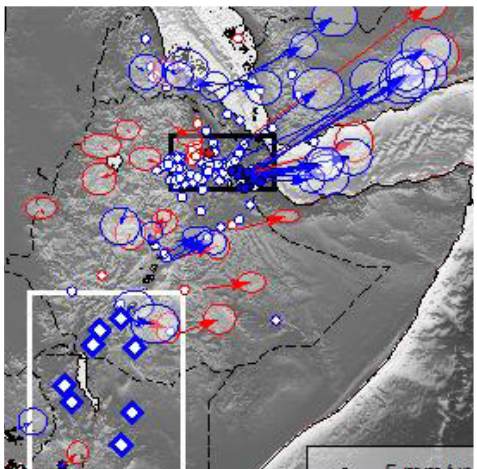

Rift Initiation & Evolution Nuggets

Collaborative Research: Active kinematics of lithospheric extension along the East African Rift

Rebecca Bendick, Robert King, Robert Reilinger, Mike Floyd

This one-year effort, supported by the GeoPRISMS program for the East Africa focus, encompassed two different primary activities. The first activity included installation of eight new campaign GPS sites, four in southernmost Ethiopia and four in northwest Kenya. These sites span the presumed actively spreading region of the Turkana Depression and will, with a subsequent measurement, provide the first estimates of the rates and location of extension in the Turkana segment of the East African Rift. Capturing observations of spreading in Turkana is critical to understanding the African Rift at the largest scale, because the Turkana segment must serve as a kinematic link between the single, focused Main Ethiopian Rift and the parallel, simultaneously active Western and Gregory Rifts in Kenya. The Turkana segment may also play a critical role in distinguishing the importance of magmatism to the form and rate of continental extension, and in deciphering the temporal evolution of the Indian Ocean monsoon and its relationship to African seasonal air masses. The second activity included collection of a huge amount of geodetic data for all of East Africa and subsequent calculation of a community velocity model. Some of these data were readily accessible through the NSF-supported UNAVCO data archive, but other data were collected by over a dozen international scientific entities and in many cases were not publically accessible or readily usable. Negotiating use of the data and then estimating velocities (Fig. 1) for all sites with a common methodological approach and in a common standard reference frame transforms the study of East African present-day kinematics from a regional to a continental scale, facilitates systematic comparisons of different structural rift segments, and provides a synoptic framework for other active tectonics research in the region. This effort also identifies critical areas for future data acquisition, either through new data sharing agreements or new experimental deployments.

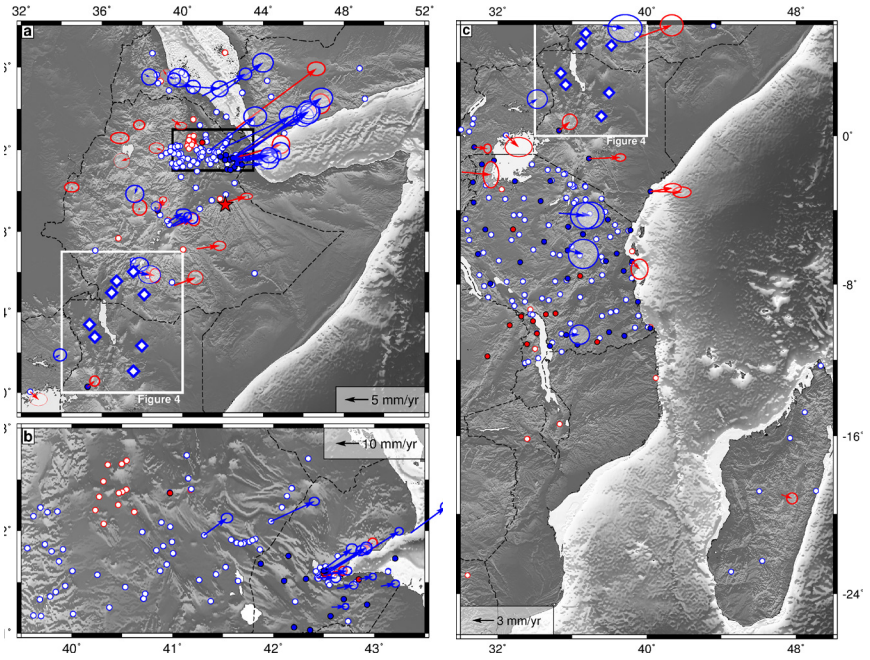

Figure. 1. GPS velocities in a Nubian reference frame and locations for cGPS (red) and sGPS (blue) sites in East Africa. Only sites with velocity uncertainty < 1 mm/yr are shown as vectors here. Other sites with a currently less precise velocity estimate are shown with a white dot but no vector. Sites without a current velocity estimate are shown as circles only. Boxed sites with diamond markers are the location of sites installed in the Turkana Depression.

Faulting processes during early-stage rifting: analysis of an unusual earthquake sequence in northern Malawi

James B. Gaherty, Donna J. Shillington, Matthew E. Pritchard, Patrick Chindandali, Ashley Shuler, Winstone Kapanje, Hassan Mdala, Nathan Lindsey, Leonard Kalindekafe, Cynthia Ebinger, Andrew Nyblade, Scott Nooner

On December 6, 2009, an unusual sequence of earthquakes occurred in the northern Malawi Rift near Karonga (Fig. 1), which lies within the weakly extended southern part of the East Africa Rift System. The sequence initiated with an Mw 5.8 event, which was followed 32 hours later by an Mw 5.9 event, and then nearly 12 days later by an Mw 6.0 event. Within this time span there were an additional eight Mw > 4.5 events, with presumably many more events that were at or below the threshold of detection. Such events are rare in the northern Malawi rift valley; prior to this sequence, the NEIC catalog (which dates to 1973) contains only three events of M > 5 within the rift valley between 9-12°S latitude. This contrasts with both the Western and Eastern Rifts through Kenya and Tanzania, which have experienced 115 M > 5 events in the same time period. Most of those events occurred on major border faults, but the locations of the Karonga events are far removed from the border fault. In addition, the events occurred just south of a young volcanic province. They offer a rare opportunity to evaluate the potential roles of magmatism and hanging-wall fault evolution in early-stage rifting. We constrain the faulting in this sequence using a unique set of aftershocks recorded over a four-month interval, combined with estimates of the distribution and mechanisms of the largest events, and models of InSAR images of deformation during the sequence.

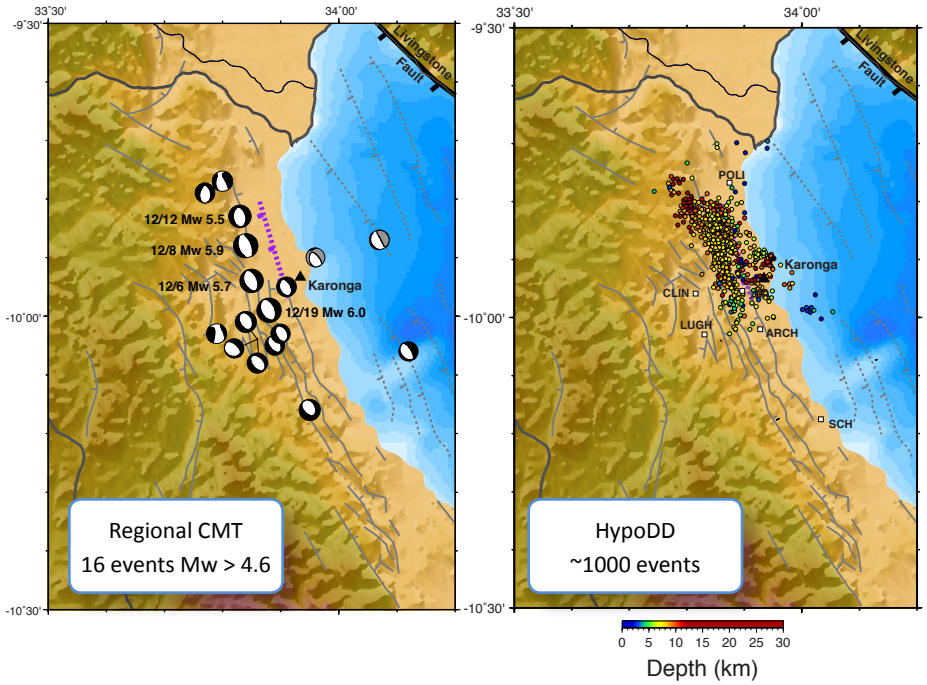

Figure 1. (left) Focal mechanisms of the largest 17 events of the 2009-2010 Karonga sequence. Surface projection of the buried St. Mary's fault, inferred from InSAR, is shown with purple line. Fault locations from PROBE and geologic data shown in grey lines. (right) Epicenters of ~1000 aftershocks relocated using HypoDD, with depth shown by color. Distribution north of Karaonga is consistent with events on the west-dipping St. Mary's fault, but beneath and south of Karonga, earthquake clusters suggest multiple west-dipping faults.

The earthquake distribution implies that a series of interacting hanging-wall faults produced the Karonga earthquakes (Fig. 1). The depths of the events are quite shallow, less than ~12 km, well above the projection of the main west-dipping border fault at depth. The majority of events appear to be associated with a previously

unidentified west-dipping fault ('St. Mary's Fault') to the north of Karonga. This fault was identified by InSAR data (Biggs et al., 2010; Fig. 2) and by field mapping by the Malawi Geological Survey, and the multiple events were interpreted to occur on this single, immature fault. Our InSAR analysis is consistent with this scenario, perhaps on a fault with listric geometry. However, the aftershock locations suggest that the events occurred on multiple west-dipping normal faults along a roughly 40-km-long north-south zone roughly centered on the village of Karonga. Most of the events north of Karonga are consistent with slip on the St. Mary's fault. However, to the south, clusters of events locate on west dipping faults 5-10 km east of the St. Mary's feature. The spacing of these clusters is consistent with west-dipping hanging-wall faults imaged within the lake (Mortimer et al., 2007). In addition, regional CMT analyses of the largest 17 events are distributed primarily along the St. Mary's feature in the northern half of the aftershock region, but show much more east-west variation to the south, with two events well into the lake. These events support the notion of multiple faults. There is no evidence of magmatic control on the sequence. Few events occurred near Rungwe volcanic province, and no geodetic deformation is observed there during this time interval.

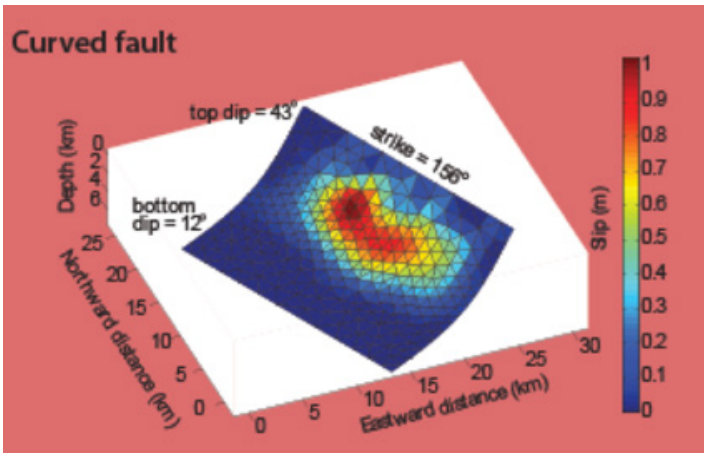

Figure. 2. Estimated slip on a listric geometry St. Mary's fault, which provides the best fit to InSAR estimates of surface deformation spanning the primary 17 events.

We envision two scenarios that can explain the fact that the seismic data suggest two or more active faults, while the InSAR is consistent with slip on a single fault. First, it is possible that primary slip on the St. Mary's fault triggered small aftershocks on the synthetic fault structures, but that no significant slip occurred on these secondary faults during the main sequence. Alternatively, since the faults are parallel and closely spaced, it is plausible that deeper slip on the parallel faults, and/or slip on faults beneath the lake, is masked by the more dominant slip on the shallower St. Mary's feature.

In addition to the significant scientific results, engagement of the Malawi GSD in both the data collection and research activities directly resulted in Malawi's first national seismic network. Based on their experience in this project, the MGSD was able to obtain funding for eight broadband seismic stations. This network represents a long-term investment by the Malawi government to better understand and mitigate seismic hazard affecting their country. Complementing this effort, LDEO hosted three staff from the MGSD for a three-week training session, analyzing the Karonga sequence and developing tools that could be used for their new national network. We also visited the MGDS headquarters to install of data analysis software and continue training.

Results from this analysis have been presented in several forums to date: 2010 and 2012 Fall AGU; 2012 AGU Science Policy conference; 2012 GeoPRISMS planning workshop for the East African Rift system; and at the MGSD and Chancellor College, Malawi. A manuscript is in preparation.

The Youngest Magmatic Event in Eastern North America

Esteban Gazel

- **Geologic Map of the VA Eocene Magmatic Event**

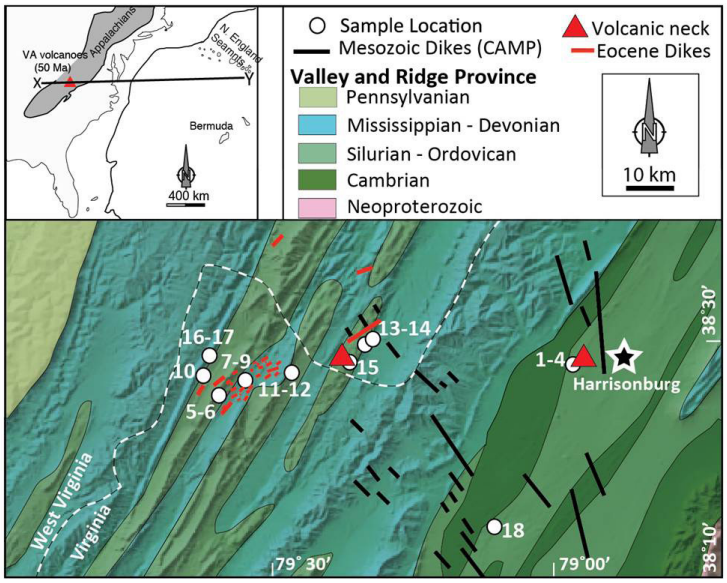

1-4: Mole Hill
5-6: Trimble Knob
7-9: State Route 63
10: Hightown Dike
11-12: Hull Farm
13-15: Sugar Grove
16-17: Hightown Quarry
18: Vulcan Quarry

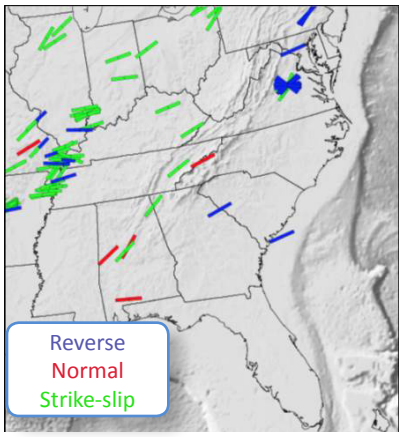

Left: From Mazza et al. (Geology, 2014).

Right: North America Moment Tensor - Saint Louis University Earthquake Center.

- **Example Ar/Ar age for the Eocene volcanic pulse in the ENAM**

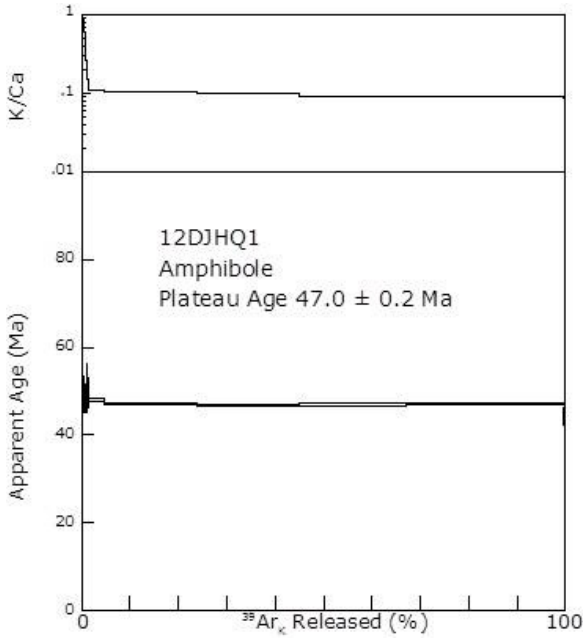

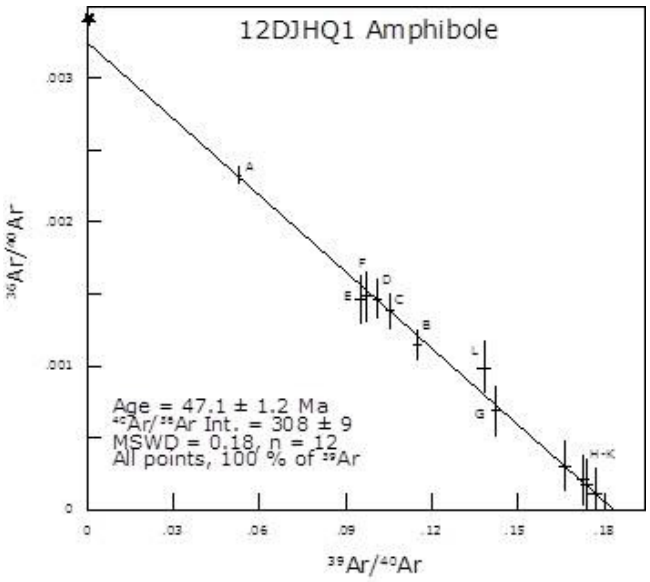

From Mazza et al. (Geology, 2014).

- **Bimodal volcanism in VA ~47-49 Ma**

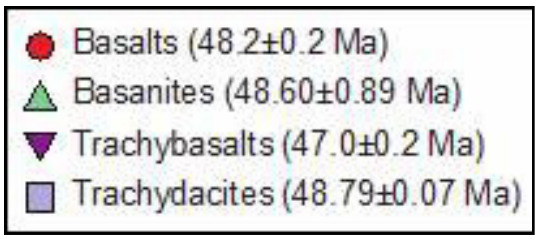

From Mazza et al. (Geology, 2014).

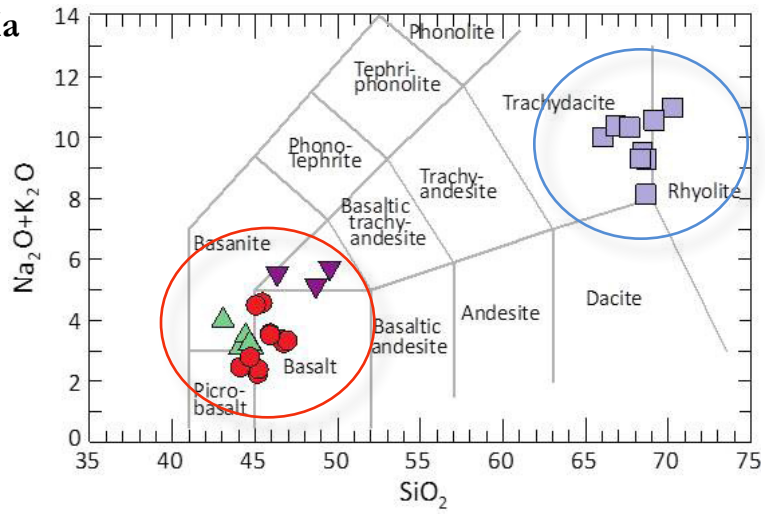

Schmandt and Lin, (GRL, 2014)

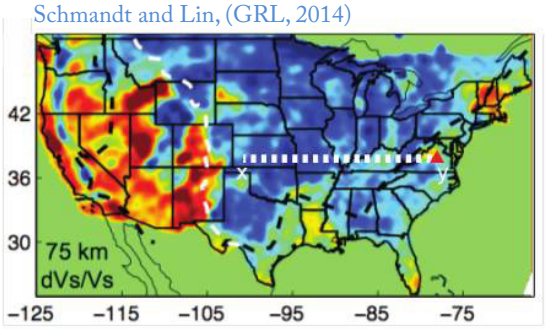

- **Tomography cross section**

Thermobarometric results agree with seismic evidence for a thin LAB below the Eocene Volcanoes

Evidence for a low-shear wave velocity "scar" below the Eocene volcanoes

$^3He/^4He$ ((R/RA >>1) from local thermal springs connects the shallow crustal fracture systems to a region deep into the mantle (Baedke and Silvis, 2009)

- **What produced the Eocene event?**

Reorganization of plate motion and change in the orientation of the regional stress field in the Eocene (Southworth et al., 1993)

Intraplate signature but T to low for a deep mantle plume (Mazza et al., 2013).

Lack of a thick lithosphere below the Eocene magmas in VA (while thick in other Appalachian locations, Wagner et al., 2012)

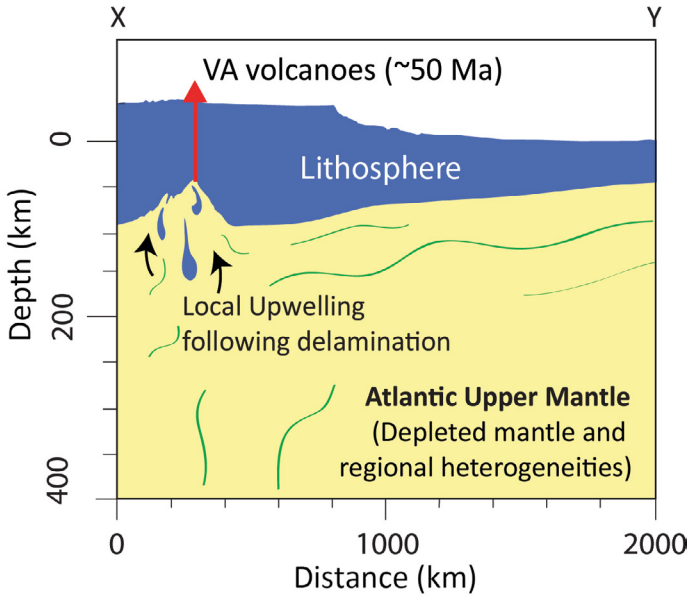

Localized upwelling, possibly lithospheric delamination

Geodynamic Modeling in Support of the MAGIC Project

Scott D. King, Shangxin Liu, Maureen D. Long, Margaret H. Benoit, Eric Kirby, Scott R. Miller

The Mid-Atlantic Geophysical Integrative Collaboration (MAGIC) includes a seismic deployment that extends from the Atlantic coast of Virginia to the western boarder of Ohio as well as using seismic data from the EarthScope Transportable Array (TA) stations and stream profile analyses that provide information about erosion and uplift over the entire eastern third of the US. Prior to the arrival of the TA, analysis of existing broadband seismic stations in the southeastern US detected a distinct pattern of shear-wave splitting: near the coast stations exhibit well-resolved null (no splitting) behavior for SKS phases over a range of back azimuths, consistent with either isotropic upper mantle or with a vertical axis of anisotropic symmetry; farther inland splitting exhibits mainly NE–SW fast directions, consistent with asthenospheric shear due to absolute plate motion (APM), lithospheric anisotropy aligned with Appalachian tectonic structure, or some combination of these (Long et al., 2010). The MAGIC deployment crosses this transition and will help determine crustal thickness and the lithosphere-asthenosphere boundary, in addition to mantle flow direction and transition zone structure.

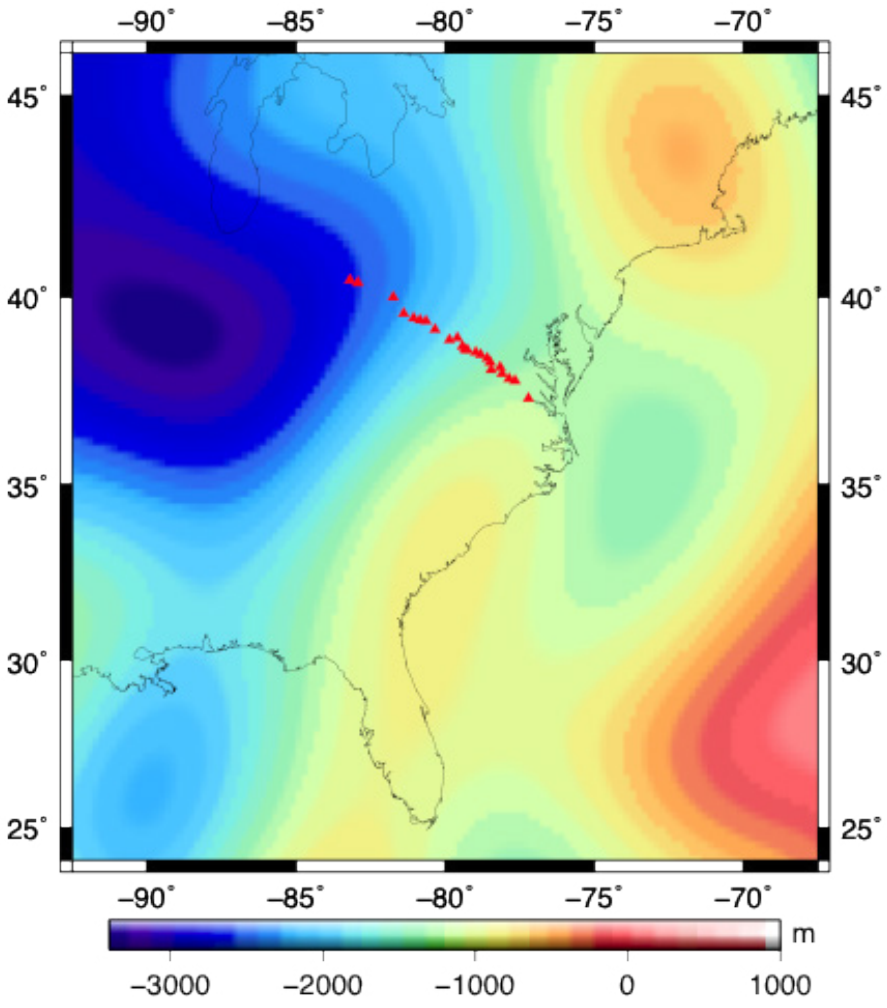

Figure 1. predicted dynamic topography from a geodynamic calculation with uniform mantle viscosity and uniform scaling of seismic velocity to density. The S40RTS seismic model, with a minimum wavelength of 1,000 km is converted to buoyancy to drive mantle flow. The red triangles denote the stations in the MAGIC deployment.

To test hypotheses regarding mantle flow and to aid the interpretation of the observations, we are building a new geodynamic model based on ASPECT (Advanced Solver for Problems in Earth ConvecTion) (Kronbichler et al. 2012) that uses buoyancy derived from seismic tomography along with realistic lithosphere and sub-lithosphere structure. We have tested seismic models S40RTS (Ritsema et al., 2011) and SAVANI (Auer et al., 2014) and we plan to compare these results with newer models, including regional models based on EarthScope data (e.g., Schmandt and Lin, 2014) in an effort to understand the uncertainty in the pattern of seismic velocities. In addition we plan to incorporate crust and lithosphere-asthenosphere boundary models for the eastern US as these become available. In addition to predicting transition zone thickness and patterns of shear-wave splitting, the geodynamic models provide estimates of heat flow, gravitational potential, and dynamic topography. Dynamic topography is the surface deformation induced by viscous stresses resulting from convective flow within the mantle. Dynamic topography varies as mantle flow changes and generally is small in amplitude and long in wavelength. Thus, dynamic topography can be difficult to remove from topographic anomalies resulting from tectonics (Braun, 2010). Most previous estimates of eastern US dynamic topography use long-wavelength seismic models (Spasojevic' et al., 2008).

References

Auer, L., L. Boschi , T. W. Becker, T. Nissen-Meyer, and D. Giardini, 2014. Savani: a variable-resolution whole-mantle model of anisotropic shear-velocity variations based on multiple datasets. J. Geophys. Res., 119, 3006-3034, doi:10.1002/2013JB010773.

Braun, J., 2010. The many surface expressions of mantle dynamics. Nature Geosci. 3,825-3,833.

Kronbichler, M., T. Heister and W. Bangerth, 2012. High accuracy mantle convection simulation through modern numerical methods. Geophys. J. Int. 191(1), 12-29.

Long, M. D., M. H. Benoit, M. C. Chapman, and S. D. King, 2010. Upper mantle anisotropy and transition zone thickness beneath southeastern North America and implications for mantle dynamics, G-cubed., 11, Q10012.

Ritsema, J., A. Deuss, A., H. J. van Heijst, and J. H. Woodhouse, 2011. S40RTS: A degree-40 shear-velocity model for the mantle from new Rayleigh wave dispersion, teleseismic traveltime and normal-mode splitting function measurements. GJI 184 (3), 1223–1236.

Schmandt, B., and F.-C. Lin, 2014. P and S wave tomography of the mantle beneath the United States, Geophys. Res. Lett., 41, doi:10.1002/2014GL061231.

Spasojevic', S., L Liu, M. Gurnis, and R. D. Müller, 2008. The case for dynamic subsidence of the U.S. east coast since the Eocene, Geophys. Res. Lett., 35, L08305, doi:10.1029/2008GL033511.

GeoPRISMS and EarthScope education and outreach to predominantly undergraduate institutions in Eastern North America via the MAGIC deployment

Maureen D. Long, Margaret H. Benoit

The Mid-Atlantic Geophysical Integrative Collaboration (MAGIC) experiment involves the deployment of 28 broadband seismometers in a dense linear transect from Charles City, VA to Paulding, OH. Data collection began in Fall 2013 and will continue through Fall 2016. The major E&O component of the MAGIC project involves outreach to faculty and students at primarily undergraduate colleges and universities in our field area, most of which do not otherwise have active ties to the GeoPRISMS and EarthScope initiatives and several of which do not have earth science departments.

Our contacts with faculty at institutions in our field areas typically begin at the siting stage, when we are searching for a suitable location for a seismometer installation in the vicinity of the college. Contacts with faculty, staff, and students at institutions in our field area have proven invaluable to siting the MAGIC experiment. Three institutions are hosting MAGIC stations on their campus (Muskingum U., Denison U., and Virginia Commonwealth U.), while faculty or staff (or their family) at several others are hosting stations on privately owned land. Meetings with faculty and students at our host institutions allow for the MAGIC PIs to learn about the local student body and departments and programs, and allow us to increase awareness of the GeoPRISMS and EarthScope initiatives at local colleges.

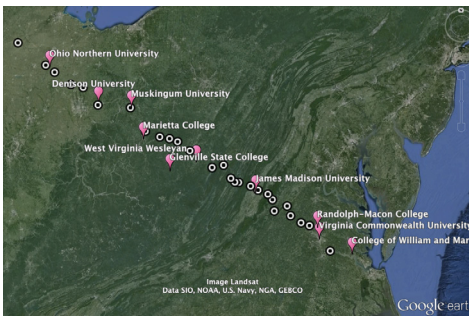

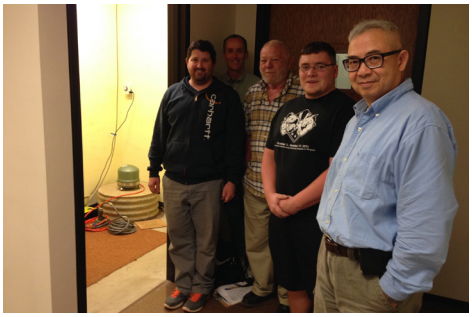

Top: Map of MAGIC station locations (white circles) along with institutions that have been involved in the MAGIC and TEENA projects (pink markers). Bottom: photograph of students and faculty from Yale U. and Muskingum U. servicing a MAGIC station (on pier in background) located in the science building on campus, May 2015.

During the course of the field work for MAGIC and its predecessor pilot project (the Test Experiment for Eastern North America, or TEENA), we have worked with faculty, students, or staff from a total of ten institutions: Ohio Northern U. (Ada, OH), Denison U. (Granville, OH), Muskingum U. (New Concord, OH), Glenville State College (Glenville, WV), West Virginia Wesleyan College (Buckhannon, WV), James Madison U. (Harrisonburg, VA), Virginia Commonwealth U. (Richmond, VA), Randolph-Macon College (Ashland, VA), and the College of William and Mary (Williamsburg, VA). At several of our stations, faculty and/or students have joined us for station installation or servicing trips. We are currently planning a MAGIC "lecture tour" to many of these institutions for Spring 2016, during which one of the PIs will visit to deliver a talk aimed at undergraduates on the geologic history of the eastern United States, the science goals of GeoPRISMS and EarthScope, the tools of observational seismology, and the MAGIC experiment. These talks will be tailored to the interests and backgrounds of the students at each institution (in particular, whether the students are physics or geology majors).

Structure and dynamics of the mid-Atlantic Appalachians from seismology, geodynamics, and geomorphology: The MAGIC project

Maureen D. Long, Margaret H. Benoit, Scott D. King, Eric Kirby, Scott R. Miller

The Mid-Atlantic Geophysical Integrative Collaboration (MAGIC) involves a collaborative effort among seismologists, geodynamicists, and geomorphologists to understand the relationships among surface processes, crustal and lithospheric structure, and deep mantle flow beneath eastern North America. The project is funded through the GeoPRISMS, EarthScope, and Geomorphology and Land Use Dynamics programs of NSF, and the science goals of the project are closely linked with those articulated by the GeoPRISMS science and implementation plans for the Eastern Margin of North America (ENAM) focus site of the Rifting Initiation and Evolution (RIE) initative.

ENAM represents a passive continental margin that has been modified by multiple episodes of orogenesis and rifting through two complete cycles of supercontinent assembly and breakup over the past 1.3 billion years of Earth history. It is unclear to what extent deep structures in the crust and mantle lithosphere have persisted over this timeframe, and what controls the pattern of mantle flow beneath the passive continental margin. Furthermore, the persistence of Appalachian topography remains a major outstanding problem in the study of landscape evolution; there is evidence for relatively recent rejuvenation of this topography, which may be

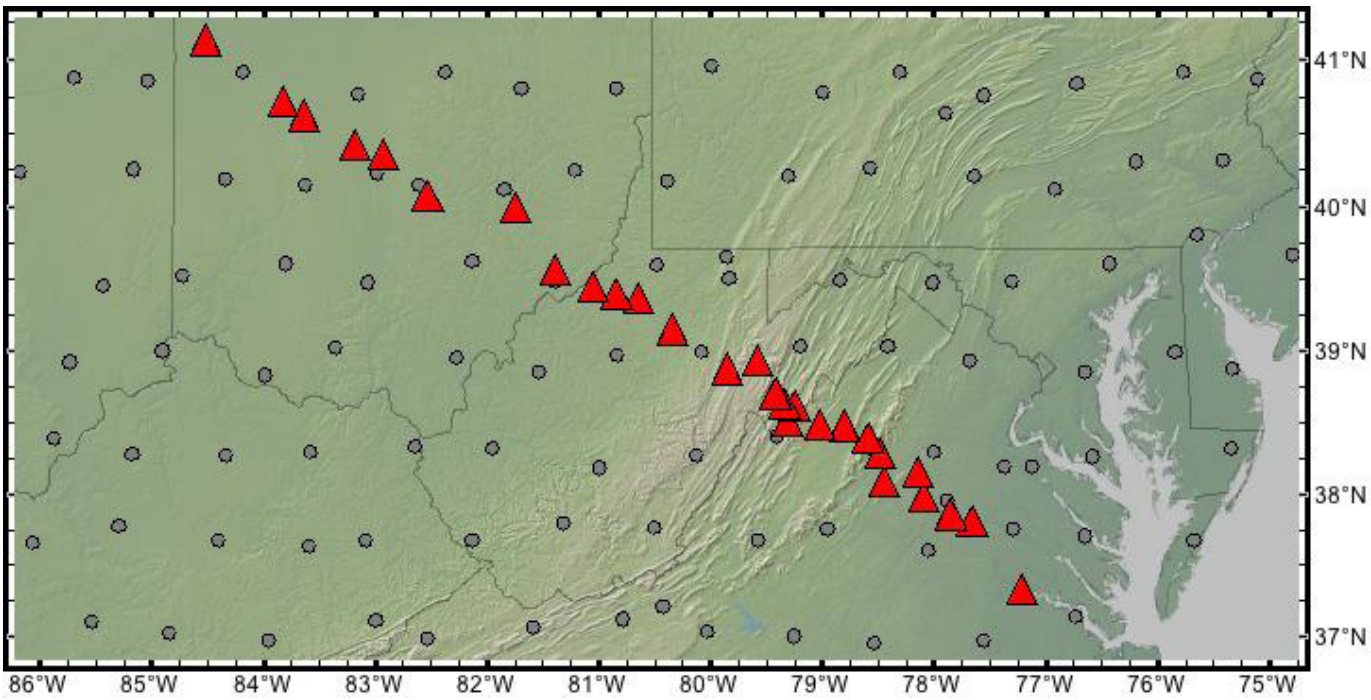

Map of MAGIC station locations (red triangles) along with Transportable Array (TA) station locations (gray circles).

connected to deep mantle flow. Although ENAM has been a passive continental margin for nearly 200 Ma, the eruption of basalts in Virginia and West Virginia during the Eocene (~40 Ma) provides evidence for its relatively recent modification [Mazza et al., 2014]. The two overarching science questions addressed by the MAGIC project are 1) What is the pattern of mantle flow beneath the eastern US continental margin and how has it affected surface topography?, and 2) How does the geological architecture and topography at the surface relate to the deeper structure of the crust and lithosphere?

To address these science questions, we are undertaking a deployment of 28 broadband seismometers as a USArray Flexible Array experiment in a dense linear transect from Charles City, VA to Paulding, OH. The first stations in the array were installed in Fall 2013, with the bulk of the stations installed in Fall 2014. As of June 2015, 27 of the 28 stations are operating, with data collection scheduled to continue through October 2016. The MAGIC data are allowing us to image isotropic and anisotropic crust and mantle structure from the coast to the continental interior, using techniques such as shear wave splitting, receiver function analysis, and tomographic inversions.

The geodynamical modeling effort focuses on quantitatively testing several different hypotheses for the pattern of mantle flow beneath eastern North America by using 3-D, time-dependent, numerical models to make testable predictions about seismic anisotropy in the mantle and (dynamic) topographic change, which will be tested against results from the seismology and geomorphology component of the project. Specific hypotheses to be tested include mantle flow driven by the ancient Farallon slab in the mid-mantle include small-scale convection at the edge of the North American craton. These hypotheses were developed based on preparatory studies of mantle anisotropy beneath ENAM [Long et al., 2010; Wagner et al., 2012] and will be tested against observations made using both the MAGIC stations and stations of the Transportable Array. The geomorphology component of the project uses quantitative stream profile data and cosmogenic isotopes to understand (past and present) erosion rates throughout the central Appalachian region; we hope to identify regional patterns in transient topographic change whose association with crustal and/or mantle features might illuminate the causes of topographic rejuvenation.

References

Long, M. D., Benoit, M. H., Chapman, M. C., and King, S. D., 2010. Upper mantle anisotropy and transition zone thickness beneath southeastern North America and implications for mantle dynamics. Geochem. Geophys. Geosyst. 11, Q10012, doi:10.1029/2010GC003247.

Mazza, S. E., Gazel, E., Johnson, E. A., Kunk, M. J., McAleer, R., Spotila, J. A., Bizimis, M., and Coleman, D. S., 2014. Volcanoes of the passive margin: The youngest magmatic event in eastern North America. Geology, 42, 483-486.

Wagner, L. S., Long, M. D., Johnston, M. D., and Benoit, M. H., 2012. Lithospheric and asthenospheric contributions to shear-wave splitting observations in the southeastern United States. Earth Planet. Sci. Lett., 341-342, 128-138.

Emplacement of regularly spaced volcanic centers in the East African Rift: Melt production or melt extraction?

Eric Mittelstaedt, Aurore Sibrant

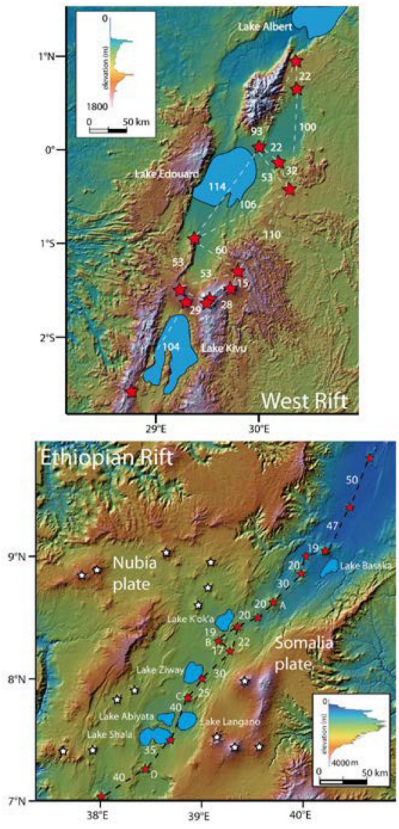

Figure 1. The active volcanoes during the last 10 ka of the West and Ethiopian Rift axis. The red and white stars indicate axial and off-axis volcanoes, respectively. The white number indicates the spacing between volcanoes.

PROJECT GOAL: This project will use coupled laboratory and numerical experiments to quantitatively assess the contribution of both melt production and melt extraction processes on the distribution of volcanic activity along the three main branches of the actively spreading East African Rift System.

As continental rifts evolve, volcanic centers within rift valleys often develop a characteristic spacing, or wavelength, such as observed in the Red Sea Rift and within the Afar depression, the Main Ethiopian Rift (MER), and the Kenya (Gregory) Rift of the East African Rift System (EARS) (Fig. 1). The surprisingly regular spacing of the volcanic centers within the EARS is attributed to lithosphere thickness, pre-existing fault systems, and mantle processes. However, little quantitative assessment of these hypotheses has been undertaken and few studies attempt to include the visco-elastic-plastic rheology of the lithosphere. The primary goal of this work is to use data from coupled numerical and laboratory experiments along with observations from the East African Rift System (EARS) to quantitatively assess the contribution of both melt production and melt extraction processes on the distribution of volcanic activity along the three main branches of the actively spreading EARS. We will perform two groups of coupled laboratory and numerical experiments; the first will simulate Rayleigh-Taylor type instabilities within the partially molten mantle (melt production), and the second will simulate the importance of pre-existing fractures and volcano loading on surface volcanism (melt extraction). Numerically, we will use a 3D marker-in-cell, finite difference code to initially match the laboratory experiments and then expand the parameter range beyond that possible in the laboratory. Both sets of experiments will vary rift opening rate, lithospheric thickness, pre-exiting fractures, and volcanic loading. Finally, we will develop predictive scaling laws that relate volcano spacing and volume to the above parameters. These scaling laws will permit the use of surface observations to estimate the relative importance of melt production below the lithosphere versus melt extraction through the lithosphere in both the EARS and other continental rifts.

CURRENT PROGRESS: This project was funded a few months ago and work has just recently began. Currently, we are determining appropriate fluids and testing laboratory experimental set-ups. Initial experiments with a mixture of Ludox and salted water (forming a gel) show great promise. Initial numerical simulations are scheduled to begin in the Fall of this year.

Reconstructing ancient passive margin dynamics by relating geomorphic and stratigraphic surfaces: a combined laboratory and field study

Kyle Straub

In the last year a student funded by this award has focused on work that is summarized in the abstract below, which we have in submission at Nature Geoscience (Fig. 1):

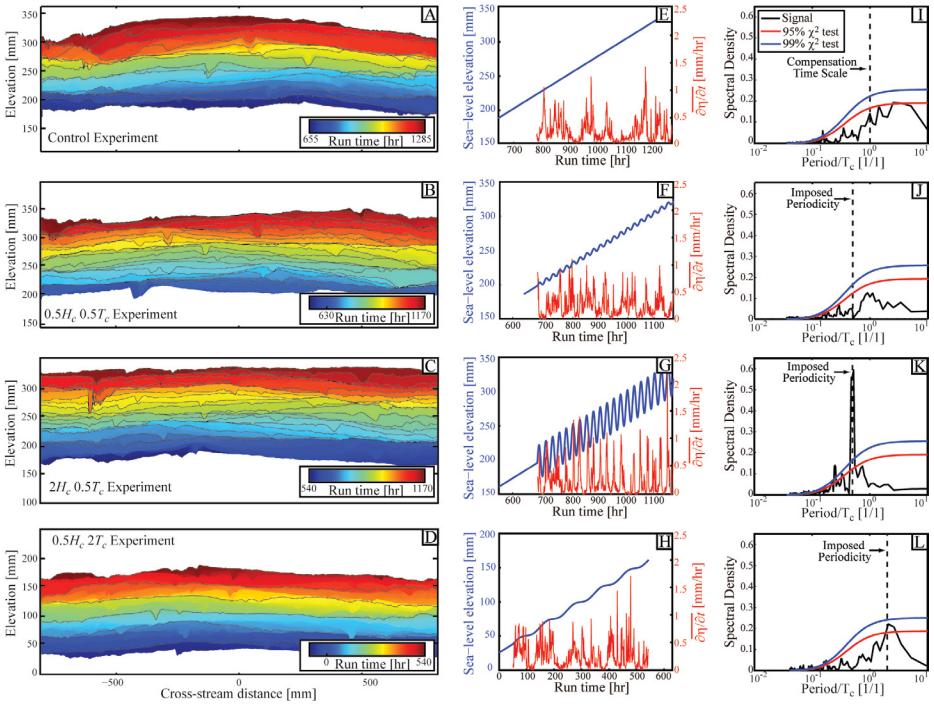

Figure 1. Time series analysis of mean deposition rate calculated from preserved stratigraphy for all experimental deltas with comparison to sea level time series. A-D) Synthetic stratigraphy along a proximal transect location illustrated in Fig. 1A. Solid black lines represent time horizons separated by 1 Tc (A) or demarcating the start of each RSL cycle (B-D). E-H) Sea level and mean deposition rate time series along proximal transects; I-L) Power spectra of mean deposition rate time series and χ_2 confidence limits

The tug of Relative Sea Level (RSL), set by climate and tectonics, is widely viewed as the most important boundary condition for the evolution of deltas. However, the range of amplitudes and periodicities of RSL cycles stored in deltaic stratigraphy remains unknown. Using experiments, we demonstrate that RSL cycles with magnitudes and periodicities less than the spatial and temporal scales of the internal (autogenic) dynamics of deltas cannot be extracted from the physical stratigraphic record. These results predict stratigraphic storage of information pertaining to RSL cycles during icehouse Earth conditions. However, these thresholds often overlap with the magnitudes and periodicities of RSL cycles for major river deltas during greenhouse Earth conditions, which suggest stratigraphic signal shredding. This theory defines quantitative limits on the range of paleo-RSL information that can be extracted from stratigraphy, which could aid the prediction of deltaic response to climate change.

Other publications that have come out in the last year in which my involvement or data was partially related to this award include:

Kim., W., Petter, A., Straub, K.M., Mohrig, D., 2014, Decoupling allogenic forcing from autogenic processes: Experimental geomorphology and stratigraphy, In: From Depositional Systems to Sedimentary Successions on the Norwegian Continental Shelf (Eds A.W. Martinius, R. Ravnås, J.A. Howell, R.J. Steel, and J.P. Wonham), IAS Spec. Publ., 46, 127-138.

Armstrong, C., Mohrig, D., Hess, T., George, T., Straub, K.M., 2014, Influence of growth faults on coastal fluvial systems: Examples from the late Miocene to Recent Mississippi River Delta, v. 301, p. 120-132, DOI: 10.1016/j.sedgeo.2013.06.010.

There will likely be two additional manuscripts submitted in the coming year that are primary products of this award. Unfortunately, the PhD student working on this has back-ended all of his publications and so a bunch will come out (hopefully) in a flurry as he gets ready to defend this year.

If I were try to summarize the key findings of the work, it's as follows: We have defined 2 nondimensional numbers important for storing environmental signals (here focused on sea-level) in stratigraphy. These numbers compare the amplitude (H*) and period (T*) of sea level cycles to the space and time scales of internal deltaic dynamics. In order for paleo-sea level information to be inverted from the stratigraphic record one of these numbers must be great than one. It turns out that in many systems important Milankovic scale cycles should not be expected to be stored in stratigraphy, if you scale our experiments up to the field through these non-dimensional numbers. This is a start (I hope a big one) towards placing quantitative limits on the fidelity of the stratigraphic record.

The GeoPRISMS Eastern North American Margin Community Seismic Experiment (ENAM CSE)

Harm Van Avendonk, Beatrice Magnani, Donna Shillington, Margaret Benoit, Brandon Dugan, Jim Gaherty, Matt Hornbach, Dan Lizarralde, Maureen Long, Steve Harder, Anne Becel, Gail Christeson

The Eastern North American Margin Community Seismic Experiment, or ENAM CSE, is an ambitious effort to collect a suite of onshore and offshore seismic data within the ENAM focus site of the GeoPRISMS Rift Initiation and Evolution (RIE) initiative as a community-driven experiment with completely open data access. The study area, focused on the East Coast margin around Cape Hatteras, North Carolina, targets the rifted margin from unextended continental lithosphere onshore to mature oceanic lithosphere offshore. Furthermore, the study area encompasses along-strike changes in margin structure and two major fracture zones that are associated with significant offsets at the modern Mid-Atlantic Ridge. The experiment was designed to allow for multiscale imaging of crustal and mantle lithospheric structure and stacked geomorphological features over a regionally extensive, shoreline-crossing footprint.

The philosophy of the ENAM CSE is that of a community experiment, as articulated in the GeoPRISMS implementation plans. Specifically, the ENAM CSE comprises a large field effort planned and executed by the community rather than by a small group of PIs, with the data made publicly available immediately. The ENAM

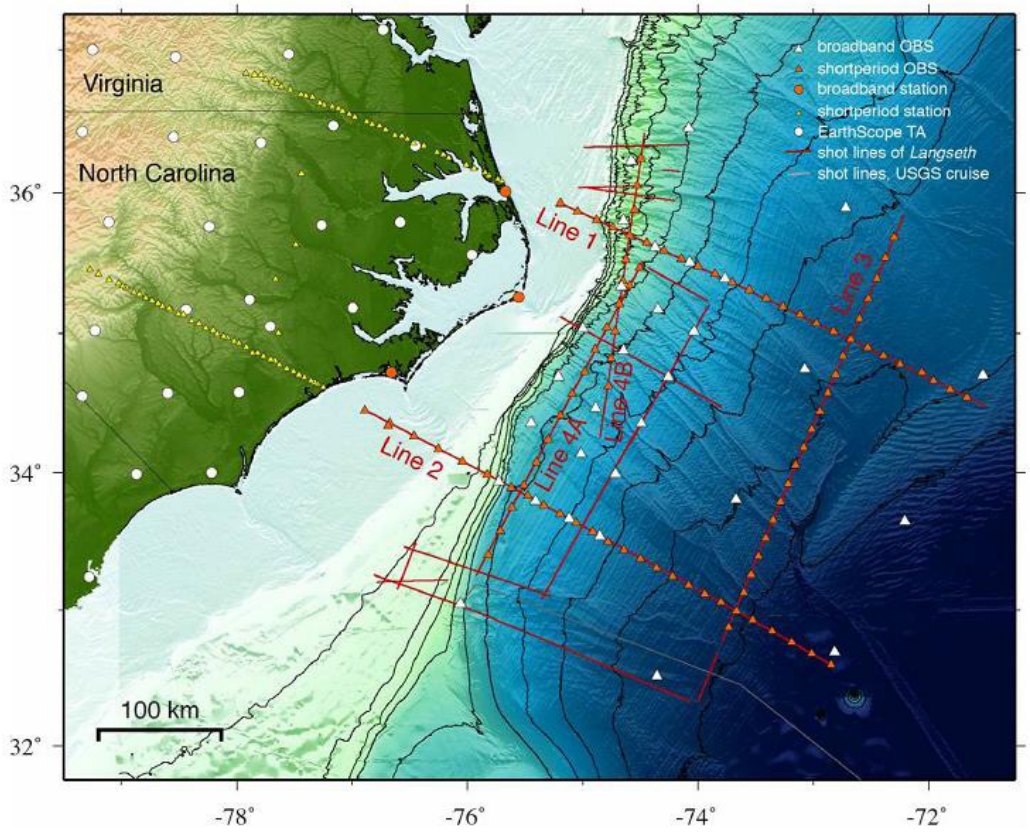

Map of ENAM CSE deployment. Broadband OBS instruments (white triangles) were deployed in April 2014 and recovered in April 2015 aboard the R/V Endeavor. Broadband onshore stations on the Outer Banks (orange circles) operated between May 2014 and May 2015. Orange triangles indicate short-period OBS stations deployed and recovered during September-October 2014 aboard the R/V Endeavor. Red lines indicate shot lines for active source seismic program on the R/V Langseth in September-October 2014; these shots were also recorded on land (yellow triangles). Active source lines were shot on land during summer 2015.

CSE was designed to address four specific goals: 1) To understand the roles of inheritance and magmatism on rifting and rupture, 2) To understand passive margin evolution from rifting to surface processes and active tectonics today, 3) To provide an open-access dataset that is openly available and useful for a variety of science targets, and 4) To increase the number of scientists taking advantage of marine seismic data through a broad training program. These big-picture goals relate to a host of more specific science questions articulated in the GeoPRISMS ENAM implementation plan, including those related to the distribution of deformation and magmatism during rifting, along-strike segmentation, the influence of deep mantle dynamics, the rift-to-drift transition, and the ongoing evolution of the passive margin.

ENAM CSE data were successfully collected during 2014-2015 and have been (or very soon will be) publicly released to the community via the IRIS Data Management Center and other data portals. Data acquisition efforts included the deployment of 30 broadband ocean bottom seismometers (OBS) in spring 2014 and their recovery in spring 2015; during this time, three onshore broadband seismometers were deployed on the Outer Banks of North Carolina. These deployments overlapped with the operation of USArray Transportable Array (TA) stations in the Carolinas and Virginia. Offshore active source data were collected in September-October 2014 with the R/V Langseth, which shot refraction data that were recorded by short-period OBS instruments deployed by the R/V Endeavor. The Langseth also acquired multi-channel seismic (MCS) data along the primary transects as well as MCS-only data along shorter ancillary lines. The Fall 2014 offshore shots were also recorded with short-period seismometers deployed onshore. Finally, a series of land seismic shots were shot in June 2015; 11 on-land shots were fired and recorded on ~1400 Texans deployed along two lines onshore.

Project URLs:

http://www.ig.utexas.edu/enam/

http://enamseismic.blogspot.com/

http://geoprisms.org/initiatives-sites/rie/enam/

http://ds.iris.edu/mda/YO?timewindow=2014-2015

Entraining young scientists in amphibious seismology through the Eastern North American Margin Community Seismic Experiment

ENAM CSE PI Team: Harm Van Avendonk, Maria Beatrice Magnani, Donna J. Shillington, James B. Gaherty, Anne Bécel, Matthew Hornbach, Dan Lizarralde, Brandon Dugan, Maureen Long, Steve Harder, Lara Wagner, Gail Christeson, Maggie Benoit

One of the goals of the GeoPRISMS Eastern North American Margin (ENAM) Community Seismic Experiment (CSE) was to involve students and young scientists in acquiring the diverse onshore/offshore, active/passive seismic datasets involved in this program and to provide them with training in data collection, analysis, and interpretation. The program was extremely successful in this regard. Overall, 79 unique individuals (students and young scientists) from 48 universities participated in the field work and data analysis training workshops held at UTIG and LDEO.

We brought students and young scientists to sea on four cruises and involved them in a suite of onshore seismic deployments/recoveries. The cruises included 1) deploying broadband ocean bottom seismometers (OBS) aboard the R/V Endeavor (April 2014), 2) acquiring seismic reflection data aboard the R/V Langseth (Sept-Oct 2014), 3) deploying and recovering short-period OBS for the active source program aboard the R/V Endeavor (Sept-Oct 2014), and 4) recovering broadband OBS aboard the R/V Endeavor (April 2015). The onshore activities included 1) deploying (May 2014), servicing (Sept 2014, Jan 2015) and recovering (May 2015) a small array of broadband seismometers; 2) deploying short period seismometers to record the offshore experiment (September 2014), 3) recovering the short period seismometers (October 2014) and 4) acquiring onshore refraction data (June 2015). We advertised the opportunity to participate in these field programs through the IRIS and GeoPRISMS listervs, and a large number of people expressed interest. In total 24 unique people participated in the research cruises and 28 in the onshore field work.

We also held data processing workshops in seismic refraction data analysis at UTIG and in

Clockwise from top: Student checks status of short period seismometer; Students and OBS Technicians prepare OBS for deployment Students put a bird on the streamer.

seismic reflection analysis at LDEO. As with the field work, we advertised the opportunity to participate in these programs through listservs and received an enormous number of applications (e.g., ~80 people applied for the MCS workshop). Twenty participants took part in the refraction workshop and learned about data processing and the basics of seismic velocity modeling using OBS data from the ENAM program. Fourteen participants attended the seismic reflection workshop held at LDEO and learned the steps required to go from raw seismic reflection data to time-migrated images.

In summary, the GeoPRISMS ENAM CSE provided tremendous educational and field opportunities to a large number of students and young scientists from across the country. We hope that this experience will empower them to take advantage of the open-access data from ENAM and other community and legacy experiments and provide training for the next generation of geoscientists.

Left: Participants in MCS training workshop processing reflection data.

Right: Participants in OBS refraction training workshop comparing tomography models.

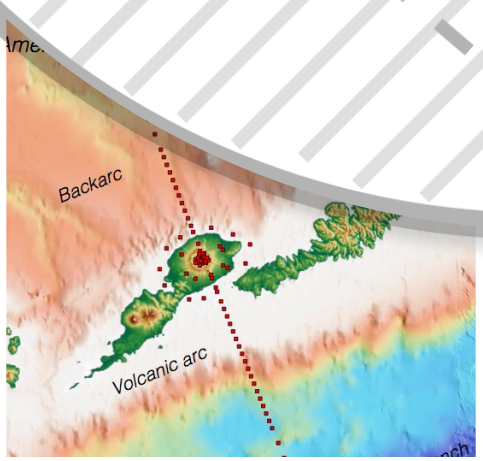

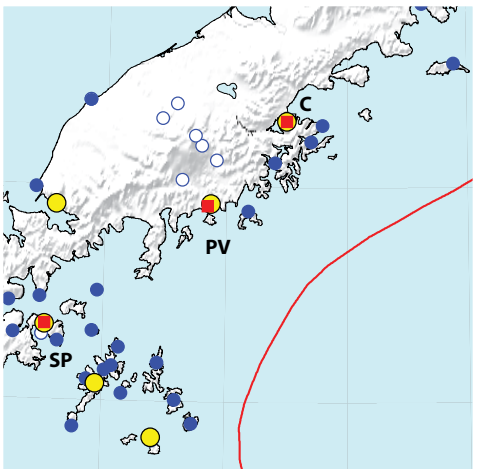

Subduction Cycles & Deformation Nuggets

Origin and evolution of the lower crust in magmatic arcs and continental crust

Mark D. Behn, Esteban Gazel, Bradley R. Hacker, Olivier Jagoutz, Peter B. Kelemen, Donna Shillington

Taking a broad view of the research supported by grants from GeoPRISMS[1] and elsewhere, we've conducted several recent reviews (Gazel et al. 2015; Hacker et al. 2015; Jagoutz & Behn 2013; Jagoutz & Kelemen 2015; Kelemen & Behn 2015; Shillington et al. 2013). A summary of our results is as follows.

Thin oceanic crust is formed by decompression melting of the upper mantle at mid-ocean ridges, but the origin of the thick and buoyant continental crust is enigmatic. Juvenile continental crust may form from magmas erupted above intraoceanic subduction zones, where oceanic lithosphere subducts beneath other oceanic lithosphere. However, it is unclear why the subduction of dominantly basaltic oceanic crust forms andesitic continental crust. Gazel et al. (2015) use geochemical and geophysical data to reconstruct the evolution of the Central American land bridge, which formed above an intra-oceanic subduction system over the past 70 Myr. We find that the geochemical signature of erupted lavas evolved from basaltic to andesitic about 10 Myr ago—coincident with the onset of subduction of more oceanic crust that originally formed above the Galápagos mantle plume. We also find that seismic P-waves travel through the crust at velocities intermediate between those typically observed for oceanic and continental crust. We develop a continentality index to quantitatively correlate geochemical composition with the average P-wave velocity of arc crust globally. We conclude that although the formation and evolution of continents may involve many processes, melting enriched oceanic crust within a subduction zone—a process probably more common in the Archaean—can produce juvenile continental crust.

The composition of much of Earth's lower continental crust is enigmatic. Seismic wavespeeds require that 10–20% of the lower third is mafic, but the available heat-flow and wavespeed constraints can be satisfied if lower continental crust elsewhere contains 49 to 62 wt% SiO_2 (Hacker et al. 2015; also see Behn & Kelemen 2003). Thus, contrary to common belief, the lower crust in many regions could be relatively felsic, with SiO_2 contents similar to andesites and dacites. Most lower crust is less dense than the underlying mantle, but mafic lowermost crust could be unstable and likely delaminates beneath rifts and arcs as invoked by Jagoutz & Behn (2013). During sediment subduction, subduction erosion, arc subduction, and continent subduction, mafic rocks

[1]*NSF OCE-1144759: "Collaborative Research: Plutons as ingredients for continental crust: Pilot study of the difference between intermediate plutons and lavas in the intra-oceanic Aleutian arc", Kelemen, PI, Steve Goldstein, Sidney Hemming, M. Rioux(UCSB) co-PI's; NSF OCE-1358091/1356132, Marine Geology and Geophysics Program, "Advanced modeling for understanding fluid & magma migration in subduction zones", Cian Wilson, lead PI, P Kelemen, M Spiegelman & Peter van Keken (Univ. Michigan) co-PI's; NSF EAR-1457293: "Collaborative Research: Focused Study of Aleutian Plutons and their Host Rocks: Understanding the building blocks of continental crust",P. Kelemen lead PI,; NSF-EAR-0742451, "Collaborative Research: Element Recycling from UHP Metasediments: Evidence and Consequences" PB Kelemen and BR Hacker, PI's; NSF EAR-1219942, "What Determines Whether the Deep Continental Crust Flows [or not]?" BR Hacker & ARC Kylander-Clark; NSF #: EAR-1322032: A field study of the liquid line of descent of hydrous alkaline-rich magmas at elevated pressures (0.5-1.0 GPa); the Dariv alkaline intrusive complex, O. Jagoutz PI*

become eclogites and may continue to descend into the mantle, whereas more silica-rich rocks are transformed into felsic gneisses that are less dense than peridotite but more dense than continental upper crust. These more felsic rocks may rise buoyantly, undergo decompression melting and melt extraction, and be relaminated to the base of the crust. As a result of this refining and differentiation process, such relatively felsic rocks could form much of Earth's lower crust (Hacker et al. 2011, Kelemen & Behn 2015).

A long-standing theory for the genesis of continental crust is that it is formed in subduction zones. However, the observed seismic properties of lower crust and upper mantle in oceanic island arcs differ significantly from those in the continental crust . Accordingly, significant modifications of lower arc crust must occur, if continental crust is indeed formed from island arcs. Jagoutz & Behn (2013) investigated how the seismic characteristics of arc crust might be transformed into those of the continental crust by calculating the density and seismic structure of two exposed sections of island arc (Kohistan and Talkeetna). The Kohistan crustal section is negatively buoyant with respect to the underlying depleted upper mantle at depths exceeding 40 kilometres and is characterized by a steady increase in seismic velocity similar to that observed in active arcs. In contrast, the lower Talkeetna crust is density sorted, preserving only relicts (about ten to a hundred metres thick) of rock with density exceeding that of the underlying mantle. Specifically, the foundering of the lower

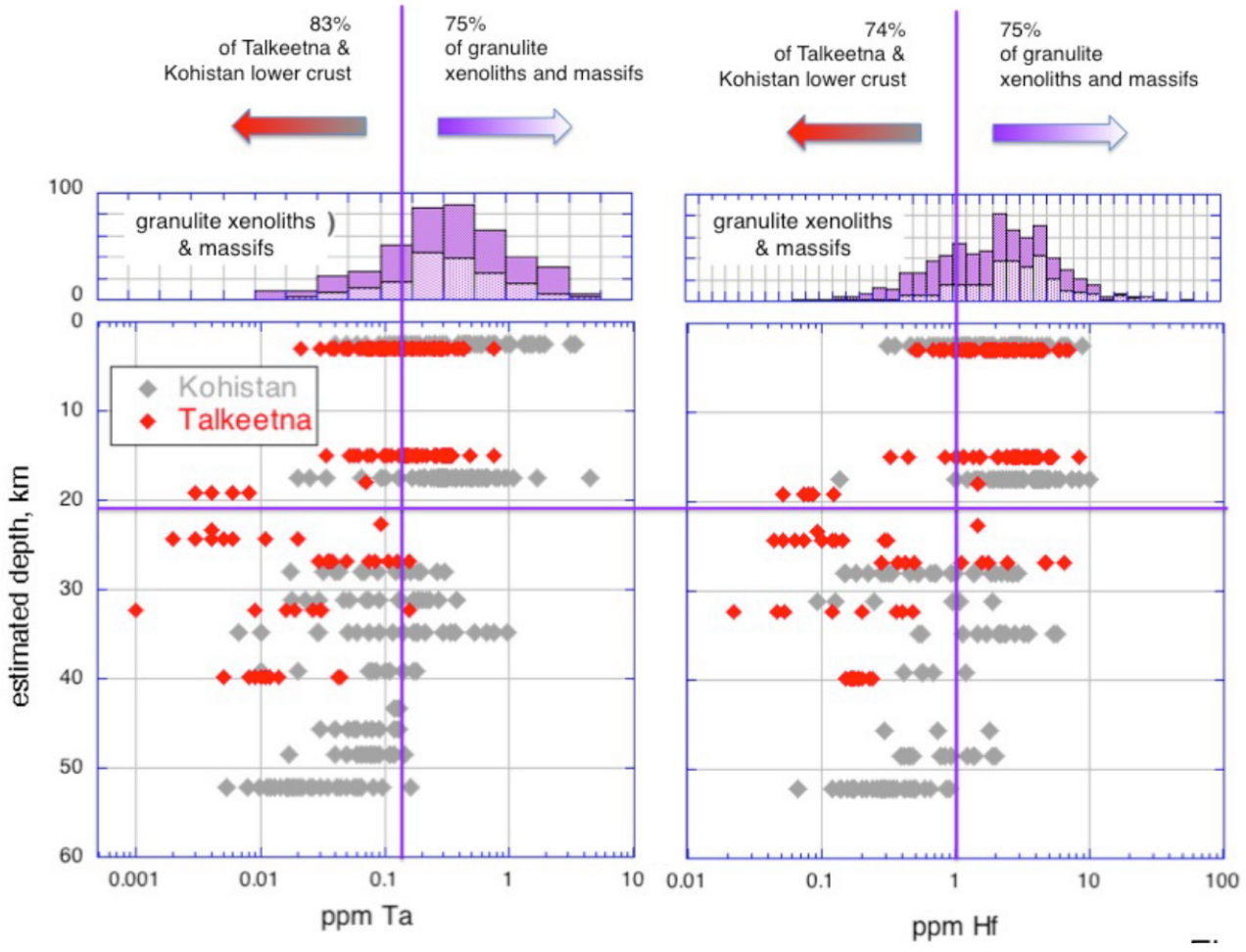

Talkeetna crust resulted in the replacement of dense mafic and ultramafic cumulates by residual upper mantle, producing a sharp seismic discontinuity at depths of around 38 to 42 km, characteristic of the continental Moho. Dynamic calculations indicate that foundering is an episodic process that occurs in most arcs with a periodicity of half a million to five million years. Because foundering will continue after arc magmatism ceases, this process ultimately results in formation of the continental Moho.

Jagoutz & Kelemen (2015) reviewed recent research on arc composition, focusing on the relatively complete arc crustal sections in the Jurassic Talkeetna arc (south central Alaska) and the Cretaceous Kohistan arc (northwest Pakistan), together with seismic data on the lower crust and uppermost mantle. Whereas primitive arc lavas are dominantly basaltic, the Kohistan crust is clearly andesitic and the Talkeetna crust could be andesitic. The andesitic compositions of the two arc sections are within the range of estimates for the major element composition of continental crust. Calculated seismic sections for Kohistan and Talkeetna provide a close match for the thicker parts of the active Izu arc, suggesting that it, too, could have an andesitic bulk composition. Because andesitic crust is buoyant with respect to the underlying mantle, much of this material represents a net addition to continental crust. Production of bulk crust from a parental melt in equilibrium with mantle olivine or pyroxene requires processing of igneous crust, probably via density instabilities. Delamination of dense cumulates from the base of arc crust, foundering into less dense, underlying mantle peridotite, is likely, as supported by geochemical evidence from Talkeetna and Kohistan. Relamination of buoyant, subducting material—during sediment subduction, subduction erosion, arc-arc collision, and continental collision—is also likely, as described more extensively by Behn et al. (2011) and Hacker et al. (2011, 2015).

Geochemical similarities between arc magmas and continental crust indicate that arc magmatic processes – and/or similar Archean processes – played a central role in generating continents. As noted above in the summary of Jagoutz & Behn (2013) an outstanding question is how arc crust formed from basaltic, mantle-derived magmas with 48 to 52 wt% SiO_2 is transformed to andesitic continental crust with more than 57 wt% SiO_2. One commonly invoked process removes dense, SiO_2-poor products of magmatic fractionation from the base of arc crust by "delamination", as in Jagoutz & Behn 2013. However, lower arc crust after delamination has significantly different trace element contents compared to estimates for the lower continental crust, and we present a simple, alternative explanation (Kelemen & Behn 2015).

In the alternative model of Kelemen & Behn (2015), buoyant magmatic rocks generated at arcs are first subducted, but upon heating these buoyant lithologies re-ascend through the mantle wedge or along a subduction channel, and are "relaminated" at the base of overlying crust. To test the relamination model, we review the average compositions of buoyant lavas and plutons for the Aleutians, Izu-Bonin-Marianas, Kohistan and Talkeetna arcs and show that they fall within the estimated range of lower continental crust compositions for major and trace elements. Relamination provides a more efficient process for generating the continental crust than does delamination and has important implications for the long-term evolution of heat producing elements in the Earth's crust.

Determining the bulk composition of island arc lower crust is essential for distinguishing between competingmodels for arc magmatism and assessing the stability of arc lower crust. Shillington et al. (2013) presented new constraints on the composition of high P-wave velocity (V_P = 7.3–7.6 km/s) lower crust of the Aleutian arc from best-fitting average lower crustal V_P/V_S ratio using sparse converted S-waves from an

along-arc refraction profile. We find a low V_P/V_S of ~1.7–1.75. Using petrologic modeling, we show that no single composition is likely to explain the combination of high V_P and low V_P/V_S. Our preferred explanation is a combination of clinopyroxenite (~50–70%) and a-quartz bearing gabbros (~30–50%). This is consistent with Aleutian xenoliths and lower crustal rocks in obducted arcs, and implies that ~30–40% of the full Aleutian crust comprises ultramafic cumulates. These results also suggest that small amounts of quartz can exert a strong influence on V_P/V_S in arc crust.

References

Behn, M.D. and P.B. Kelemen, Relationship between seismic velocity and the composition of anhydrous igneous and meta-igneous rocks, Geochemistry, Geophysics, Geosystems (G-cubed), 2002GC000393, 2003.

Behn, M.D., P.B. Kelemen, G. Hirth, B.R. Hacker, and H.-J. Massonne, Diapirs as the source of the sediment signature in arc lavas, Nature Geoscience 4, 642-646, 2011.

Gazel, E., J. Hayes, K. Hoernle, P. Kelemen, E. Everson, W.S. Holbrook, F. Hauff, P. van den Bogaard, E.A. Vance, S. Chu, M.J. Carr and G.M. Yogodzinski, The youngest continents, Nature Geoscience 8, 321-327, 2015

Hacker, B.R., P.B. Kelemen and M. Behn, Differentiation of the continental crust by relamination, Earth Planet. Sci. Lett. 307, 501-516, 2011.

Hacker, B.R., P.B. Kelemen and M.D. Behn, Continental lower crust, Ann Rev Earth Planet Sci 43,167–205, 2015

Jagoutz O. and M.D. Behn, Foundering of lower arc crust as an explanation for the origin of the continental Moho. Nature 504, 131–34, 2013.

Jagoutz, O. and P.B. Kelemen, Role of arc processes in the formation of continental crust, Ann Rev Earth Planet Sci. 43, 363–404, 2015

Kelemen, P.B. and M.D. Behn, Formation of continental crust by relamination of buoyant arc lavas and plutons, in revision for Nature Geoscience, July 2015.

Shillington, D.J., H.J.A. Van Avendonk, M.D. Behn, P.B. Kelemen, and O. Jagoutz, Constraints on the composition of the Aleutian arc lower crust from Vp/Vs, Geophys. Res. Lett., 40, 2579–2584, 2013.

Collaborative Research: Magnetotelluric and Seismic Investigation of Arc Melt Generation, Delivery, and Storage beneath Okmok Volcano

Ninfa Bennington, Kerry Key

Project Summary

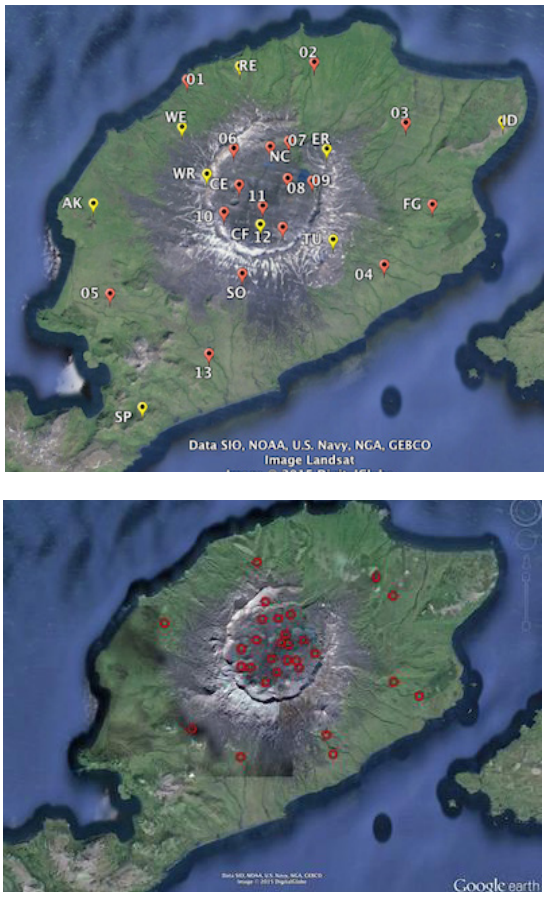

Figure 1. (a) Distribution of seismic instruments at Okmok volcano where broadband and short period instruments are indicated as orange and yellow flags, respectively. Lettered station labels designate the Alaska Volcano Observatory seismic instruments and temporary, year-long seismic installation is indicated via two-number designation. (b) Distribution of the 29 onshore magnetotelluric stations.

Alaska accounts for nearly 99% of the seismic moment release within the US. Much of this is associated with the Aleutian volcanic arc, the most tectonically active region in North America, and an ideal location for studying arc magmatism. The arc contains numerous small- to moderate-sized calderas; such calderas suggest low mantle magma production rates and associated small volumes of melt ascending from the mantle and accumulating within the crust. Future caldera forming eruptions would likely be small and locally focused in such a volcanic setting. In contrast, geochronologic and volumetric estimates of mantle magma production are high and argue in favor of large volumes of magma generated in the mantle and ubiquitous magma storage within a thermally and mechanically weakened crust. Such crustal magma reservoirs could host large future caldera forming eruptions. Gaining a greater understanding of Aleutian arc melt generation, migration, and storage beneath an active caldera should help resolve these two disparate views of the arc's magmatic system.

Okmok is an active volcano located in the central Aleutian arc, which hosts a 10 km diameter caldera. The subdued topography of Okmok, relative to other Aleutian volcanoes, improves access and permits dense sampling of the volcanic edifice. We have selected Okmok as the site of study for this project due to frequent volcanic activity and the presence of a crustal magma reservoir as inferred from previous seismic studies. At least two caldera forming eruptions are recognized, and Okmok is believed to be representative of volcanos both within the Aleutian arc and worldwide, where long periods of effusive eruptions are punctuated by much larger explosive caldera forming eruptions. As one of the most active volcanos in the Aleutian arc, Okmok also poses a major hazard to trans-Pacific air travel, hence understanding crustal magma storage and transport is a critical component in assessing future volcanic hazards at the volcano.

This project uses geophysical techniques to characterize the magmatic system beneath Okmok. During the summer of 2015 we collected onshore and offshore magnetotelluric data and installed a temporary year long seismic deployment. These new geophysical data will be used to test hypotheses regarding the role of slab fluids in arc melt generation, melt migration within the crust, and the crustal magmatic plumbing and storage system beneath Okmok caldera. Analysis of these data will include a suite of seismic and magnetotelluric modeling efforts (ambient noise and earthquake tomography, surface wave anisotropy, 3D onshore and 2D amphibious magnetotelluric inversion, joint ambient noise/body-wave and seismic/magnetotelluric tomography), as well as petrologic modeling using SIGMELTS. These analyses will result in geophysical models of seismic velocity and electrical conductivity that in turn will constrain the distribution of temperature, fluids and melts from the top of the slab through the shallow crust.

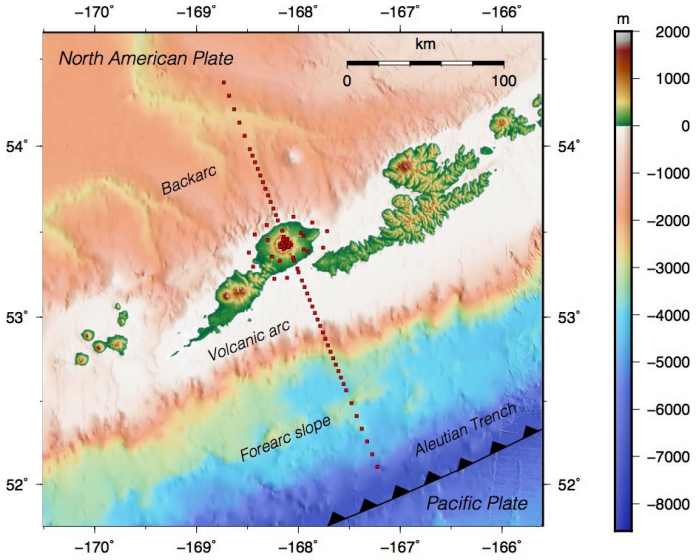

Figure 2. Distribution of the 53 offshore and 29 onshore magnetotelluric stations shown along with the regional tectonic framework.

Field Work

In June-July 2015 we carried out the amphibious field deployment. The onshore work was based out of Bering Pacific Ranch at Fort Glenn, an abandoned WWII military base, with a helicopter transporting the seismic and MT teams and equipment during the 19 days of field operations. Offshore MT deployments were made during a four day cruise on the RV Thompson, with the instruments being recovered three weeks later during a six day cruise on the new RV Sikuliaq.

We installed 13 temporary broadband seismometers both in and around the Okmok caldera (Fig. 1a). In tandem with the Alaska Volcano Observatory's 12 permanent seismic stations, there are now 12 seismic instruments within/at the rim of the caldera and 14 seismic instruments outside the caldera. The temporary array will record seismic data until its retrieval in summer 2016.

Onshore magnetotelluric data were collected in a 3D array using a combination of long-period and wide-band MT systems, with 19 stations within the caldera and 10 stations outside (Fig. 1b). Offshore magnetotelluric stations were deployed along a 2D tectonic profile spanning the trench, volcanic arc and backarc in order to constrain melt formation and migration to the crust and the hydration state of the forearc mantle (Fig. 2). A ring of offshore stations surrounding the eastern portion of Umnak island supplements the onshore 3D MT data and will be used to constrain the distribution and migration of melt within the crust. Of the 54 offshore deployments, 53 instruments were successfully recovered while one instrument was lost in Umnak pass due to strong tidal currents in the shallow water. Initial analysis of the data shows strong MT signals, especially from data collected during a geomagnetic storm in late June.

Highlight pictures from fieldwork

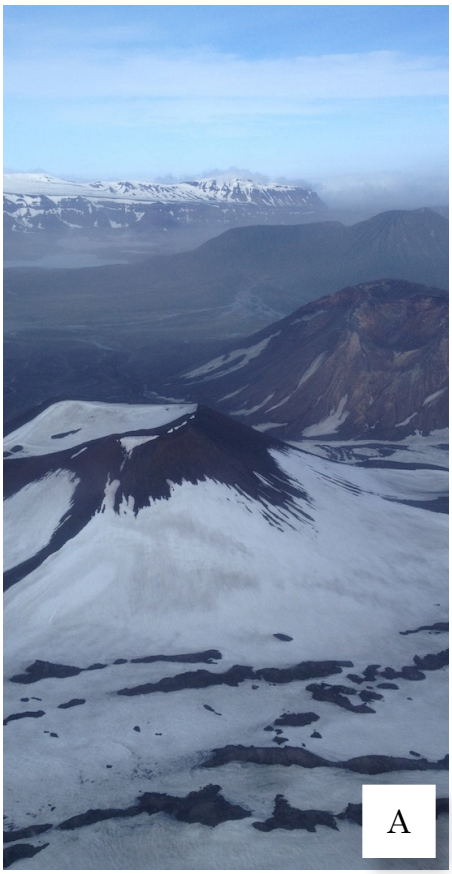

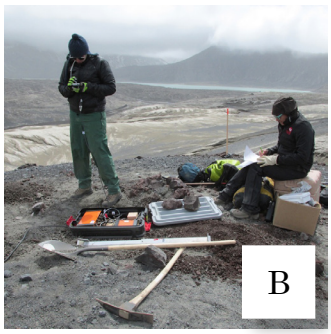

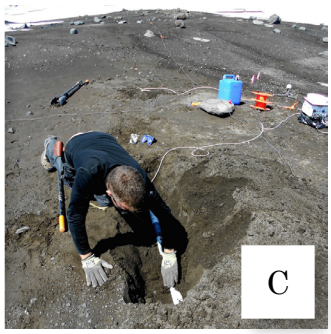

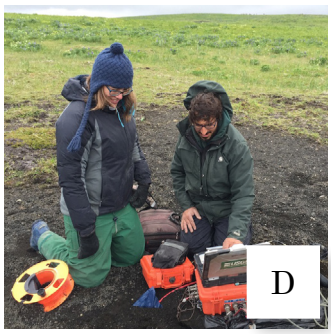

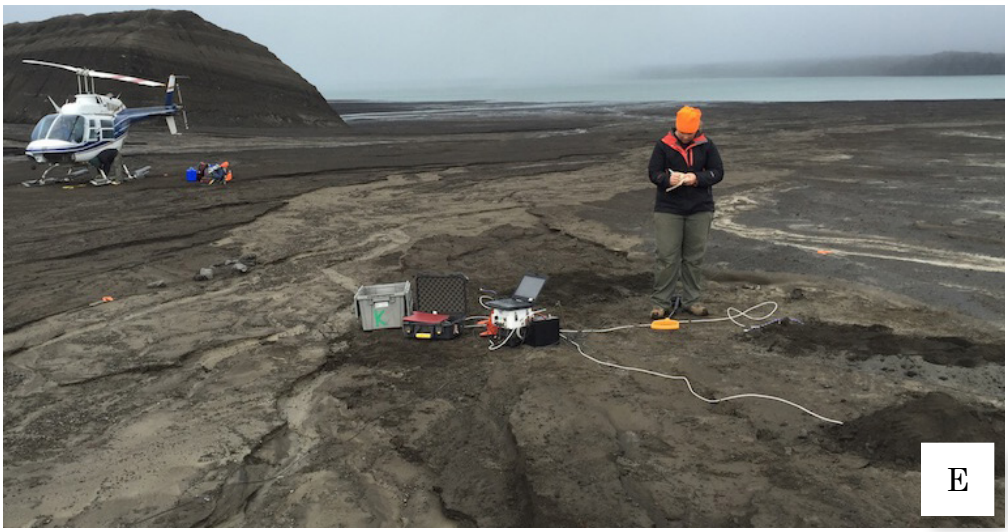

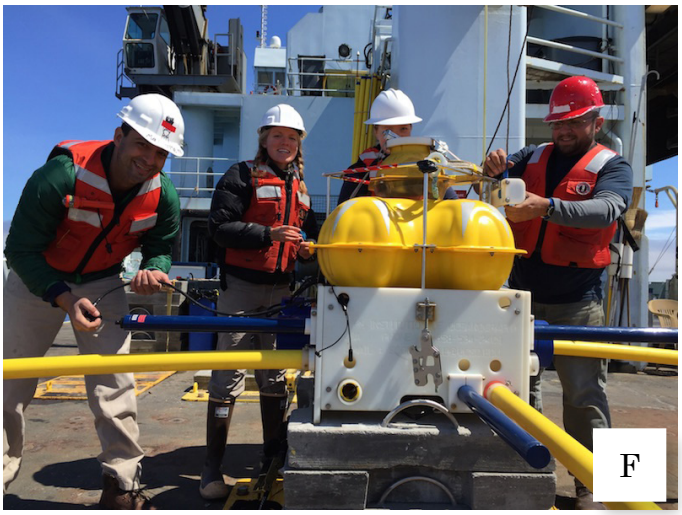

A: Okmok caldera (cone F in the foreground, cone C in mid-ground, and cone D and new cone from the 2008 eruption in the background). Seismic Fieldwork: B: Seismic station being installed inside Okmok caldera. Onshore magnetotelluric fieldwork: C: MT magnetometer being buried inside the caldera floor, D: and an MT station outside the caldera, E: MT station in the caldera. Offshore magnetotelluric fieldwork: F: Scripps broadband MT receiver being prepared for deployment on the RV Thompson, G: Image from a drone video of an MT receiver being recovered on the RV Sikuliaq with Umnak Island in the background (video available at http://okmok.ucsd.edu).

Different parental magmas for plutons versus lavas in the central Aleutian arc

Merry Y. Cai, Matthew E. Rioux, Peter B. Kelemen, Steven L. Goldstein, Louise Bolge, Andrew R.C. Kylander-Clark

The oceanic, Aleutian magmatic arc has never been rifted, the crust is relatively thick compared with other Pacific arcs, the islands are relatively large, and thus the islands host extensive exposures of Eocene to Miocene plutons as well as Eocene to Holocene lavas. These large outcrops of plutonic rocks are unique among oceanic arcs worldwide, and offer an exceptional opportunity to study the mid-crust in such settings. Most geochemical work on the Aleutians has focused on Holocene lavas. With a pilot grant from NSF GeoPRISMS[1], we obtained samples of plutons from the Aleutians collected by the US Geological Survey from 1950 to 1980, and made modern trace element and isotope analyses of these samples. Prior to this, there were very few similar studies of Aleutian plutons. The results of our preliminary study are as follows.

Cenozoic plutons that comprise the middle crust of the central and eastern Aleutians have distinct isotopic and elemental compositions compared to Holocene tholeiitic lavas in the same region, including those from the same islands (Cai et al. 2013, 2014, 2015). Therefore the Holocene lavas are not representative of the net magmatic transfer from the mantle into the arc crust. Compared to the lavas, the Eocene to Miocene (9-39 Ma) intermediate to felsic plutonic rocks show higher SiO_2 at a given Mg/(Mg+Fe). In other words, the plutons are "calc-alkaline" whereas the lavas are dominantly tholeiitic. Crucially, the plutons also have higher εNd-εHf values and lower Pb and Sr isotope ratios than the lavas. In all of these ways, the plutonic rocks strongly resemble calc-alkaline, Holocene volcanics with "depleted" isotope ratios in the western Aleutians, whose composition has been attributed to significant contributions from partial melting of subducted basaltic oceanic crust. The new isotope data on the plutons data reflect temporal variation of central and eastern Aleutian magma source compositions, from predominantly calc-alkaline compositions with more "depleted" isotope ratios in the Paleogene, to tholeiitic compositions with more "enriched" isotopes more recently. Alternatively, the differences between central Aleutian plutonic and volcanic rocks may reflect different transport and emplacement processes for the magmas that form plutons versus lavas. Calc-alkaline parental magmas, with higher SiO_2 and high viscosity, are likely to form plutons after extensive mid-crustal degassing of initially high water contents. In any case, our isotope data have overarching importance because the plutonic rocks are chemically similar to bulk continental crust, whereas the central Aleutian lavas are not. Formation of similar plutonic rocks worldwide may play a key role in the genesis and evolution of continental crust.

During fieldwork in summer 2015, funded by a second GeoPRISMS grant[2], we will sample older volcanic rocks that are intruded by Paleogene plutons on Unalaska, Umnak and Atka Islands, ensuring that we have overlapping age coverage for volcanic and plutonic rocks in the central Aleutians. We can then test whether the isotopic and compositional differences between central Aleutian plutons and lavas reflect a temporal evolution in the arc, or the continuous presence of two distinct magma series throughout arc history.

We will also make detailed studies of some of the larger plutons in the Aleutians, including the Shaler pluton on Unalaska Island. There are fewer than five published analyses of the Shaler pluton, which is the largest exposed pluton in the arc. Prior to our pilot work there was only a single, imprecise, biotite $^{40}Ar/^{39}Ar$ age on the pluton from the Shaler.

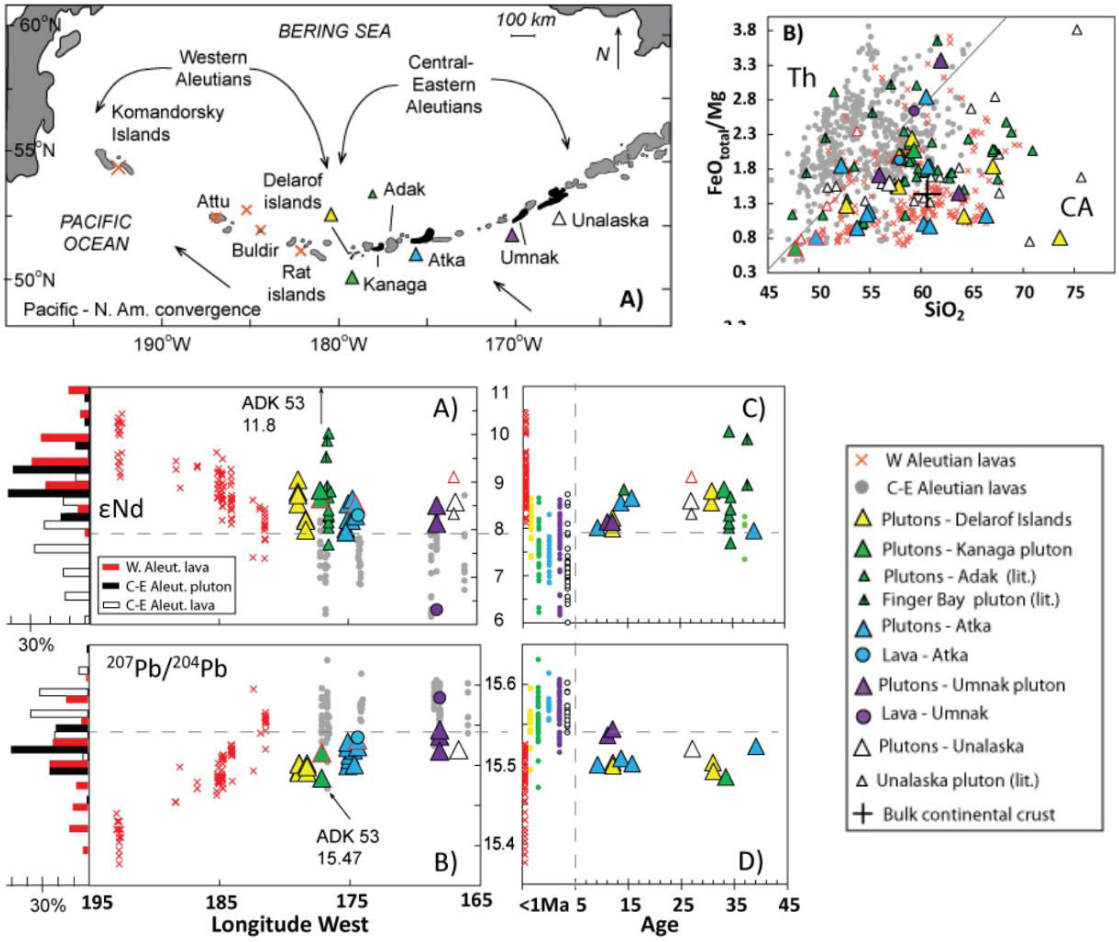

Cai, Y., M.E. Rioux, P.B. Kelemen and S.L. Goldstein, Geochemical and temporal relationships between plutonic and volcanic rocks from the Aleutian arc: A pilot study, Fall Meeting AGU Abstract, V21C-2743, 2013

Cai, Y., M. Rioux, P. Kelemen, S. Goldstein, L. Bolge and A. Kylander-Clark, Distinctly different parental magmas for plutons and lavas in the central Aleutian arc, Fall Meeting AGU Abstract,, V43C-4909, 2014

Cai, Y., M.E. Rioux, P.B. Kelemen, S.L. Goldstein and L. Bolge, Distinctly different parental magmas for calc-alkaline plutons and tholeiitic lavas in the central and eastern Aleutian arc: New isotope, trace element and geochronological data, Earth Planet. Sci. Lett., revised and in review, July 2015

[1]Research reported here was funded by NSF OCE-1144759: "Collaborative Research: Plutons as ingredients for continental crust: Pilot study of the difference between intermediate plutons and lavas in the intra-oceanic Aleutian arc", Peter Kelemen, PI, Steve Goldstein, Sidney Hemming, M. Rioux(UCSB) co-PI's, $150,000, 2011-2014.

[2]Ongoing field work in the is funded by NSF EAR-1457293: "Collaborative Research: Focused Study of Aleutian Plutons and their Host Rocks: Understanding the building blocks of continental crust",P. Kelemen lead PI, $200,000, 2015-17

Seafloor Geodesy

Dave Chadwell

This project (OCE-1249876 "Constraining slip distribution of the Cascadia Subduction Zone Offshore Central Oregon with Seafloor Geodesy") initiates seafloor geodetic measurements of plate motion on the submerged continental slope of the Cascadia Subduction zone to constrain the distribution of slip on the megathrust. One site (NNP1) is located at latitude 44.6 N offshore Newport, Oregon. A second site (NGH1) is located at 46.7 N offshore Grays Harbor, Washington. A third site (JNP1) is farther offshore Newport on the incoming Juan de Fuca plate and measures the present-day convergence rate with North America.

In June 2014, using R/V Thompson and ROV Jason, site JNP1 was re-established with new transponders on permanent benchmarks placed next to old transponders, which were deployed in 2000 and where the position of JNP1 was measured in 2000, 2001, 2002 and 2003. The global position of the old transponders was transferred to the new ones with centimeter resolution. This allows us to continue the time series from 2000 to 2014 and beyond. In September 2014, the GPS-Acoustic Wave Glider was deployed at JNP1 and operated for approximately 60 hours. During that time it self-guided along a nominal circular track within approximately 30 meters of the center of the seafloor transponders. Both the GPS data and acoustic ranging data were collected for 30 of the 60 hours. These data have been processed successfully. Two important results were achieved:

(1) The GPS-Acoustic method from a Wave Glider is viable in the nominally deep waters (JNP1 site is 3000 m deep). The Wave Glider can act as a replacement for high-cost ships in Cascadia and likely other subduction zones (e.g., offshore Alaska). The Wave Glider costs a few dollars a day to operate (i.e., for status and command/control communications using Iridium) compared to several tens-of-thousands of dollars per day for a ship that has dynamic positioning, which is needed to hold station within 30 meters

(2) The re-measurement of the site JNP1 now spans 2000 to 2014, incidentally the longest seafloor position time series anywhere. Preliminary results show that the convergence velocity is comparable to the geologically predicted rate. This supports the hypothesis that creep may be occurring at the CSZ in central Oregon. Scientifically useful data can be collected from a Wave Glider based GPS-Acoustic system.

Also in September 2014, from the R/V Atlantis, the transponders were deployed at sites NNP1 and NGH1. Here, we successfully demonstrated the capability to deploy the transponder package free-fall from the sea surface. In part, the site selection was determined using results from modeling supported by project OCE-1144493 "Potential contributions of Seafloor Geodesy to understanding slip behavior along the Cascadia Subduction Zone". Support for developing the Wave-Glider-based GPS-Acoustic and benchmark is from NSF OTIC program.

As of summer 2015, the Wave Glider will be deployed from a small vessel a few miles offshore Newport and

then directed to sites NNP1, JNP1 and NGH1 to collect the next epoch of positions in the time series.

This project is the first implementation of an autonomous approach to collecting GPS-Acoustic data greatly reducing costs of data collection by no longer relying upon research ships, permanent seafloor benchmarks for horizontal positioning that ensures the time series of positions can be continued into the future, and reuse of commercial seafloor transponders. These three changes in methodology are transformative for GPS-Acoustic seafloor geodesy.

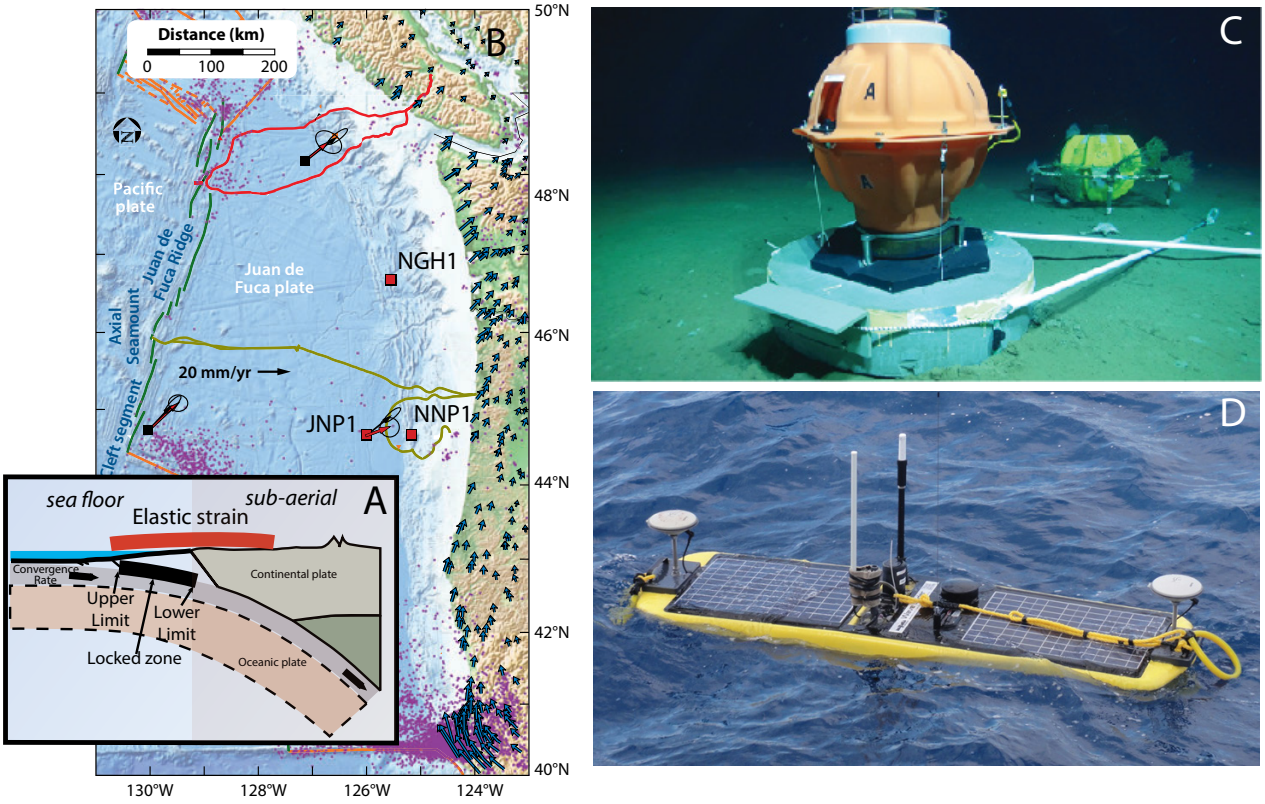

Figure 1. (A) Subduction process showing incoming plate in contact along interface with upper plate which accumulates elastic strain as uplift and contraction. Much of the deformation occurs offshore, highlighting the significance of seafloor measurements in a space geodetic frame to bridge the sub-aerial and marine regions. (B) In 2014, two sites NNP1 and NGH1 were established, the first sites on the seaward slope of Cascadia subduction zone. Also in 2014, site JNP1 offshore Newport was reestablished and its position re-measured. Two earlier GPS-Acoustic sites (black squares) are also shown. Red and black arrows show the GPS-Acoustic and geomagnetically-derived plate motions relative to North America, respectively. (C) Foreground shows new seafloor benchmark with commercial transponder placed approximately 2 m from old (circa 2000) transponder at site offshore Oregon. In June 2014, successfully demonstrated ROV Jason removing and replacing the transponders with millimeter-level repeatability. (D) Wave Glider conFig.d for GPS-Acoustic operations underway at sea. (Note: recovery line has since been rerouted around solar panel.)

The Subduction Margin Carbon Cycle: A Preliminary Assessment of the Distribution Patterns of Multicycle Carbon (NSF, OCE-1144483)

Laurel B. Childress, Neal E. Blair

Over geologic time scales, the burial of organic carbon in sediment plays an important role in global carbon and oxygen cycling. The burial of carbon in active margins is of particular interest for several reasons. When compared with passive margins, active margins are particularly efficient in the burial of organic carbon due to the close proximity of highland sources to marine sedimentary sinks and high sediment transport rates. Of particular interest is the ancient (rock) carbon, also known as kerogen, which comprises 25 – 45% of the organic carbon buried on active margins (Blair et al., 2004). The sequestration of organic carbon on active margins can provide a record of the terrestrial environment spanning millions of years. Differences through time in the volume and nature of exported organic carbon from terrestrial environments have implications for the regulation of the carbon cycle and can also provide information on storm frequency, sea level, precipitation regimes, vegetation type, erosion rate, climate shift, and tectonic movement/uplift. As part of the Alaska and Aleutian Subduction Zone (AASZ) Primary Site of the Subduction Cycles and Deformation (SCD) Initiative, the Southern Alaska Margin represents an ideal active margin system in which to study the relationship between tectonic and glacial changes and organic carbon.

To investigate these relationships, we use samples from Site U1417 of Integrated Ocean Drilling Program (IODP) Expedition 341. Located in the distal portion of the Surveyor Fan and extending into the Miocene, this core allows for the investigation of sedimentary and organic carbon provenance over broad tectonic and

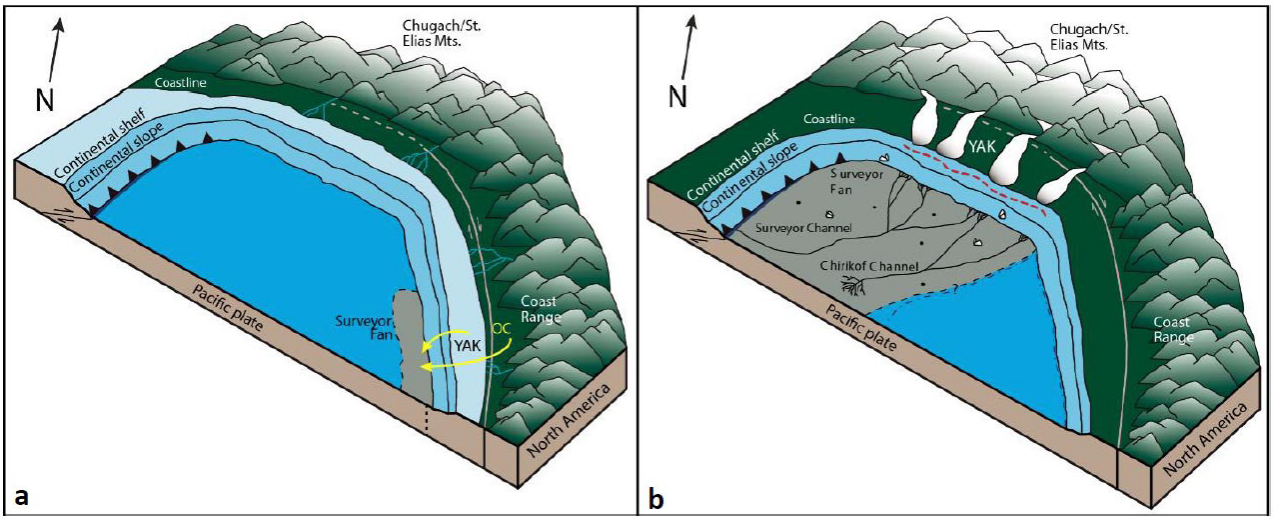

Figure 1. From Reece et al. (2011) (modified), schematic illustration of the southern Alaska margin sedimentary evolution from (a) ~20 Ma, first terrigenous sediment deposition to (b) ~1 Ma, glacial intensification following tidewater glaciation. Yakutat terrane (YAK), organic carbon transport (yellow), glacial restriction to terrestrial carbon export (red dashed line).

climate dynamics. Initial interpretations of core material from Site U1417 suggest at least three distinct sedimentary packages linked to the tectonic convergence of the Yakutat Terrane and the onset of glaciation (Expedition 341 Scientists, 2014). Observations of discrete coal and plant fragments, coupled with initial shipboard measurements, imply good preservation of a traceable terrestrial organic carbon signal at this site (Jaeger et al., 2014). Variations in the volume or nature of kerogen input could indicate an altered terrestrial erosion pattern, which is likely driven by a combination of tectonics/uplift and glacial incision of bedrock in the Southern Alaska Margin. Furthermore, interpretation of organic carbon sources downcore and into the Miocene will be an important component in the source-to-sink study of connections between glaciation, climate change, and tectonic uplift.

To assess connections between the marine and terrestrial environments Site U1417 sediments and rock samples of the Yakutat Terrane, including the Kulthieth, Yakataga, and Poul Creek Formations (Perry et al., 2009), were analyzed for carbon concentration and stable carbon isotope values by elemental analysis – isotope ratio mass spectrometry (EA-IRMS) and compound specific hydrocarbon analyses (polycyclic aromatic hydrocarbons [PAH], alkanes) via coupled pyrolysis-gas chromatography-mass spectrometry (pyr-GCMS). Elemental, isotopic, and hydrocarbon data from rock samples of the Yakutat Terrane provides a valuable constraint on the biogeochemistry of the terrestrial end member(s). Principal component analaysis of data from the three primary terrestrial formations clearly distinguishes the oldest formation (Kulthieth), from the younger, partially reworked formations (Poul Creek, Yakataga) by carbon content and alkane chain length.

Recorded at Site U1417 in the organic carbon record are important changes in the tectonic and erosional dynamics of the landscape. Through the Miocene, sediment and associated organics are erosionally derived from the tectonic uplift and transport of the Yakutat Terrane. During this period, records in the Surveyor Fan are higher in organic carbon concentration and isotopic values are consistent with Yakutat/Coastal Range derived material (Fig. 1a). Following the onset of regional glaciation near the Pliocene-Pleistocene boundary, a dramatic shift in erosional patterns is recorded in the organic carbon record of the Surveyor Fan. As tidewater glaciation progressed to more intensive regional glaciation (Fig. 1b), the source and/or volume of material eroded from the margin transformed. Previous sediment delivery by river systems from the Yakutat Terrane/ Coastal Range sources was restricted by glaciation, greatly diminishing terrestrial organic carbon export and preservation in the Surveyor Fan.

References

Blair, N.E., Leithold, E.L., and Aller, R.C., 2004, From bedrock to burial: The evolution of particulate organic carbon across coupled watershed-continental margin systems: Marine Chemistry, v. 92, p. 141–156, doi: 10.1029/2002JC001467.

Expedition 341 Scientists, 2014, Southern Alaska margin: interactions of tectonics, climate, and sedimentation. IODP Prel. Rept., 341, doi: 10.2204/iodp.pr.341.2014

Jaeger, J.M., Gulick, S.P.S., LeVay, L.J., Asahi, H., Bahlburg, H., Belanger, C.L., Berbel, G.B.B., Childress, L.B., Cowan, E. a., Drab, L., Forwick, M., Fukumura, A., Ge, S., Gupta, S.M., et al., 2014, Site U1417: Proceedings of the Integrated Ocean Drilling Program, v. 341, doi: 10.2204/iodp.proc.341.103.2014.

Perry, S.E., Garver, J.I., and Ridgway, K.D., 2009, Transport of the Yakutat Terrane, Southern Alaska: Evidence from Sediment Petrology and Detrital Zircon Fission-Track and U/Pb Double Dating: The Journal of Geology, v. 117, p. 156–173, doi: 10.1086/596302.

Reece, R.S., Gulick, S.P.S., Horton, B.K., Christeson, G.L., and Worthington, L.L., 2011, Tectonic and climatic influence on the evolution of the Surveyor Fan and Channel system, Gulf of Alaska: Geosphere, v. 7, no. 4, p. 830–844, doi: 10.1130/GES00654.1.

Magmatic Evolution Leading Up to the Modern Aleutian Arc on the Alaska Peninsula

Ron Cole

Project Overview and Relevance to GeoPRISMS Program

The Alaska/Aleutian subduction zone was selected as the highest priority site for the Subduction Cycles and Deformation (SCD) initiative in the NSF GeoPRISMS program. This project, started in May 2015, is a two-year synoptic study that will yield new age and geochemical data on Eocene to Quaternary igneous rocks along the continental segment of the Aleutian arc on the Alaska Peninsula (Fig. 1). The Alaska Peninsula contains over 20 volcanoes with historic activity, five with major eruptions in the past 25 years, and includes Katmai-Novarupta which in 1912 produced the largest eruption of the 20th century. With exposed igneous rocks that span more than 100 million years, the Alaska Peninsula is one of the best places in the world to investigate long-term magmatism and crustal growth along a convergent margin. Yet the Alaska Peninsula is a region where "the availability of isotopic data is poor and insufficient to provide anything beyond the most basic conclusions about geochemical variability in the continental part of the AASZ" (GeoPRISMS, 2013, section 2.2.5). As such, this study aims to capture the inception and growth of the Aleutian arc on the Alaska Peninsula, in concert with the

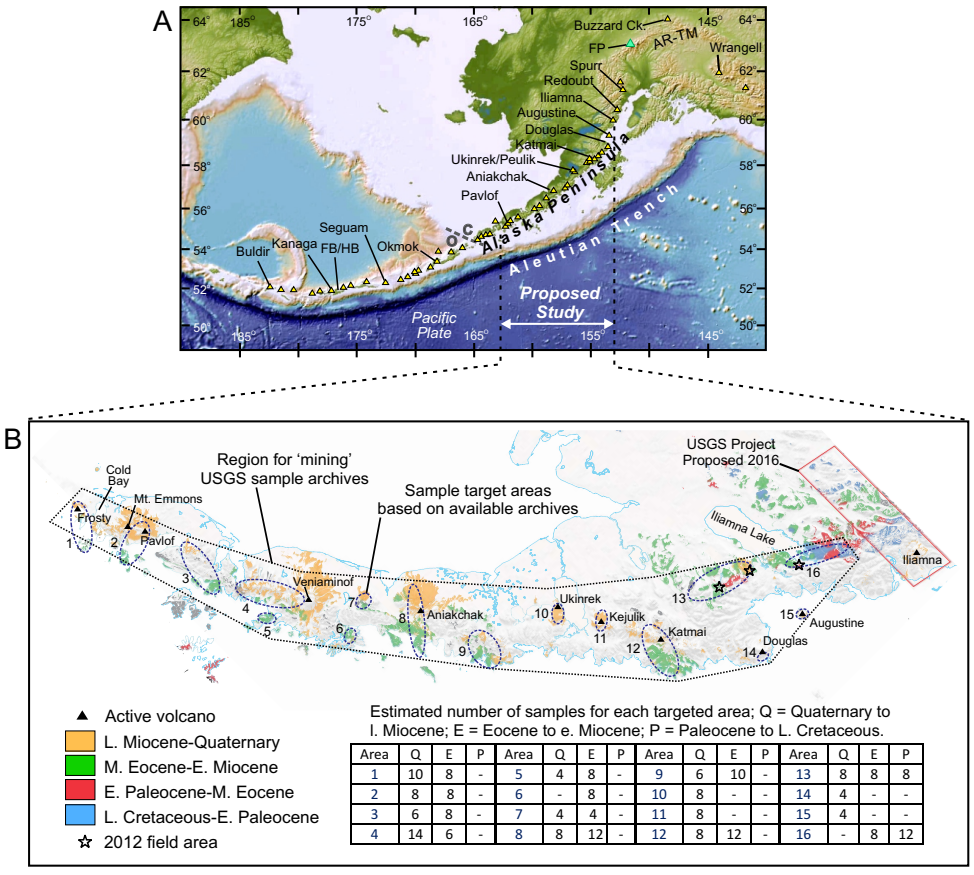

Area	Q	E	P	Area	Q	E	P	Area	Q	E	P	Area	Q	E	P
1	10	8	-	5	4	8	-	9	6	10	-	13	8	8	8
2	8	8	-	6	-	8	-	10	8	-	-	14	4	-	-
3	6	8	-	7	4	4	-	11	8	-	-	15	4	-	-
4	14	6	-	8	8	12	-	12	8	12	-	16	-	8	12

Figure 1. A) Map of south-central Alaska showing proposed study region on the Alaska Peninsula between Cold Bay and Iliamna volcano, Quaternary volcanoes of the Aleutian and Wrangell arcs (yellow triangles), and selected Eocene igneous rocks (green triangles). FP = Foraker pluton; AR-TM = Alaska Range-northern Talkeetna Mt.ains; FB/HB = Finger Bay and Hidden Bay plutons on Adak Island. Thick gray dashed line shows boundary between oceanic (O) and continental (C) crust. B) Simplified geologic map showing Late Cretaceous through Quaternary igneous rocks in the proposed study region. Blue dashed outlines show the targeted sample areas. The table shows the targeted number of samples in each area for major and trace element analyses.

SCD initiatives to "focus on long-term margin evolution and material transfer" and "the growth and evolution of volcanic arcs and continents" (GeoPRISMS, 2013; section 2.1). Results of this project will contribute to the following fundamental objectives as outlined for the GeoPRISMS program: test for along-arc variations of the Aleutian system, document geochemical products of subduction through time, and evaluate the timing and cause(s) of subduction initiation. Three undergraduate students from Allegheny College are participants in this project.

Current Status and Forthcoming Work

To accomplish this regional study, we are using existing samples and data from legacy U.S. Geological Survey mapping projects and recent Alaska Volcano Observatory projects, capitalizing on prior field campaigns. With logistical support from the U.S. Geological Survey, about 250 samples were successfully gathered in May 2015 from the Alaska Geologic Materials Center in Anchorage, covering all of the proposed study areas (Fig. 1). The samples include sets of volcanic and plutonic rocks with a range of mafic to felsic compositions. From these samples, about 200 were cut for thin sections and splits were made for major and trace element analyses. The thin section billets and geochemical splits were sent to commercial labs at the end of June 2015 with thin sections and geochemical data expected by early August 2015. Forthcoming data will include $^{40}Ar/^{39}Ar$ ages, zircon U/Pb ages, zircon Hf-isotopes, and whole-rock Nd-Sr isotopes on subsets of representative samples. We anticipate roughly 80 new radiometric dates and about 40 new isotope samples from this work. The project involves multiple levels of collaboration including: undergraduate institution-research university, academic-government, and an international collaboration. The collaborators include: Dr. Erin Todd (U.S. Geological Survey, Anchorage), Dr. Brian Jicha (University of Wisconsin at Madison), Dr. Jin-Hui Yang (Institute of Geology and Geophysics of the Chinese Academy of Sciences in Beijing), and Dr. Chris Nye (retired, Alaska Volcano Observatory, Fairbanks).

Friction of megathrust gouges at in-situ subduction zone conditions

Sabine den Hartog, Demian Saffer, Chris Marone

The objective of this project is to investigate the frictional behavior of natural subduction megathrust fault rocks representative of a range of in situ conditions from the trench to the downdip reaches of the seismigenic zone (T>350-400 °C). One important and novel aspect of this ongoing effort is the incorporation of a unique suite of natural megathrust fault zone samples obtained by drilling and from extraordinarily well-characterized exhumed subduction paleo-décollements (Fig. 1), thus allowing friction experiments on relevant, natural megathrust materials at their in-situ pressures and temperatures (i.e. in their natural "habitat"). Specifically, the work focuses on:

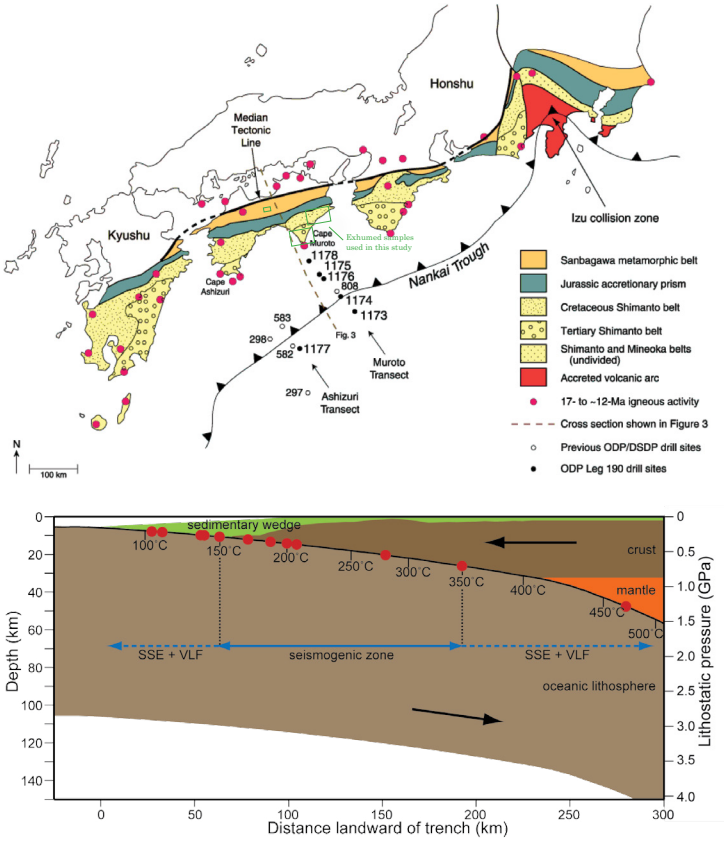

1. Using samples from (1) the Shimanto & Sanbagawa Belts: exhumed subduction fault rocks as analogs for the in situ megathrust at depth; and (2) drillcore from IODP/ODP expeditions in which the shallow plate boundary initiates. These collectively sample conditions along the megathrust from ~50- 450°C;

2. Conducting direct and rotary shearing experiments under hydrothermal conditions to reproduce the in situ P-T conditions for each sample;

3. Evaluating the frictional stability of these megathrust materials in their natural "habitat" in order to better understand the processes and compositional factors controlling the limits of the seismogenic zone; and

4. Linking frictional behavior to micromechanical models in order to extrapolate to other compositions and conditions, and to generalize our results.

Figure 1. A) Map of south-central Alaska showing proposed study region on the Alaska Peninsula between Cold Bay and Iliamna volcano, Quaternary volcanoes of the Aleutian and Wrangell arcs (yellow triangles), and selected Eocene igneous rocks (green triangles). FP = Foraker pluton; AR-TM = Alaska Range-northern Talkeetna Mt.ains; FB/HB = Finger Bay and Hidden Bay plutons on Adak Island. Thick gray dashed line shows boundary between oceanic (O) and continental (C) crust. B) Simplified geologic map showing Late Cretaceous through Quaternary igneous rocks in the proposed study region. Blue dashed outlines show the targeted sample areas. The table shows the targeted number of samples in each area for major and trace element analyses.

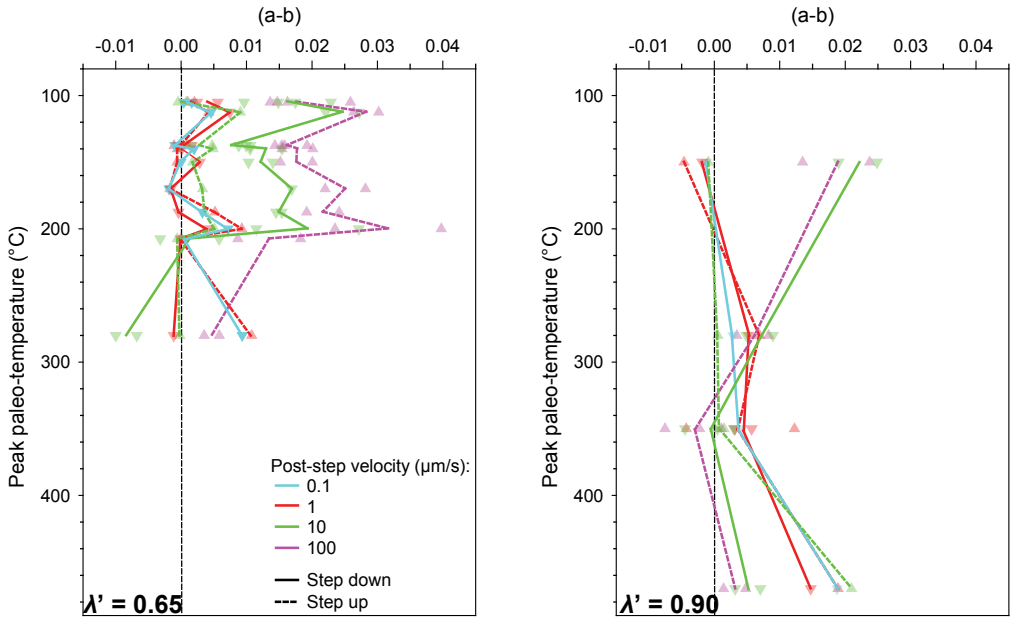

Figure 2. Results of friction experiments, showing frictional rate-dependence (a-b) determined from velocity-stepping tests, as a function of peak burial/past temperature for each sample, for a scenario in which effective stress in the experiments corresponds to a modestly overpressured megathrust (λ = 0.65; panel A), and a highly overpressured megathrust (λ = 0.90; panel B). Colors indicate stepping tests conducted at different sliding velocities (as noted).

The project is thematic in scope, but closely linked to the GeoPRISMS SCD primary site at Alaska, and to the former MARGINS focus Site in SW Japan, through the use of natural subduction zone material collected from the exhumed subduction zone sediments and faults found on Kodiak Island, Alaska, from Shikoku Island, SW Japan, and recovered from the modern Nankai megathrust during ODP Leg 190.

Our results to date are in general agreement with previous studies of synthetic phyllosilicate-quartz mixtures under hydrothermal conditions, in which gouges show stable, velocity-strengthening (or near-neutral) behavior at low temperatures (Regime 1), potentially unstable, velocity-weakening at intermediate temperatures (Regime 2) and velocity-strengthening at the highest temperatures (Regime 3) [den Hartog et al., 2012, 2013]. For our samples, rate-weakening (Regime 2) occurs between ~300-400 °C is experiments that simulate low effective stress conditions (λ = 0.90); this behavior is shifted to lower temperatures under higher effective stress conditions (λ = 0.65), consistent with previous work on synthetic mixtures (Fig. 2). The three-regime behavior is well-explained by a microphysical model in which frictional behavior is governed by a competition between rate-independent frictional slip on aligned phyllosilicates and thermally activated deformation of intervening quartz clasts by pressure solution [den Hartog et al., 2012, 2013].

Our initial data also show that at their in situ conditions, the fault rocks are, overall, nearly rate-neutral (a-b =~0), and exhibit a decrease to rate-weakening behavior (negative (a-b)) for lower slip velocities, and for T between ~250-350°C. The rate weakening of friction is greater at slower slip velocities. This behavior also raises the interesting possibility that these rocks could host slow slip, wherein unstable slip may nucleate at low velocity (where we observe rate weakening), but is damped by rate-strengthening at higher slip velocities [e.g., Rubin, 2011].

This project has also provided extensive mentoring experience for post-doctoral researcher Sabine den Hartog. She has supervised the work of a PhD student on high-temperature friction tests, and has gained broad experience in the lab working with a new direct shear system and supervising a second graduate student in our engineering program.

Publications to date from this project

den Hartog, S.A., Saffer, D.M., Spiers, C.J., The roles of quartz and water in controlling unstable slip in phyllosilicate-rich megathrust fault gouges, Earth, Planets and Space, Frontier Letter, 66:78, doi:10.1186/1880-5981-66-78 (2014).

den Hartog et al., Friction of Megathrust Gouges at in-Situ Subduction Zone Conditions: Strength, Rate Dependence, and Microphysical Mechanisms, AGU Fall Meeting, S11B-4348 (2014).

Hirauchi, K., Yamamoto, Y., den Hartog, S., and Spiers, C., Effect of Metasomatic Alteration on Frictional Behavior of Subduction Megathrusts. AGU Fall Meeting. San Fransisco, CA (2014).

Fisher, D.M., and den Hartog, S. Role of Silica Redistribution in the Rate-State Behavior of Megathrusts: Field Observations and Experimental Results. AGU Fall Meeting. San Francisco, CA (2014).

den Hartog, S.A., A. Niemeijer, D.M. Saffer, C. Marone. Frictional behavior of exhumed subduction zone sediments from the Shimanto Belt, Japan, at in-situ P-T conditions and implications for megathrust seismogenesis. EGU Annual Meeting. Vienna (2014).

References

Den Hartog S.A.M., et al.. New constraints on megathrust slip stability under subduction zone P-T conditions. Earth and Planetary Science Letters 353-354, 240-252 (2012).

Den Hartog S.A.M., et al., Friction on subduction megathrust faults: beyond the illite-muscovite transition. Earth and Planetary Science Letters 373, 8-19 (2013). doi:http://dx.doi.org/10.1016/j.epsl.2013.04.036

Rubin, A. M. Designer friction laws for bimodal slow slip propagation speeds. Geochem. Geophys. Geosyst. 12, Q04007 (2011).

Interseismic Slip Deficit at the Edge of a Locked Patch: Shumagin Islands, Alaska

Jeff Freymueller

This project was funded in spring/summer 2015, and activity so far has focused on obtaining permits needed to go out in the field in late August to early September. Most permits are now in hand, but one key permit appears to be stalled due to personnel changes at the Alaska Maritime National Wildlife Refuge. If permits are obtained in time, we plan to carry out fieldwork in early September.

The primary goal of the project is to begin to study what controls along-strike variations in the behavior of the seismogenic zone, by using a region that shows a substantial lateral variation in this property. The Shumagin segment of the Alaska subduction zone is the ideal location to study the transition from a wide locked region on the plate interface to a dominantly creeping section, and a trench-normal chain of islands in the forearc provides an ideal measurement setting. This data will be used to determine the distribution of slip deficit within the Semidi and Shumagin segments, for the first time providing a detailed view of how the seismogenic zone varies along strike across a locked to creeping transition.

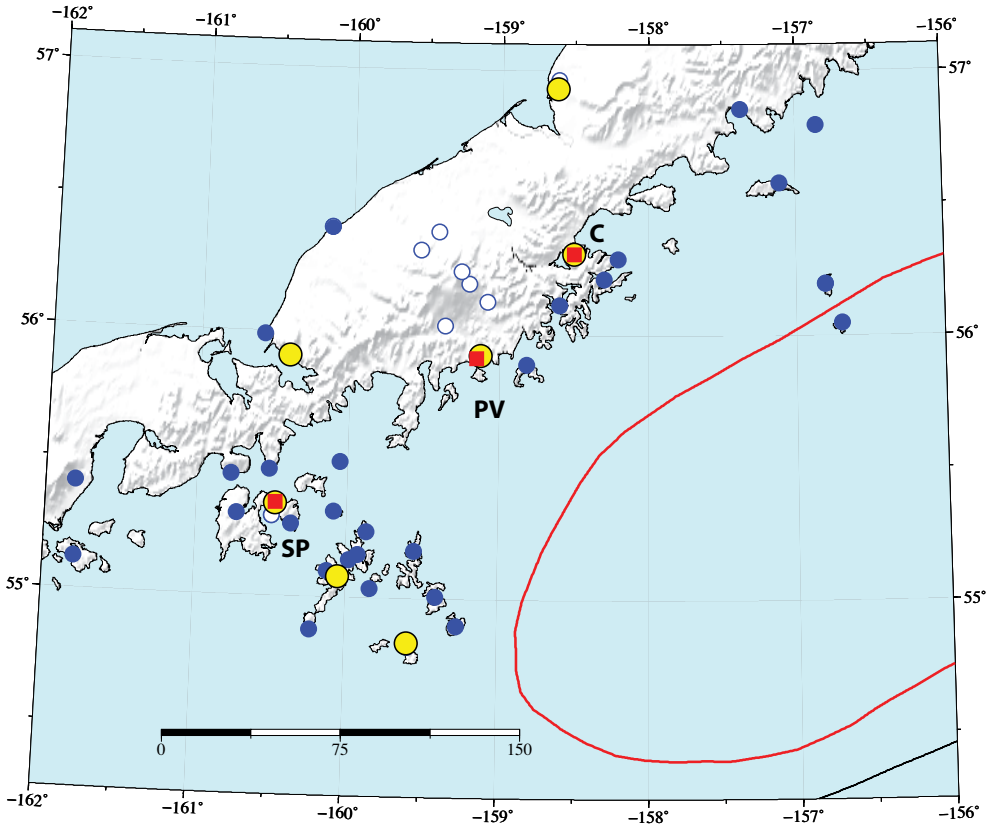

This project will repeat surveys at campaign GPS sites (blue dots) to measure rates of motion from the early 1990s to present. Large yellow dots are continuous GPS sites, and those with red squares have campaign sites nearby that need to be resurveyed for a survey tie to link the measurements together. White dots are other campaign GPS markers that are not planned for repeat surveys (mainly on Veniaminof volcano).

A systematic study of very low frequency earthquakes (VLFEs) in Cascadia

Abhijit Ghosh

Very low frequency earthquakes (VLFEs) are rich in 0.02-0.05 Hz energy and depleted in higher frequencies compared to local earthquakes of similar magnitudes. They are thought to represent a mode of fault slip that is typically associated with slow earthquakes. So far, VLFEs are found in a handful of subduction zones worldwide including Japan and Royuku trench [Ando et al., 2012; Ito et al., 2010]. They are typically located downdip of the seismogenic zone and near the subduction trench as well, making them a critically important event to study the interaction between different frictional/stress regime and near-trench tsunamigenic earthquakes.

VLFEs are recently found in Cascadia during an episodic tremor and slip (ETS) event [Ghosh et al., 2015]. A grid-search moment tensor method is used to obtain the best locations and source parameters. They are located downdip of the seismogenic zone, and migrate alongstrike with tremor activity (see figure). Their focal mechanisms indicate double-couple sources, and are consistent with shallow subduction thrust geometry in the study area. The Mw ranged between 3.3 and 3.7. VLFEs releases more moment than the total cumulative moment released by tremor activity during an entire ETS event. They are providing a unique way to investigate fault heterogeneity, the wide spectrum of fault slip and energy partitioning across the frequency spectrum of seismic radiation during faulting.

References

Ando, M., Tu, H. Kumagai, Y. Yamanaka, and C.-H. Lin (2012), Very low frequency earthquakes along the Ryukyu subduction zone, Geophys. Res. Lett., 39, L04303, doi:10.1029/2011GL050559.

Ghosh, A., E. Huesca-Pérez, E. Brodsky, and Y. Ito (2015), Very low frequency earthquakes in Cascadia migrate with tremor, Geophys. Res. Lett., 42, doi:10.1002/2015GL063286.

Ito, Y., K. Obara, K. Shiomi, S. Sekine, and H. Hirose (2007), Slow earthquakes coincident with episodic tremors and slow slip events, Science, 315, 503-506, doi:10.1126/science.1134454.

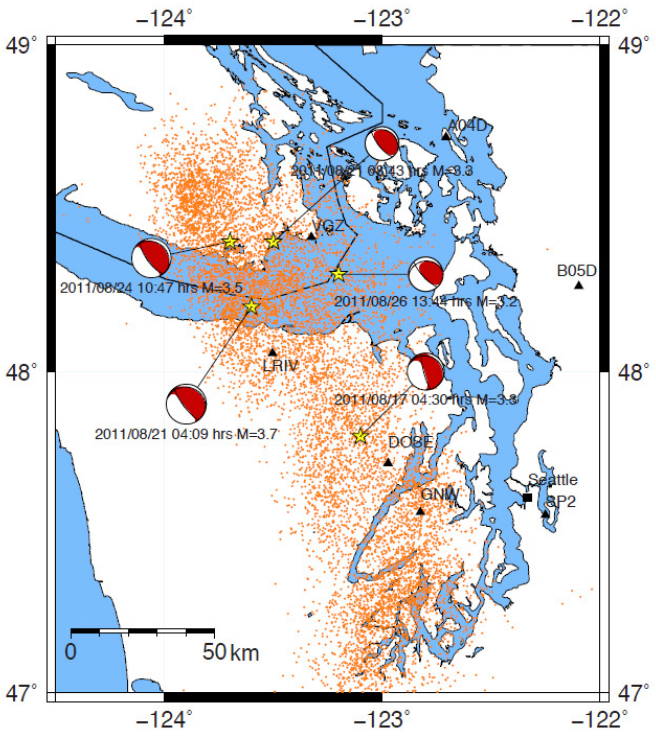

Tremor (orange dots), VLFEs (yellow stars), and their focal mechanisms during August 2011. The date of occurrences and moment of magnitudes (Mw) of VLFEs are noted. Black triangles are the seismic stations used to obtain source parameters of the VLFEs. The tremor catalog is obtained from htt://pnsn.org/tremor. Tremor detected between 31 July and 2 September 2011 is used to show the tremor distribution during the episodic tremor and slip event. Fig. is modified from Ghosh et al., 2015.

An investigation of fault zone hydrogeology in subducting plates

Shuoshuo Han, Nathan Bangs

Faults in the oceanic plate facilitate plate hydration near the trench and provide pathways for fluid migration during subduction. However, the internal structure and hydraulic conductivity of these faults and their variation over time and space have not been examined and quantified. In this recently awarded project, we will investigate the structure and fluid content in the faults within representative segments of the subducting plate using existing multichannel seismic (MCS) data (see Fig.). We will conduct amplitude preserved prestack-depth migration, 2D waveform modeling of fault plane reflections, and fluid flow modeling on the 2D MCS data at Nicaragua, Cascadia, Nankai (offshore southwestern Japan), and Alaska to explore the limits on the fluid content of the fault zones in the oceanic plate seaward of the trench. From these results we will quantitatively assess the hydration state of incoming plate at different subduction zones. We will also conduct seismic attribute analysis of the decollement, near-basement sediment, and basement crustal rocks, and carry out waveform modeling of the faults in the downgoing plate beneath the trench and the slope at Nankai and Costa Rica. The 3D MCS data sets from these two sites will allow us to examine some of the along strike variability in the fluid exchange between the hydrologic systems of upper and lower plate. This study will improve our understanding of the transfer of fluids through subducting plate faults both seaward and landward of the trench, and will provide constraints for future investigations in plate hydration and dehydration zones.

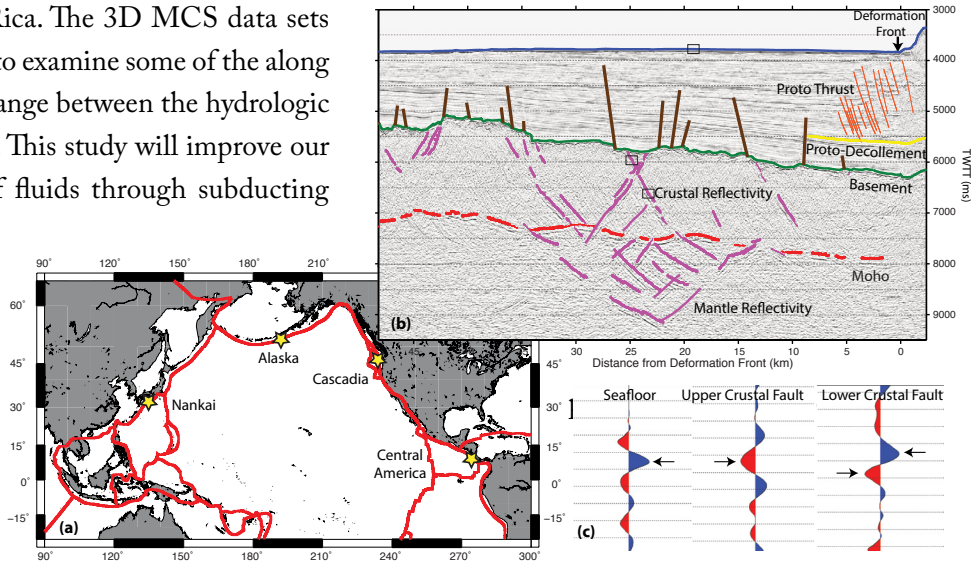

(a) Locations of the four subduction zones: Cascadia, Nankai, Central America, and Alaska (marked by yellow stars) that are to be examined in this study. (b) Prestack-time migrated multichannel seismic image of the incoming Juan de Fuca plate seaward of Cascadia Subduction Zone with interpretation. Seafloor, top of the oceanic crust, and Moho are shown as blue, green, and red lines; Normal faults, protothrust faults, and protodecollement in the sediment section are shown as brown, orange, and yellow lines. Crustal and mantle reflections that are interpreted as fault plane reflections are shown in magenta lines (from Han et al., submitted.) (c) Waveform of the reflections of seafloor, upper crustal fault, and lower crustal fault in the black rectangles of (b).

References

Han, S., Carbotte, S.M., Canales, J.P., Carton, H., Nedimović, M., Gibson, J., Horning, G. Seismic reflection imaging of the Juan de Fuca plate from ridge to trench: new constraints on fault evolution and crustal structure prior to subduction. submitted to, J. Geophys. Res

Experimental Constraints on the Rheology and Seismicity of Subducting Lithosphere and the Slab-Wedge Interface

Greg Hirth, David Goldsby

1. Experiments on antigorite and lawsonite to investige the role of dehydration reactions on fault strength and slip stability at high pressure and temperature conditions.

2. Development of techniques and approaches to control pore-fluid pressure at high P&T conditions and to scale results to natural settings.

3. Experiments and supporting thermal models to investigate dynamic frictional weakening in serpentinite.

Publications

Chernak, L., G. Hirth, Syn-deformational antigorite dehydration produces stable fault slip, Geology, 39, 847-850, doi:10.1130/G31919.1, 2011.

Kohli, A. H., D. L. Goldsby, G. Hirth, T. E. Tullis, Flash weakening of serpentinite at near-seismic slip rates, J. Geophys. Res., doi:10.1029/2010JB007833, 116, B03202, 2011.

Kelemen, P. B., G. Hirth, Reaction-driven cracking during retrograde metamorphism: Olivine hydration and carbonation, Earth and Planet. Sci. Lett., 345-348, 81-89, http://dx.doi.org/10.1016/j.epsl.2012.06.018, 2012.

Hirth, G., S., Guillot, Rheology and tectonic significance of serpentinite, Elements, 9, 107-113, doi:10.2113/gselement.9.2.107, 2013.

Proctor, B., T. M., Mitchell, G. Hirth, D. Goldsby, F. Zorzi, G. Di Toro, Dynamic weakening of serpentinite gouges and bare-surfaces at seismic slip rates, J. Geophys. Res., 119, 8107-8131, doi:10.1002/2014JB011057, 2014.

Auzende, A. -E., J. Escartin, N. P. Walte, S. Guillot, G. Hirth, D. J. Frost, Deformation mechanisms of antigorite serpentinite at subduction zone conditions determed from experimentally and naturally deformed rocks, Earth and Planet. Sci. Lett., 411, 229-240, doi:10.1016/j.epsl.2014.11.053, 2015.

Proctor, B., G. Hirth, Role of pore fluid pressure on transient strenght changes and fabric development during serpentinite dehydration at mantle wedge conditions, Earth and Planet. Sci. Lett., provisionally accepted.

Deformation experiments on antigorite and lawsonite show very different behavior during dehydration: for antigorite, we observe “slow slip” events with little AE (acoustic emission). In contrast, for lawsonite, we observe unstable slip (stick-slip) with prominent AE. These data have implications for understanding the role of dehydration reactions on seismicity in subducting slabs. Results from Okazaki et al., in prep. (Fig. 1).

Motivated by our earlier work (Chernak and Hirth, 2011) - we developed a new technique to drain the pore-fluid produced during dehydration reactions in high P experiments (this is routinely done for low P experiments, by preivously not accomplished for experiments at mantle conditions). The data document the large effect of pore-fluid pressure on the weakening produced during dehydration. Weakening shown for the undrained experiment occurs after <1% reaction. Nonetheless, in all experiments on antigorite, deformation remains stable. Microstructural observations indicate deformation involving a "pressure solution" type process - which is inherently stable. Results from Proctor and Hirth - provisionally accepted (Fig. 2).

To scale these results to natural conditions, we use the ratio of the temperature ramp rate (controlling reaction rate) to the strain rate (or displacement rate). For slabs, this ratio is in the range of 0.1 to C/micron based on thermal models of the subduction interface. Fig. 3 shows that unstable slip observed for lawsonite is insensitive to the ratio. In contrast, the unloading slope observed for the stable antigorite samples scales almost linearly with the ratio of T ramp rate/displacement rate. (Okazaki et al., in prep.).

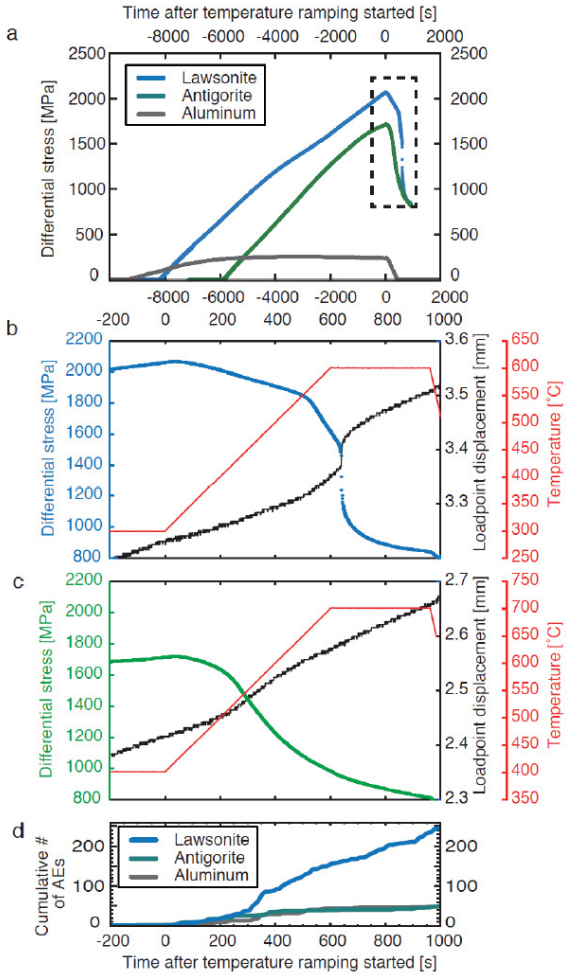

Figure 1.

We also performed experiments to evaluate what happens when rapid slip is imposed onto a fault zone rich in serpentine - for example when an earthquake ruptures into a stably creeping serpentinite patch (Fig. 4). These test document extreme dynamic weakening. The slip velocity at which dynamic weakening is observed increases in the presence of gouge - but for

Figure 2.

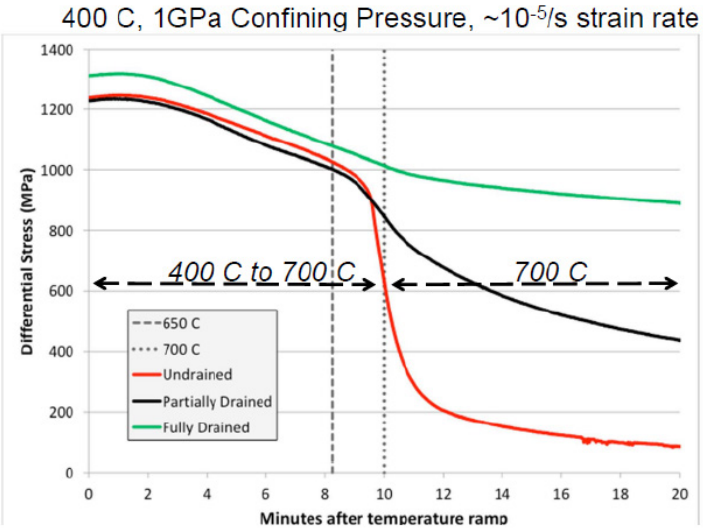

Figure 3.

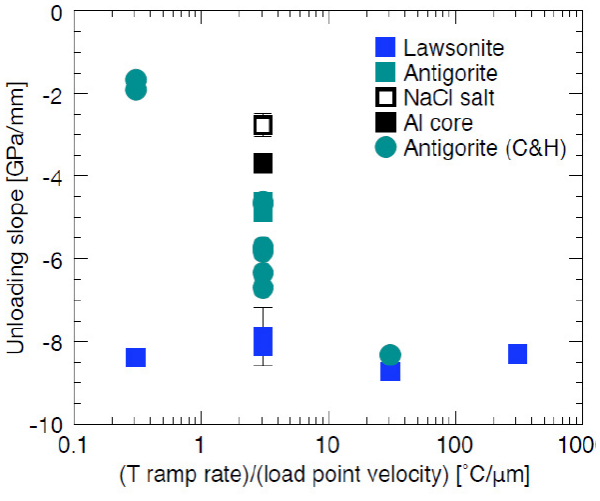

experiments on either bare surfaces or with a layer of gouge - the onset of weakening is well-explained by flash weakening at asperity contacts.

Fig. 4a shows data from small displacement and large displacement experiments. In this case, we observed a significant difference in the "deceleration" path, which reflects the onset of melting for the large displacement tests. The micrograph shows glass and vesicles quenched on the slip surface of a high displacement test. The bottom two plots show comparison to friction models that incorporate flash weakening. Results from Proctor et al., JGR 2014.

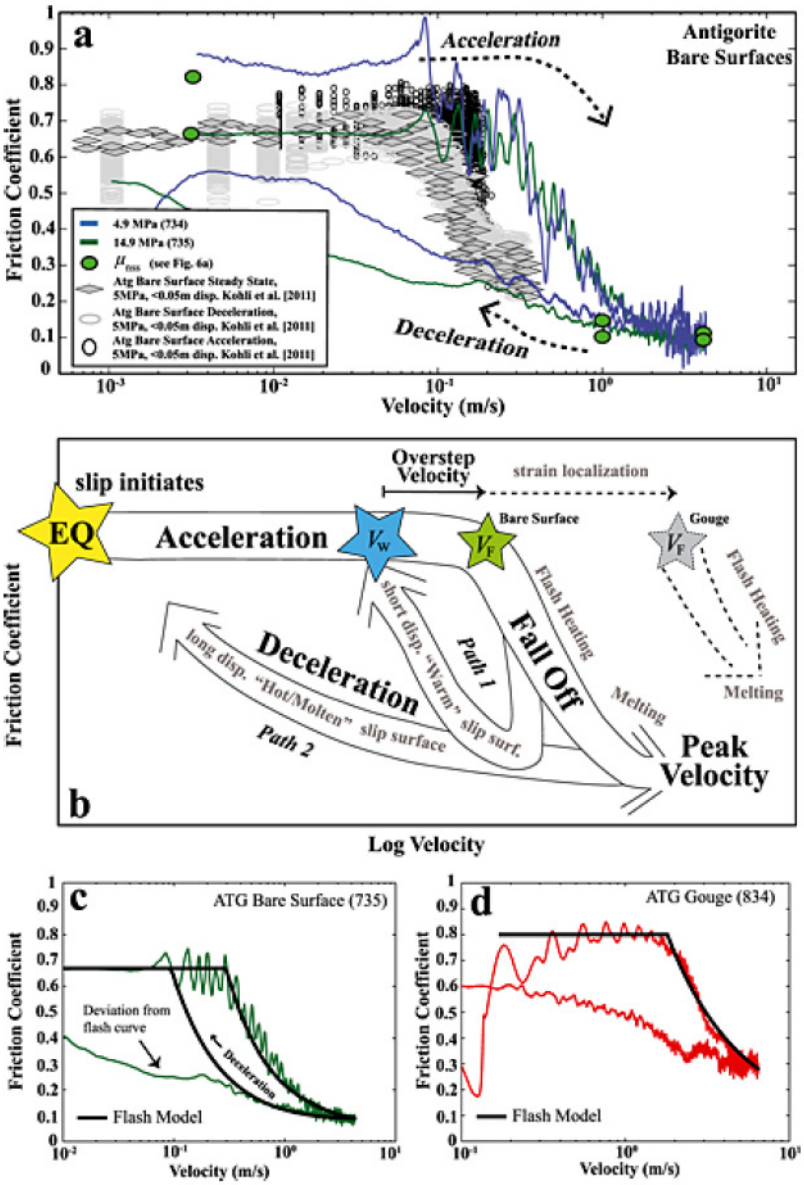

Figure 4.

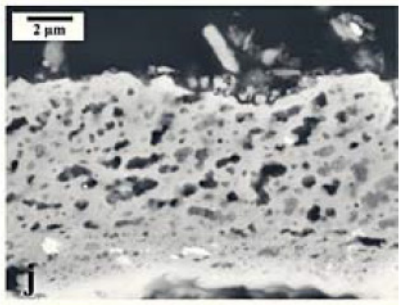

Evolution of the Chemically Diverse Aleutian Island Arc

Brian R. Jicha, Suzanne M. Kay

The Alaska-Aleutian Arc extends for more than 3500 km westward from central Alaska to the Kamchatka Peninsula. The timing of Aleutian Arc inception and subsequent compositional evolution through the initial stages of arc growth are poorly known. Early estimates of Aleutian Arc inception varied from 70 to 40 Ma (e.g., Grow and Atwater, 1970; Scholl et al., 1986), but were based on very little data. Determining precisely how and when the Aleutian Arc began to form was one of the initial goals of this project. By addressing a central question of the GeoPRISMS Program (What are the physical and chemical conditions that control the development of subduction zones, including subduction initiation and the evolution of mature arc systems?), we intended to help link subduction initiation in the Aleutians with similar tectonic events at subduction zones in the western Pacific.

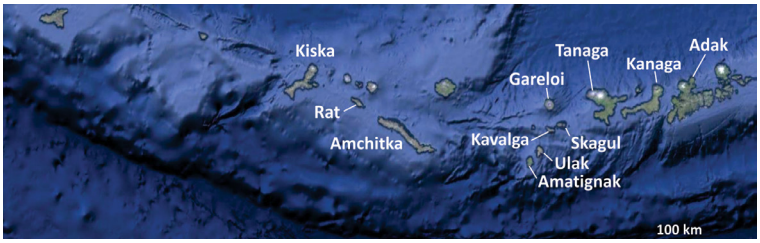

Figure 1. Google Earth image of western Aleutian arc showing islands studied as part of this project.

We identified outcrops on several islands that appeared to have a high probability of providing new limits on the timing of arc inception. Specifically, we focused on mafic 'basement' rocks and intrusives that cut the mafic lavas on Amatignak, Ulak, and Amchitka Islands (Fig. 1). These islands were interpreted to host remnants of the very early growth of the Aleutian Arc prior to northward arc migration. We also aimed to acquire new samples of the Vega Bay formation on Kiska Island and investigate the Finger Bay Volcanics on Adak Island (Rubenstone, 1984; Kay and Kay, 1994) from the extensive sample suite in the collections at Cornell University.

Two reconnaissance field campaigns were conducted in the summer of 2012 and 2013 with the help of the U.S. Fish and Wildlife service vessel M/V Tiglax. In 2012, we (Jicha and Cornell Ph.D. student Ashley Tibbetts) spent two weeks in the central and western Aleutians sampling lavas from Adak, Kiska, Ulak, Amatignak, and Kagalaska islands. Initial $^{40}Ar/^{39}Ar$ incremental heating experiments and geochemical analyses revealed that most of the subaerial samples of the older portions of the central and western Aleutians are < 40 Ma and thus provide little information on subduction initiation. As a result, we refocused our priorities and aimed to constrain the along- and across-arc chemical evolution of the central and western Aleutians over the last 40 Myr of arc history (e.g., Kay and Kay, 1994). In August 2013, we (Jicha, Kay, UW-Madison M.S. student Allen Schaen) conducted another sampling campaign with an emphasis on two regions: a SW-NE trending transect from the southern (Amatignak and Ulak) and central (Kavalga, Ogliuga, and Skagul) Delarof Islands to the Pleistocene-Holocene volcanoes on Gareloi and Tanaga Islands, and the Rat Island to Attu island segment of the western Aleutians (Fig. 1, 2). The first transect is the focus of the Master thesis of UW-Madison student Allen Schaen, which aims to compare the temporal evolution of igneous and tectonic processes in the Delarofs

with similar studies on the Adak Island to the east (e.g., Kay and Kay, 1994) and the Attu Island to the west (e.g., Yogodzinski et al. 1993). The thesis of Tibbetts focuses on the evolution of the Aleutian basement on the islands of Attu, Kiska and Rat.

Overall, we have conducted $^{40}Ar/^{39}Ar$ laser incremental heating experiments and major, trace-element, and Sr and Nd isotope analyses on more than 130 samples. A summary of the findings is provided here:

1. Twenty-two $^{40}Ar/^{39}Ar$ ages reveal that magmatism in the Delarof region spanned 37 million years and was coincident with two arc-wide magmatic flare ups in the late Eocene/early Oligocene and latest Miocene/Pliocene (e.g., Jicha et al., 2006). A significant transition in arc chemistry of the lavas in this region occurs in the Pleistocene where lavas from nearby volcanoes Gareloi and Tanaga exhibit higher sediment signatures (e.g., Th/La) and lower $^{143}Nd/^{144}Nd$ compared to older Delarof Islands closer to the trench. Similar findings from Eocene-Miocene lavas within the western Aleutians from Amchitka to Adak suggest that a sediment melt component was unavailable early in the development of the western Aleutian Arc, but has become more pronounced in the Quaternary.

Figure 2. Allen Schaen (top) and Suzanne Kay (bottom) collecting samples from Rat and Skagul Islands, respectively in 2013.

2. As part of our attempt to understand the evolution of the Central Aleutian arc lower crust we have studied and dated gabbroic composition granulite xenoliths from the Cornell collection of ~200 samples from Kanaga Island. The mafic xenolith suite is composed of plagioclase-clinopyroxene ±orthopyroxene-titanomagnetite-bearing gabbroic xenoliths with rare olivine and adcumulate textures, pyroxene granulites with granoblastic textures, and deformed recrystallized mafic granulites. The variable textures, mineral chemistries and isotopic ratios of these xenoliths show they had experienced a complex history before being incorporated into their ~7 Ma Mg-rich basalt host lava. These mafic xenoliths, along with the ultramafic xenoliths, are interpreted as lower crustal cumulates of basaltic to mafic andesitic arc magmas (e.g., Kay et al., 2014). It is from a mafic two-pyroxene granulite xenolith that we have surprisingly obtained the oldest ages yet reported in the Aleutian arc. This age comes from extremely challenging $^{40}Ar/^{39}Ar$ incremental heating experiments on low K ($\sim An_{68}Or_{0.4}Ab_{31.6}$) plagioclase, which yield complicated spectra, but give a plateau age of 47.8±4.3 Ma. We interpret this age as a time of metamorphism and recrystallization of mafic arc cumulates by younger arc magmas intruding the existing arc crust.

3. Calc-alkaline I-type plutons, like those thought to be major crustal building blocks of continental margins are rare in oceanic island arcs, but are present in the pre-Pliocene record of the Aleutian arc (e.g., Kay et al., 1990). The oldest and most calc-alkaline of these is the ~10 km wide Hidden Bay pluton on Adak Island, which intrudes the early Tertiary Finger Bay Formation. Published K-Ar (Citron et al., 1980) and new $^{40}Ar/^{39}Ar$ and U-Pb zircon ages from 16 gabbro, porphyritic diorite, diorite, granodiorite, leucogranodiorite and aplite units show the pluton evolved from 34.6 to 30.9 Ma in a series of events during a waning magmatic phase. The similarity of chemical analyses of the isotropic gabbros with modern Aleutian high-Al basalts supports minimal evolution of the central Aleutian magmatic source since at least 34 Ma. Mineralogical, trace element, and isotopic evidence suggest the plutonic units largely evolved in the deep crust with final crystallization and

segregation of aplites occurring at shallow levels. Overall, the diorites are cumulates, whereas the volumetrically dominant granodiorites (58-63% SiO_2) along with the leucogranodiorites (67-70% SiO_2) approach melt compositions. The presence of calc-alkaline plutons in the central Aleutian arc by 34 Ma requires stability of pargasitic hornblende, crustal thicknesses approaching those of the modern arc by 34 Ma (~ 37 km on Adak; Janiszewski et al., 2013), a parental magma similar to that from the present-day arc, and a contractional stress regime. Such a scenario requires a very rapid build-up of the Aleutian ridge in the Eocene.

4. Building on the model of Yogodzinski et al. (1993), we have also been investigating the early evolution of the western arc. Our new chemical and $^{40}Ar/^{39}Ar$ analyses show that both the host rock (40.3±0.1 Ma) and the gabbroic units (34.7 to 27.2 Ma) have depleted epsilon Nd values (+9-10.8) and Marianas-like trace element chemistry (e.g., depleted LREEs). These NE-striking units are bordered on the west by 35.6 to 28.8 Ma altered MORB-like pillow lavas, breccias and dikes. Still further west lies a band of MORB-like rhyolite-albite granites with one rhyolite giving a $^{40}Ar/^{39}Ar$ age of 16.2±0.1 Ma. Thus, our new data indicates the oldest units on Attu formed in a Marianas-like arc between 40 and 16 Ma. To our knowledge, similar magmatic rocks are virtually unknown east of Attu. In contrast, the youngest Attu volcanic rocks form an east-west trending band of 8-6 Ma calc-alkaline andesites with lower εNd (+7.5-9.0) that erupted as calc-alkaline volcanism was occurring all along the arc. Combining this change in the strike of magmatic centers on Attu with published paleomagnetic data from Kiska (Minyuk and Stone, 2009) suggests a ~40-50° clockwise rotation of the western Aleutians along with uplift on Attu after 16 Ma and before 8 Ma.

Our ongoing and future efforts for the samples collected in 2012 and 2013 coupled with the vast collection at Cornell University will be focused on quantifying subduction erosion and subsequent northward migration of the arc with time, and evaluating the evolution of the different parts of the central and western Aleutian arc in comparison to the Attu-Rat, Delarof, and Kanaga-Adak segments.

References

Citron, G.P., Kay, R.W., Kay, S.M., Snee, L., and Sutter, J. (1980) Tectonic significance of early Oligocene plutonism on Adak Island, central Aleutian Islands, Alaska, Geology, v. 8, p. 375-379.

Grow, J.A., and Atwater, T. (1970) Mid-Tertiary tectonic transition in the Aleutian arc, Geological Society of America Bulletin, v.81, p. 3715-3722.

Janiszewski, H. A., Abers, G. A., Shillington, D. J. and Calkins, J. A. (2013), Crustal structure along the Aleutian island arc: New insights from receiver functions constrained by active-source data, Geochemistry, Geophys. Geosystems, 14(8), 2977–2992, doi:10.1002/ggge.20211.

Jicha, B.R., Scholl, D.W., Singer, B.S., Yogodzinski, G.M., Kay, S.M. (2006) Revised age of Aleutian Island Arc formation implies high rate of magma production, Geology, v. 34, p. 661-664.

Kay, S.M., and Kay, R.W. (1994) Aleutian magmas in space and time, in Plafker, G., and Berg, H.C., eds., The Geology of Alaska: The Geology of North America, v. G-1: Boulder, Geological Society of America, p. 687-722.

Kay, S.M., R.W. Kay, G.P. Citron and M. Perfit, (1990) Calc-alkaline plutonism in the intra-oceanic Aleutian Arc, Alaska, In Kay, S. M. and Rapela, C.W. (eds.), Plutonism from Antarctica to Alaska, Geological Society of America Special Paper 241, 233-255.

Kay, S.M., Romick, J, Jicha, B.R., Kay, R.W., 2013, Mafic basement xenoliths from Kanaga Island and their implications for Aleutian arc initiation and evolution, Abstract for 2013 Fall Meeting, AGU, San Francisco, CA, V131-06.

Minyuk, P.S., Stone, D.B. (2009) Paleomagnetic determination of paleolatitude and rotation of Bering Island (Komandorsky Islands) Russia: comparison with rotations in the Aleutian Islands and Kamchatka, Stephan Mueller Spec. Publ. Ser., 4, 329–348.

Rubenstone, J.L. (1984) Geology and geochemistry of early Tertiary submarine volcanic rocks of the Aleutian Islands, and their bearing on the development of the Aleutian arc [Ph.D. Thesis]: Ithaca, New York, Cornell University, 350 p.

Scholl, D.W., Vallier, T.L., and Stevenson, A.J. (1986) Terrane accretion, production, and continental growth: a perspective based on the origin and tectonic fate of the Aleutian-Bering Sea region, Geology, v.14, p. 43-47.

Yogodzinski, G.M., Rubenstone, J.L., Kay, S.M., and Kay, R.W. (1993) Magmatic and Tectonic Development of the Western Aleutians: An Oceanic Arc in a Strike-Slip Setting, Journal of Geophysical Research, v. 98, p. 11807-11834.

Heat Flow at the Cascadia Subduction Zone

H. Paul Johnson, Evan A. Solomon, Robert N. Harris

This currently active research grant has the objective of determining the heat flow and fluid flux regime on the Washington State portion of the Cascadia Subduction Zone. The underlying goal of the program is to determine the temperature of the decollement (tectonic plate slip zone), a critical parameter in identifying the potential slip area for the next large megathrust (Magnitude 9) earthquake in the Pacific Northwest. Determining the intersection points of critical isotherms with the decollement will inform temperature-dependent numerical models of the up- and down-slope boundaries of the region where inter-seismic stress is stored.

A field program on the R/V Atlantis, using the Remotely Operated Vehicle Jason II was supported by this GeoPRISMS grant in August, 2013. This 3-week cruise successfully collected an unusual aMt. of heat flow and fluid flux measurements on a corridor of the Washington margin off Greys Harbor, WA. At the present time, initial processing of all of the heat flow, fluid flux and geochemical data has been completed, and we are now at the penultimate stage of integrating the diverse data sets and developing numerical models of both fluid circulation and isotherm distribution within the sedimentary wedge. In addition to the heat flow and fluid flux data, we are also processing acoustic backscatter data from the R/V Atlantis EM302 swath bathymetry system to identify areas of high intensity reflections due to authigenic carbonate deposition. These sites represent areas of the Cascadia sedimentary wedge where fluid and methane emissions have been persistent over thousands of years, and will provide a geological history of the evolving hydrologic system within the accretionary prism over time.

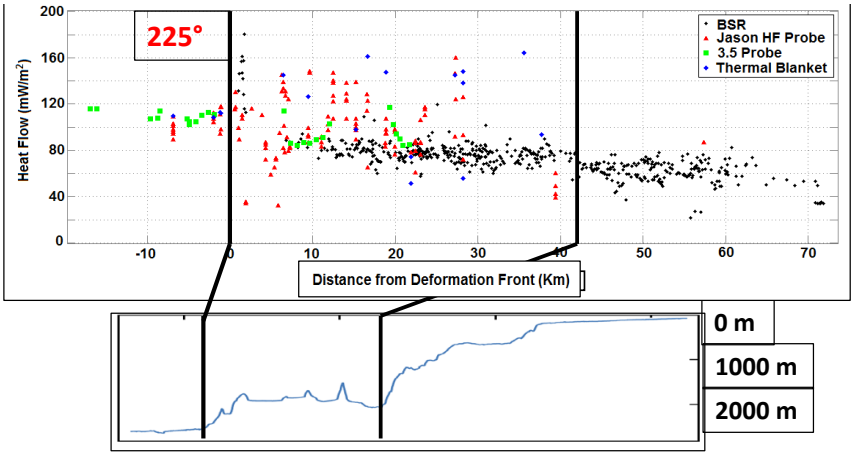

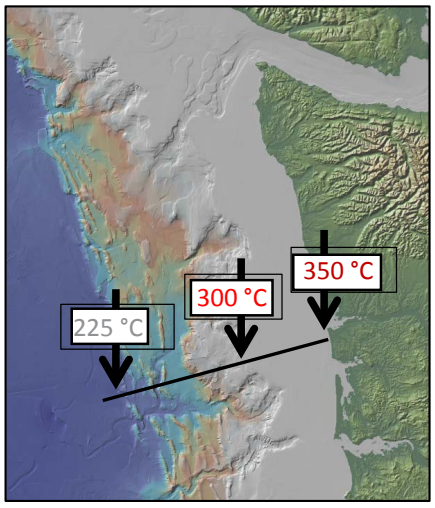

Top: Profile of compiled heat flow data from the August, 2013 GeoPRISMS cruise. Black dots are heat flow from Bottom Simulating Reflectors from the Langseth 2012 cruise over the same margin. Red triangles are Jason HF probe measurements, green squares are the OSU long HF probe, and blue dots are UW thermal blankets. Temperature of the incoming plate west of the decollement is 225°C. Middle: bathymetric profile of the margin where the heat flow data were acquired. Bottom, temperatures of the decollement beneath the accretionary wedge of sediments.

Publications and Talks

Johnson, H. Paul, Evan A. Solomon, Robert N. Harris, Marie S. Salmi, and Richard D. Berg. "Heat Flow and Fluid Flux in Cascadia's Seismogenic Zone." Eos, Transactions American Geophysical Union 94, no. 48 (2013): 457-458.

Johnson, H. Paul, Evan Solomon, Robert Harris, Marie Salmi and Richard Berg; A Geophysical and Hydrogeochemical Survey of the Cascadia Subduction Zone, GeoPRISMS Newsletter Issue No. 32 Spring 2014

Hautala, Susan L., Evan A. Solomon, H. Paul Johnson, Robert N. Harris, and Una K. Miller. "Dissociation of Cascadia margin gas hydrates in response to contemporary ocean warming." Geophysical Research Letters (2014).

Homola, Kira, H. Paul Johnson, and Casey Hearn. "In situ measurements of thermal diffusivity in sediments of the methane-rich zone of Cascadia Margin, NE Pacific Ocean." Elementa: Science of the Anthropocene 3, no. 1 (2015)

Johnson, H. Paul, Una Miller, Marie Salmi, Evan Solomon, Analysis of Bubble Plume Distributions to Evaluate Methane Hydrate Decomposition on the Continental Slope submitted to G-cubed June, 2015.

Atwater, Brian F., Bobb Carson, Gary B. Griggs, H. Paul Johnson, and Marie S. Salmi*. "Rethinking turbidite paleoseismology along the Cascadia subduction zone." Geology 42, no. 9 (2014): 827-830.

Salmi, M. and U. Miller. The Silent Subduction Zone. Ocean Shores Community Environmental Group Meeting. May 1st, 2014. Galway Bay Community Center. Quinault Tribal Nation outreach talk.

Salmi, M., H.P Johnson, E. Solomon, R. Harris. 2014. Heat Flow Survey on the Washington Margin of the Cascadia Subduction Zone. AOGS Annual Meeting, July 28 - August 1st, 2014. Sapporo, Japan

Salmi, M., H.P. Johnson, E.A. Solomon, R.N. Harris. 2014. Heat Flow Survey on the Washington Margin of the Cascadia Subduction Zone. AGU Fall Meeting, 15-19 December 2014, San Francisco, CA

Berg, R.D., Solomon, E.A., Johnson, H.P., Culling, D., Harris, R.N., 2014. Fluid and solute fluxes from the deformation to the upper slope at the Cascadia margin. AGU Fall Meeting, 15-19 December 2014, San Francisco.

The Tadpole Zone: High temperatures and density filtering of Indian continental crust along the Moho beneath southern Tibet

Peter B. Kelemen, Bradley R. Hacker

Supported in part by past and present GeoPRISMS and related grants[1], we are preparing a paper outlining the following hypothesis.

Data indicate that the thick middle and lower continental crust of the central southern Lhasa block is hot and largely felsic. These data include: (1) the presence of 10–18 Ma volcanic rocks including primitive andesites and dacites formed by interaction between crustal melts and mantle peridotite, (2) thermobarometry on xenoliths in a 12.7 Ma dyke indicating temperatures greater than 1000°C in the lowermost crust (2.6 GPa), (3) low seismic wavespeeds (VP < 7 km/s) characterize the upper 70 km of the crust, (4) an abrupt transition from low to high VP/VS ratios interpreted as the α/β quartz transition at 50 km depth and ~ 950°C, and (5) high wavespeeds (VP > 7.5 km/s) between 70 and 85 km depth. Though these data indicate that the Moho has been at ~ 1000°C or more since the Miocene, there are also (6) earthquakes at Moho depths in this region.

The well-defined Moho at ~ 80 km depth throughout this region may be due to the transition from garnet granulite to eclogite facies in the imbricated Indian crust subducting beneath Tibet. Along this horizon, as the Indian continental crust continues to be thrust northward beneath Tibet, mafic lithologies become dense eclogites that form diapirs sinking into the upper mantle, while buoyant, felsic lithologies remain in a steadily thickening crust. High temperatures close to the Moho arise from a combination of radioactive heating of thick, felsic crust and upward return flow of mantle material around descending eclogite diapirs. There is a belt of primitive, potassic magmas (Mg/(Mg+Fe) of 0.6 to 0.7) extending for ~ 1500 km, 0 to 100 km north of the Indus-Tsangpo Suture Zone, with an isotopic component derived from continental crust. These magmas probably formed via chemical interaction between mantle peridotite and partial melts of foundering eclogite. Earthquakes at Moho depth occur at high temperature, perhaps due to localized, non-Newtonian deformation coupled with thermal runaway in compositionally weak layers and/or the margins of diapirs.

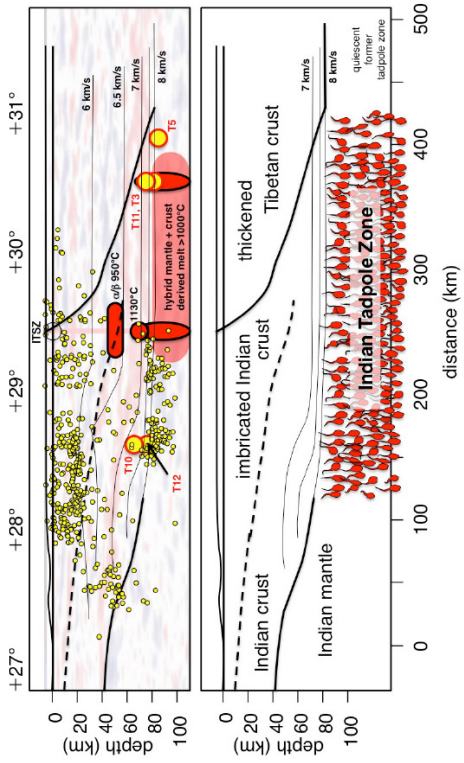

[1]*NSF OCE-1144759: "Collaborative Research: Plutons as ingredients for continental crust: Pilot study of the difference between intermediate plutons and lavas in the intra-oceanic Aleutian arc", Kelemen, PI, S Goldstein, S Hemming, M Rioux (UCSB) co-PI's; NSF OCE-1358091/1356132, Marine Geology and Geophysics Program, "Advanced modeling for understanding fluid & magma migration in subduction zones", C Wilson, lead PI, P Kelemen, M Spiegelman & P van Keken (U. Michigan) co-PI's; NSF EAR-1457293: "Collaborative Research: Focused Study of Aleutian Plutons and their Host Rocks: Understanding the building blocks of continental crust",P. Kelemen lead PI; NSF-EAR-0742451, "Collaborative Research: Element Recycling from UHP Metasediments: Evidence and Consequences" P Kelemen and B Hacker, PI's; NSF EAR-1219942, "What Determines Whether the Deep Continental Crust Flows [or not]?" B Hacker & ARC Kylander-Clark*

Reevaluating carbon fluxes in subduction zones: What goes down, mostly comes up

Peter B. Kelemen, Craig E. Manning

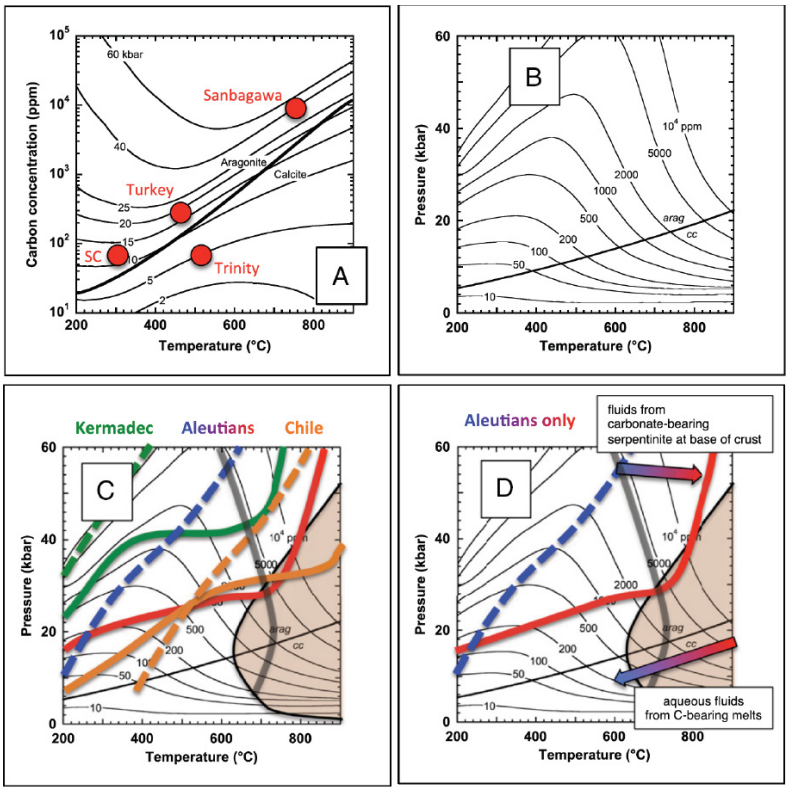

We recently reviewed carbon fluxes in subduction zones (Kelemen & Manning 2015), supported in part by grants from GeoPRISMS and other sources . Carbon fluxes in subduction zones can be better constrained by including new estimates of carbon concentration in subducting mantle peridotites, consideration of carbonate solubility in aqueous fluid along subduction geotherms (Caciagli & Manning 2008; Dolejs & Manning 2010; Manning et al. 2013; Manning 2013), and diapirism of carbon-bearing metasediments (e.g., Kelemen et al. 2003; Behn et al. 2011).

Whereas previous studies concluded that about half the subducting carbon is returned to the convecting mantle, we find that relatively little carbon may be recycled. If so, input from subduction zones into the overlying plate is larger than output from arc volcanoes plus diffuse venting, and substantial quantities of carbon are stored in the mantle lithosphere and crust. Also, if the subduction zone carbon cycle is nearly closed on time scales of 5–10 Ma, then the carbon content of the mantle lithosphere + crust + ocean + atmosphere must be increasing. Such an increase is consistent with inferences from noble gas data. Carbon in diamonds, which may have been recycled into the convecting mantle, is a small fraction of the global carbon inventory.

[1]*NSF OCE-1144759: "Collaborative Research: Plutons as ingredients for continental crust: Pilot study of the difference between intermediate plutons and lavas in the intra-oceanic Aleutian arc", Kelemen, PI, S Goldstein, S Hemming, M Rioux (UCSB) co-PI's; NSF OCE-1358091/1356132, Marine Geology and Geophysics Program, "Advanced modeling for understanding fluid & magma migration in subduction zones", C Wilson, lead PI, P Kelemen, M Spiegelman & P van Keken (U. Michigan) co-PI's; NSF EAR-1457293: "Collaborative Research: Focused Study of Aleutian Plutons and their Host Rocks: Understanding the building blocks of continental crust",P. Kelemen lead PI; NSF-EAR-0742451, "Collaborative Research: Element Recycling from UHP Metasediments: Evidence and Consequences" P Kelemen and B Hacker, PI's; NSF EAR-1219942, "What Determines Whether the Deep Continental Crust Flows [or not]?" B Hacker & ARC Kylander-Clark*

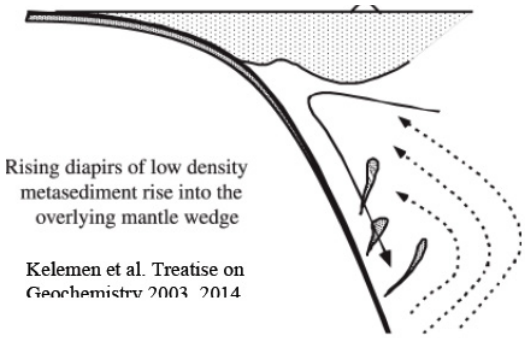

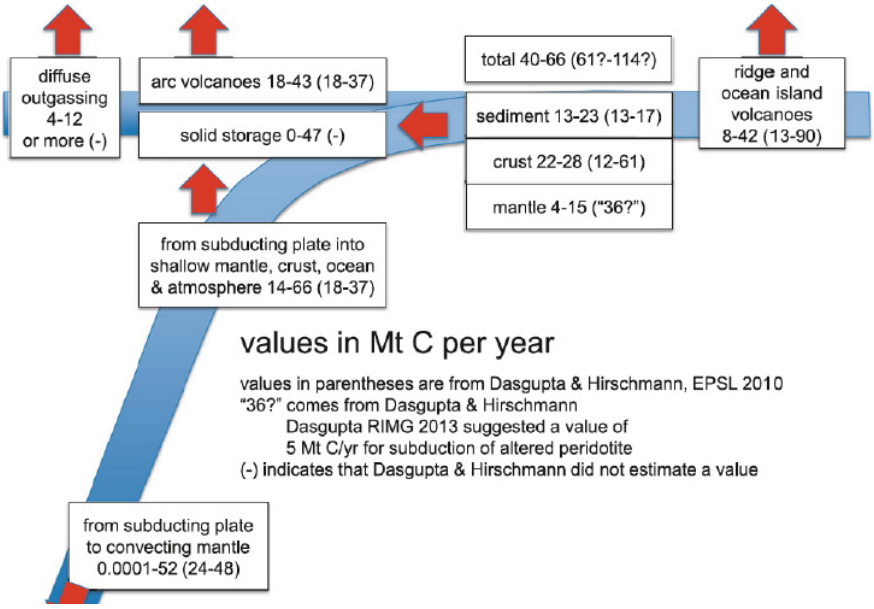

References

Behn, M.D., P.B. Kelemen, G. Hirth, B.R. Hacker, and H.-J. Massonne, Diapirs as the source of the sediment signature in arc lavas, Nature Geoscience 4, 642-646, 2011.

Caciagli NC, Manning CE (2003) The solubility of calcite in water at 6–16 kbar and 500–800 °C. Contrib Mineral Petrol 146:275–285.

Dolejs, D., and C. E. Manning (2010), Thermodynamic model for mineral solubility in aqueous fluids: Theory, calibration and application to model fluid-flow systems, Geofluids, 10, 20-40

Kelemen, P.B. and C.E. Manning, Re-evaluating carbon fluxes in subduction zones: What goes down, mostly comes up, Proc. National Acad. Science, published ahead of print June 5, 2015, doi:10.1073/pnas.1507889112, 2015.

Kelemen, P.B., K. Hanghøj, and A.R. Greene, One view of the geochemistry of subduction-related magmatic arcs with an emphasis on primitive andesite and lower crust, in The Crust, (R.L. Rudnick, ed.), Vol. 3, Treatise on Geochemistry, (H.D. Holland and K.K. Turekian, eds.), Elsevier-Pergamon, Oxford, 593-659, 2003.

Manning CE (2013) Thermodynamic modeling of fluid-rock interaction at mid-crustal to upper mantle conditions. Rev Mineral Geochem 76:135–164.

Manning CE, Shock EL, Sverjensky DA (2013) The chemistry of carbon in aqueous fluids at crustal and upper-mantle conditions: Experimental and theoretical constraints. Rev Mineral Geochem 75:109–148

Collaborative Research: The role of oxygen fugacity in calc-alkaline differentiation and the creation of continental crust at the Aleutian arc

Katherine A. Kelley, Elizabeth Cottrell, Mattia Pistone, Matthew Jackson

Among the key characteristics shared by bulk continental crust and some subduction zone magmas is calc-alkaline affinity, a rapid draw-down in Fe concentration early in a magma's cooling history. Resolving the key roles that H_2O, fO_2, and magmatic bulk composition play in controlling calc-alkaline trends will have important implications for models of how Earth's continents initially formed and have grown through time. This project combines study of volatile contents, radiogenic isotopes, and oxidation conditions of melt inclusions from natural Aleutian arc magmas, which is paired with an experimental study of the independent controls of H_2O and fO_2 on phase equilibria of Aleutian magmas. Our first major results focus on quantifying the effects of H2O and fO_2 on magmatic phase appearance, and assessing the relationship between H_2O, fO_2, and calc-alkaline affinity of natural Aleutian magmas. In fall 2015, we will venture into the field through the NSF-sponsored shared platform for Aleutians research to collect new samples of the most strongly cal-alkaline Aleutians magmas.

Correlations both among global magmas and within the Aleutians suggest fO_2, H_2O, and Fe-depletion (i.e., calc-alkaline affinity) are linked at arcs • Phase equilibria experiments suggest that fO_2 is the main control on oxide vs. silicate crystallization, and early oxide saturation is linked to Fe-depletion in magmas.

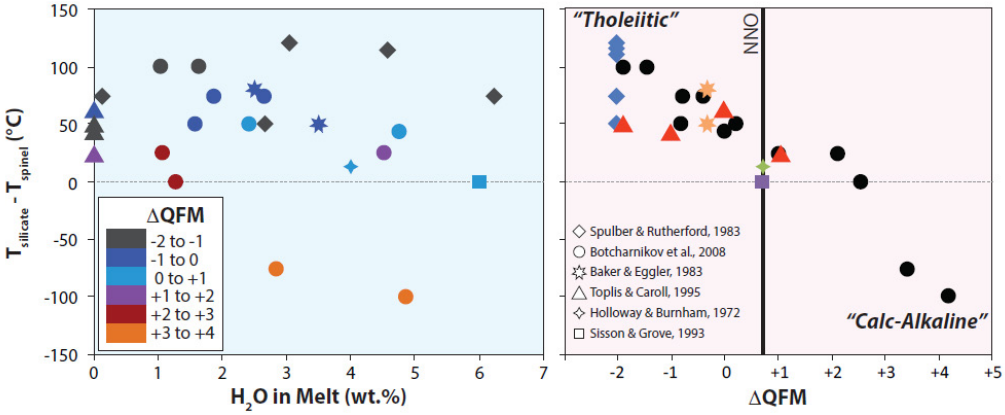

Compilation of experimental data showing how the suppression or enhancement of magnetite relative to silicates varies as a function of H_2O and oxygen fugacity. No trend is apparent with magmatic H_2O content, but there is a strong correlation with oxygen fugacity. Moreover, experimental liquids follow a tholeeitic trend in cases where silicates crystallize early relative to magnetite, whereas liquids follow a calc-alkaline trend when magnetite appears early. Redox conditions more oxidized than the Ni-NiO (NNO) solid oxygen buffer are apparently required to generate a true Fe-depletion trend in experimental liquids

Published Abstracts

Kelley, K. A., E. Cottrell, M. N. Brounce, and Z. Gentes (2014), Roles of magmatic oxygen fugacity and water content in generating signatures of continental crust in the Alaska-Aleutian arc, EOS Transactions AGU, presented at 2014 Fall Meeting, AGU, San Francisco, Calif., 15-19 Dec., T11A-4531.

Ferm GeoPRISMS: Retreating Glacier in Homogeneous Valley

Peter Koons (with contributions from Sean Birkel)

Reduction of ice buttressing constitutes the major influence of glacier wasting. Over steepening at the sides along the valley floor by excavation during advance, together with concomitant reduction of strength due to strain damage, causes valley walls to fail immediately on shallow and deep-seated failure planes, consequently, contributing a large sediment pulse associated with glacial retreat. In the high stress, post -buttress environment, time-dependent strength reduction and pore pressure fluctuation typically leads to landslide decay over centuries following glacier retreat. These regions are particularly susceptible to failure from strength/stress ratio (Σ/τ) perturbations from seismic induced dynamic stress contributions.

Advancing Glacier in a Fault Damage Zone controlled valley (Model Fairweather Fault)

An advancing glacier produces a transient perturbation to the stress state of the bedrock with an increase at the snout of down-valley normal and shear component stresses (σ_{yy}, τ_{yz}) and a steep gradient in the vertical stress (σ_{zz}), both causing a decrease in strength/stress ratio (Σ/τ). Along the valley sides, the transient stress pulse is influenced by the increase in Σ/τ due to the glacial buttress, but, concurrently, valley-parallel shear introduces σ_{yx} and σ_{yy}, reducing Σ/τ. The net Σ/τ pattern is one of failure ($\Sigma/\tau<1$) at the snout where concentrations of glacier induced stresses coincide with topographic stress maxima in a region already close to failure. The result of this stress concentration is to allow significant bulldozing/excavation in front of the snout. This is accompanied by stability on the lower lateral sides of the glacier ($\Sigma/\tau>1$), and failure ($\Sigma/\tau<1$) at the upper margins of the glacial sides.

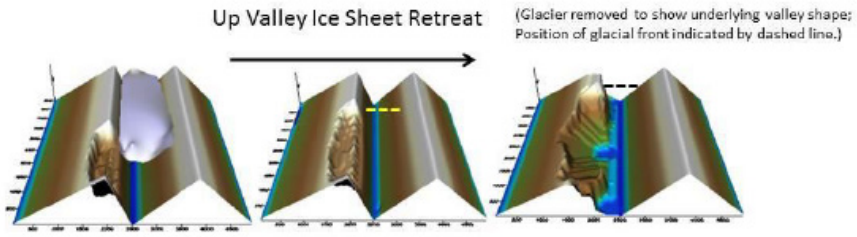

Retreating Glacier
Notes: Reduction of ice buttressing constitutes the major influence of glacier wasting. Over-steepening at the sides along the valley floor by excavation during advance, together with concomitant reduction of strength due to strain damage, causes valley walls to fail immediately on shallow and deep-seated failure planes. In the high stress, post -buttress environment, time-dependent strength reduction and pore pressure fluctuation typically leads to landslide decay over centuries following glacier retreat. These regions are particularly susceptible to failure from perturbations to the local Strength/Stress ratio from seismic-induced dynamic stress contributions (co-seismic landslides).

Advancing glacier flowing from back to front along weak fault damage, vertical zone ~ Fairweather (*glacier removed to expose land surface*)

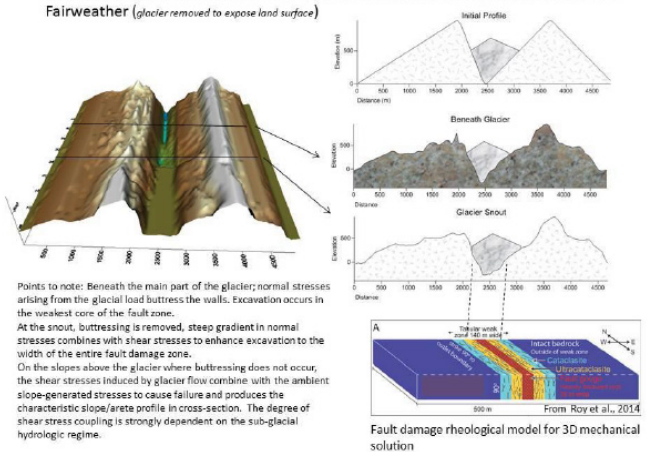

Points to note: Beneath the main part of the glacier; normal stresses arising from the glacial load buttress the walls. Excavation occurs in the weakest core of the fault zone.
At the snout, buttressing is removed, steep gradient in normal stresses combines with shear stresses to enhance excavation to the width of the entire fault damage zone.
On the slopes above the glacier where buttressing does not occur, the shear stresses induced by glacier flow combine with the ambient slope-generated stresses to cause failure and produces the characteristic slope/arete profile in cross-section. The degree of shear stress coupling is strongly dependent on the sub-glacial hydrologic regime.

Fault damage rheological model for 3D mechanical solution

Some Background to FERM: Current models of Earth

surface evolution and of Earth geodynamics have been stunningly successful in producing a general description of topographic development as partial functions of fluid transport and topographic slope. These standard models, which focus on the change of elevation (h) with time (dh/dt), rely on fluid-related erosion laws (fluvial, glacial, coastal) to apportion some fraction of channel incision as a function of fluid flux, with hillslope expressions based primarily on linear and non-linear diffusion laws. A basic limitation in the application of these traditional models arises from the use of multiple, different physical descriptions for the response of any Earth element depending upon the ambient erosion regime. For instance, terrain influenced by fluvial processes is modeled by a different set of mechanics than the same terrain influenced by a topographic slope, or by glacial, or by coastal processes, which in turn differ from the widely-used tectonic descriptions for that same Earth element.

By recognizing that an element of Earth consists of the same material, independently of what processes act on it, we draw together the various physical descriptions of surface evolution and tectonic evolution into a single, Earth-centric framework, the Failure Earth Response Model (FERM), that unifies the physical description of dynamics within and between the geomorphic

and tectonic domains. FERM is constructed on the two, basic assumptions about the three-dimensional stress state and rheological memory:

I) Material displacement, whether tectonic or geomorphic in origin, at or below Earth's surface, is driven by local forces overcoming local resistance;

II) Large displacements, whether tectonic or geomorphic in origin, irreversibly alter Earth material properties enhancing a long term strain memory mapped into the topography. i.e. the earth is a memory material

The FERM formulation with its explicit inclusion of material history, geomorphic and tectonic processes, including seismic accelerations and pore pressure fluctuations, allows closer examination of tectonic:geomorphic interactions and predicts evolutionary trends that differ significantly from the traditional approach.

Contributions from Sean Birkel

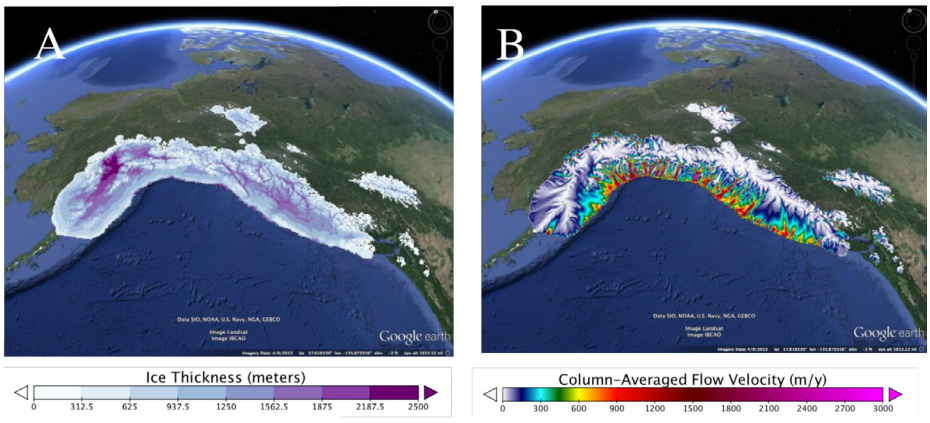

Figure 1. University of Maine Ice Sheet Model (UMISM) simulation of the Cordilleran Ice Sheet during the Last Glacial Maximum (domain excludes the Laurentide Ice Sheet) shown in Google Earth. UMISM calculates both steady state and transient solutions and produces output parameters including ice thickness (A), column-averaged flow velocity (B), basal water production, and bed depression that can be used to derive erosion rates and sediment transport. UMISM solves ice flow using a shallow-ice approximation that ignores longitudinal stresses. Solutions are generally valid to ~ 1 km horizontal grid resolution. The benefit to shallow ice models is that they run orders of magnitude faster than those that incorporate full Stokes solutions. Our strategy is to use UMISM for big picture problem solving, and then to focus on areas of interest using higher order solutions that are possible in software such as FLAC3D. Part of the GeoPRISMS work has involved co-PI Birkel adapting UMISM (a 25-year old Fortran program) to be more readily accessible for student use. This includes the implementation of gridded netCDF output, and improvements to the model preprocessor written in MATLAB.

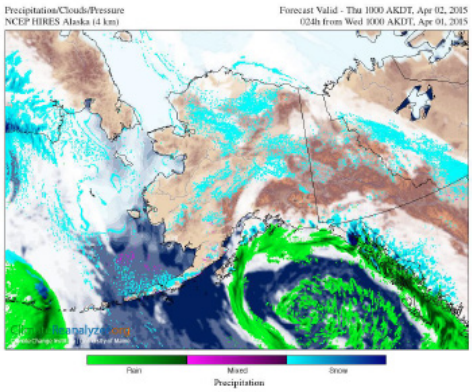

2A

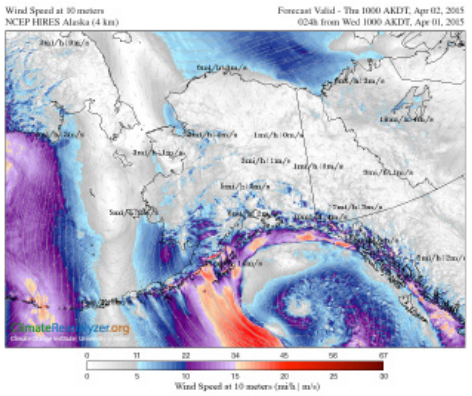

2B

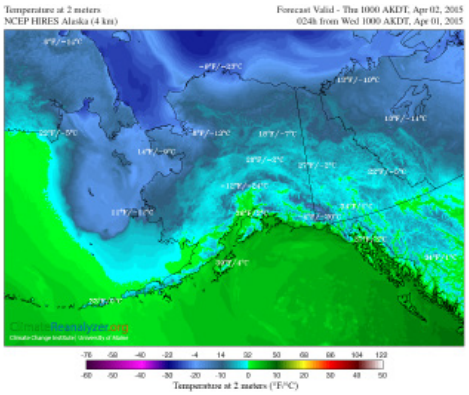

2C

Figure 2. Co-PI Birkel runs a website called Climate Reanalyzer (http://cci-reanalyzer.org), which is a visualization framework for reanalysis, GCM, and weather forecast models. Climate Reanalyzer receives >700 users each day. The website includes daily-updated 48-hour forecast graphics for Alaska from the 4km NCEP NAM-WRF model framework (see [A] precipitation and cloudcover; [B] wind at 10 meters, and [C] temperature at 2-meters). High resolution daily forecast graphics, now archived on our servers for 2013-2014, have provided valuable information about Alaskan climate and the spatial distribution of precipitation that is integral to understanding climate-erosion linkages across the region.

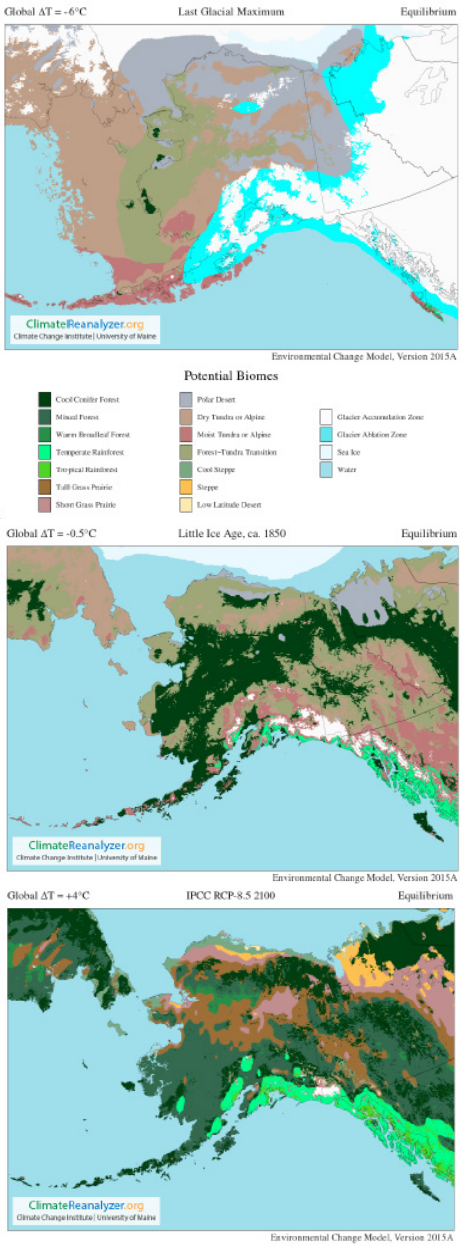

3A

3B

3C

Figure 3. Co-PI Birkel is developing a teaching resource relevant to GeoPRISMS called the Environmental Change Model (ECM) (http://cci-reanalyzer.org/ECM). ECM is a program that estimates snow/ice mass balance and potential biomes across the globe for climate boundary conditions ranging from Last Glacial Maximum (LGM; ~ 20,0000 years ago) to 2100 CE. Using the ECM, students can run simulations to see the equilibrium response of biomes to different climate boundary conditions. Shown below are potential biome solutions for Alaska for the (A) Last Glacial Maximum, (B) Little Ice Age, and (C) 2100 CE. Solutions are calculated from gridded inputs of monthly temperature and precipitation using a degree day solver and biome rubric. Boundary conditions for a given experiment are derived by blending reanalysis (modern climate) and general circulation model (GCM; past/future climate) climatologies. The ratio of reanalysis to past or future climate depends on a user-selected global temperature departure value, ΔT. For the LGM, ΔT = -6 °C; for modern climate, ΔT = 0 °C; for 2100, ΔT = +4 °C. And so on. The mass balance algorithm used in the ECM is also used in the UMaine Ice Sheet Model Alaska simulations. Documentation is available on the website, and a publication is in preparation.

Results from the iMUSH Active Source Seismic Experiment

Alan Levander, Eric Kiser, Imma Palomeras, Colin Zelt, Brandon Schmandt, Steve Hansen, Steven Harder, Ken Creagar, and John Vidale

iMUSH (imaging Magma Under Saint Helens) is a U.S. NSF sponsored multi-disciplinary investigation of Mt. Saint Helens (MSH), currently the most active volcano of the Cascades arc in the northwestern United States. The project consists of active and passive seismic experiments, extensive magnetotelluric sounding, and geological/geochemical studies involving scientists at 7 institutions in the U.S. and Europe. The long-term goal of the project is to produce a comprehensive 3D model of the volcanic plumbing system from the surface to the subducting Juan de Fuca slab.

Here we describe preliminary results of the iMUSH active source seismic experiment, conducted in July and August 2014. The active source experiment consisted of fifteen 454 and eight 908 kg weight shots recorded by ~3500 seismographs deployed at ~6000 locations. Of these instruments, ~940 Nodal Seismic instruments were deployed continuously for two weeks in an areal array within 10 km of the MSH summit (Fig. 1-2). 2500 PASSCAL Texan instruments were deployed twice for five days in 2 areal arrays and 2 dense orthogonal linear arrays that extended from MSH to distances > 80 km.

Overall the data quality from the shots is excellent, registering very clear Pg, pre- and post-critical PmP phases, and surprising strong Sg, and SmS signals. The seismograph arrays also recorded dozens of micro-earthquakes beneath the MSH summit and along the MSH seismic zone, numerous other local and regional earthquakes, and at least one low frequency event.

At this point we have completed various types of analysis of the data set: We have determined an average 1D Vp structure from stacking short-term/long-term average ratios, and the 2-D Vp, Vs and Vp/Vs structure from ray-trace inversion and finite-frequency tomography along the two orthogonal profiles (in the NW-SE and NE-SW directions, Fig.s 1-2). We also have made low-fold CMP stacks of the profile data. Below the MSH summit, the 2-D ray-trace inversions have identified a large Vs, and Vp/Vs (Vp/Vs ~ 2) anomaly at 4-10 km depth below sea level. We identify this anomaly as the feeder magma chamber below the shallowest magma chamber at 1-3 km depth below the caldera, imaged previously in local earthquake tomography (Waite and Moran, 2009, Journal of Volcanology and Geothermal Research, 182, 113-209). A low Vp anomaly extending to the Moho dips to the southeast away from the Mt. St. Helens caldera, outlining a likely pathway for melt and fluid migration in the crust. Low frequency events are associated with this anomaly. The PmP phases image the Moho at depths varying from 35-40 km directly beneath the MSH plateau and to the east beneath the backarc. We have also identified a continuous landward dipping reflection from within the uppermost mantle, the source of which is under discussion.

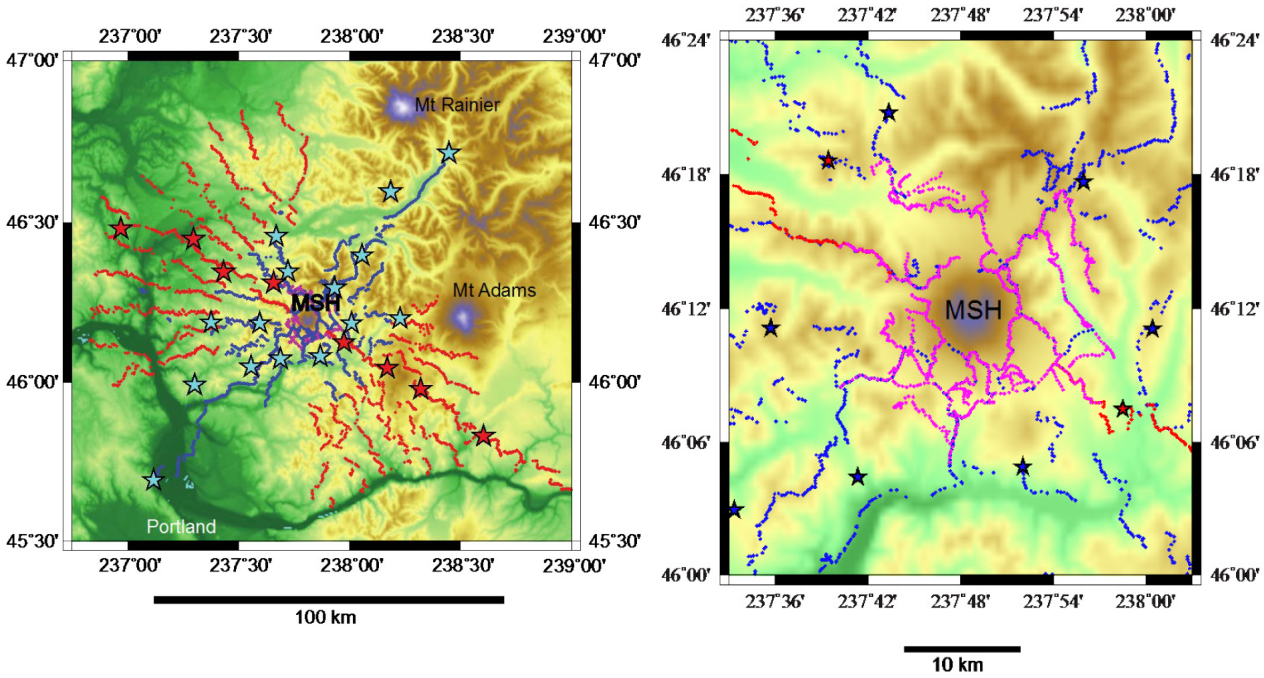

Figure 1 (left). iMUSH active seismic experiment. The ~2450 blue dots are Texans used in the first deployment that recorded 15 shots denoted by blue stars. The ~2550 red dots are Texans from the second deployment that recorded 8 shots denoted by red stars. The ~940 magenta dots are Nodal Seismic instruments which recorded all 23 shots. Approximately 1200 seismographs were hiked into the MSH region (Fig. 2).

Figure 2 (right). Map showing detail of instrument deployments near Mt. St. Helens (MSH). Magenta dots are ~940 Nodal Seismic recorders which recorded continuously for 2 weeks. Deployment teams of foot hiked in the 1200 instruments that were within 7.5 km of MSH. Blue and red dots are Texans deployed during the first and second deployments. Also shown is the inner ring of shots, denoted by blue and red stars, which were ~15 km from the center of MSH.

Geochemical constraints on the source, flux, migration and seismic signatures of volcanic fluids, Katmai Volcanic Cluster, Alaska

Taryn Lopez

Fluid movement in the subsurface of active volcanoes is frequently thought to produce elevated seismicity; however the actual type of fluid (i.e. magma, volatiles, or hydrothermal waters) and the implications of the fluid movement are not well constrained. Knowledge of the type of fluid/s in the subsurface is critical for both forecasting and estimating the explosivity of the impending volcanic eruptions. In open-system volcanoes, low-solubility volatiles can be released from magma during ascent and outgassed at the surface of the volcano in advance of the source magma. This provides a useful tool to aid in eruption forecasting. The chemical and isotopic composition of these volatiles can provide insights into both the source (i.e. subducted slab, mantle wedge, or crust) and the type of volatiles at depth, which can help elucidate subduction and magma generation processes. Further, advanced knowledge of a hydrothermal and/or meteoric water system in a volcano's subsurface may help scientists to better interpret the monitoring data and evaluate potential hazards during periods of unrest. Finally, if magma movement can be directly identified from seismic data, then scientists could provide robust constraints on the likelihood and/or timing of impending eruptions.

In this project we aim to utilize these geochemical tools to address several fundamental science questions for three active volcanoes within the Katmai region of the Aleutian Arc, Alaska. Specifically, we will use geochemical and complementary seismic datasets to (1) identify volatile sources, (2) determine proportions of magmatic,

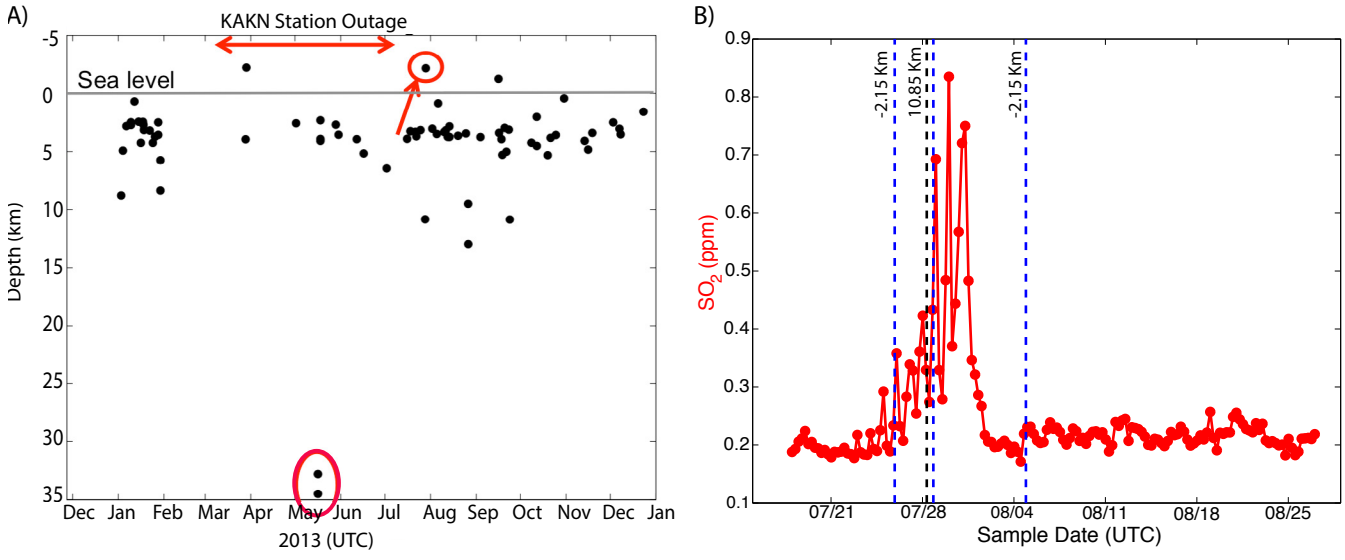

Figure 1. AVO located earthquakes within 5 km of Trident Volcano (A) and measured MultiGas SO_2 concentration from Trident's fumarole field and repeating earthquakes detected during the 2013 field campaign (B).

volatile and/or hydrothermal fluids within the subsurface, and (3) distinguish trends in gas composition that correlate with seismic signatures of fluid movement. Mt. Martin, Mt. Mageik, and Trident Volcanoes are selected as the targets of this study due to their continuous gas emissions, active hydrothermal systems, and abundant seismicity likely related to subsurface "fluid" movement. A two-week field campaign was conducted in July 2013 during which (1) fumarolic gases were sampled for chemical and isotopic analysis from Mt. Mageik and Trident Volcano, (2) MultiGas instruments where installed adjacent to the active fumarole fields for in situ sampling of plume CO_2, SO_2, and H_2S composition at all three target volcanoes, (3) and broadband seismometers were co-located with MultiGas instruments at Mt. Mageik and Mt. Martin to complement the existing Alaska Volcano Observatory (AVO) seismic network and measure local seismicity.

We use the chemical and isotopic compositions of the sampled volcanic fluids along with simple 2- and 3-component mixing models to distinguish mantle, crust, and sediment volatile sources at Mt. Mageik and Trident Volcano. Similar chemical and isotopic trends are observed at both volcanoes. Specifically, $^3He/^4He$ ratios of the fumarolic gases ($R/R_A \geq 7.3$) are similar to that of the upper mantle (~8±1 R_A) and are consistent with magma degassing in the subsurface. $\delta^{15}N$ values combined with N_2/He ratios indicate that sediment is the primary N_2 source, while $\delta^{13}C$ of CO_2 combined with $CO_2/^3He$ ratios indicate decreasing abundances of limestone, sediment and mantle C sources. Because the basement rock beneath the target volcanoes is comprised primarily of Jurassic limestone and sediments, we cannot conclusively distinguish subducted slab from crustal sedimentary volatile sources. Finally, $\delta^{18}O$ and δD isotopes from steam condensate within the fumarole samples reflect mixing of meteoric and subducted (i.e. andesitic) water, with meteoric water being the predominant water source at both volcanoes. Specifically, Trident's steam condensate is comprised of ~56% meteoric water and 43% andesitic water; while Mageik's steam condensate is comprised of ~71% meteoric water and 29% andesitic water.

Based on the gas composition from measured fumarole samples (Mageik and Trident only), the MultiGas measurements, and previous results in the literature, and through comparison with other well-studied volcanoes, we conclude that (1) preferential removal of (acidic) magmatic gases by hydrothermal waters (a process known as scrubbing) is occurring in the subsurfaces of both Mt. Mageik and Trident Volcano, and (2) shallow magma is degassing beneath Mt. Martin. Elevated CO_2 concentrations relative to SO_2 and HCl in the fumarolic samples from both Mt. Mageik and Trident Volcano are consistent with scrubbing of magmatic gases by hydrothermal waters, when combined with the strong meteoric signature of the steam condensate described above, suggest that both Mt. Mageik and Trident Volcano have well-developed hydrothermal systems. Additionally, changes in the relative composition of CO_2, HCl and S within gaseous emissions since the 1990's indicate that Mt. Mageik's hydrothermal system has increased in volume with respect to the magmatic system, while Trident's hydrothermal system has decreased in volume with respect to the magmatic system. A relatively low CO_2/SO_2 ratio (<1) at Mt. Martin observed in the MultiGas data is consistent with magma degassing at relatively shallow depths and a relatively dry pathway to the surface.

Changes in gas composition are also compared with seismicity to help constrain seismic signatures of subsurface fluid flow. Here we present preliminary results from Trident Volcano. Earthquakes located within ~5km of Trident by AVO are shown in Fig. 1A. Note that Trident seismicity tends to cluster at depths of ~3-7 km below sea level, which is consistent with proposed depths of magma storage in this region. Two deep (~32-35 km),

low frequency earthquakes were located beneath Trident ~2 months prior to our field study. Such events are frequently seen at Alaska Volcanoes (e.g. Pavlof, Redoubt) and are often associated with the influx of magma from the mantle. Observations of ~1 month of MultiGas data from Trident Volcano find an ~6 day period from 7/25/13 – 8/1/13 during which emissions of SO_2, a magmatic gas, increase to detectable levels before returning to below detection limit levels for the remainder of the study period (Fig. 1B). The initial increase in SO_2 corresponds with the occurrence of a small and near-surface (+2.15 km) volcano-tectonic earthquake located within 2 km of the fumarole field that repeated twice more within the next week (marked by red arrow in Fig. 1A and by blue dashed lines in Fig. 1B). We speculate that this earthquake may have been related to the ascent and surface release of magmatic gas. Additionally, during this time period a swarm of 12 low-frequency repeating earthquakes occurred over a 14 minute period on 7/28/13 (black dashed line, Fig. 1B) at a depth of ~10.8 km. We propose that these earthquakes may be related to ascent of a small batch of magma within the crust and resulting volatile release. Additional data over a longer time period are required to more robustly constrain the relationship between subsurface fluid movement, seismicity and surface outgassing at Trident Volcano. Future work will involve similar data comparisons and analyses at Mt. Mageik and Mt. Martin volcanoes.

High-resolution numerical modeling of outer-rise fault development and evolution

Magali Billen, John Naliboff

The complexity of deformation patterns found within subduction zones reflects the competition between forces driving and resisting subduction. In the outer-rise region of subduction zones, slab-pull forces and bending stresses overcome compressional stresses generated at the plate boundary interface, giving rise to extensional stresses and subsequent normal faulting. On the seismic timescale, such faulting may generate significant magnitude earthquakes (e.g. Lynnes and Lay, 1988) and serve as a potential indicator earthquake for larger underthrusting events (Christensen and Ruff, 1988). Over longer timescales, observational (e.g., Ranero et al. 2003) and numerical (Faccenda et al., 2009, 2012) studies suggest that outer-rise normal faults provide pathways for fluid migration deep into slabs and consequently a mechanism for volatile recycling into the deep mantle. Building on these studies, this investigation aims to discern the relationship between outer-rise deformation, plate driving forces and lithospheric rheology at both short- (<10,000 years) and long-term (> 10 Myr) time scales.

Our approach to examining the factors controlling outer-rise deformation combines high-resolution numerical modeling with global observations of subduction dynamics, flexural rigidity and seafloor faulting. On a global scale, outer rise faulting patterns show little to no correlation with slab pull magnitudes, convergence rates or oceanic plate ages despite wide variations in these parameters across modern subduction systems (Naliboff et al., 2013). 2-D numerical models of long-term (> 10 Myr) outer-rise deformation in oceanic-continental

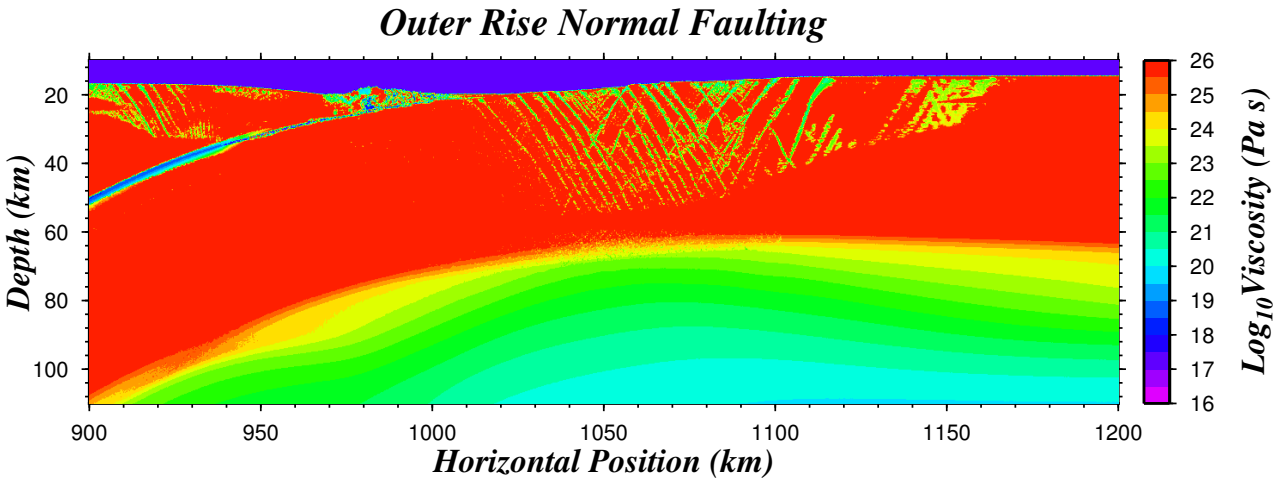

Figure 1. Viscosity structure of the overriding- (upper left) and downgoing-plate after ~ 400,000 years of deformation. Normal faults (brittle shear zones) develop seaward of the trench in the outer rise region in response to extensional bending stresses and slab pull forces.

systems suggest that this lack of correlation likely reflects that downgoing plate age and velocity, slab pull magnitude and plate boundary coupling all significantly affect outer-rise faulting patterns (Naliboff et al., 2013). Conversely, variations in the brittle rheology of downgoing oceanic lithosphere produce little to no changes in time-averaged outer-rise faulting patterns.

To further elucidate any connection between the rheology of downgoing oceanic lithosphere, plate boundary interface strength and outer rise faulting patterns, we have developed 2-D models of the Tonga subduction system incorporating observations of slab geometry, bathymetry and overriding plate structure. Rather than develop a subduction system through time-dependent processes, these experiments impose a 'cross-sectional' slice of the modern Tonga subduction system as an initial condition that approximates the modern forces driving and resisting subduction. In addition, high numerical resolutions in the vicinity of the trench (200 m) permit the definition of a narrow (1 km), rheologically distinct shear zone marking the plate boundary interface. The resulting models thus allow for direct comparisons to observed regional patterns of outer-rise deformation and an assessment of their relationship to plate boundary rheology. Preliminary results show the development of outer-rise normal faults penetrating deep into the mantle lithosphere after ~ 400,000 years of deformation (Fig. 1)).

Explosive pulse following the late Neogene initiation of the Central Oregon High Cascades

Bradley W. Pitcher, Adam J. R. Kent, Anita L. Grunder, Robert A. Duncan, Daniel Eungard

The Deschutes Formation of Central Oregon (~7.4- 4.0 Ma) preserves a remarkable stratigraphy that records the initial stages of the High Cascade arc following an eastward shift in volcanism ~7.5 Ma. Over 120 (uncorrelated) tephra fall units and 130 ignimbrite units are contained within the formation, suggesting that the arc may have been much more magmatically productive and explosive during this phase than at any other time within the last 17 Ma. This study aims to evaluate this history of explosive volcanism by establishing a comprehensive record of the ages, volumes, composition, and petrogenesis of each explosive deposit in the within the Deschutes Fm.

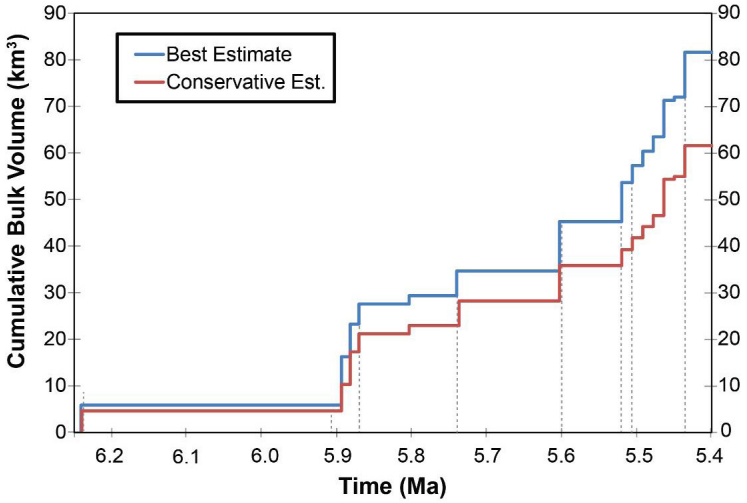

Figure 1. Cumulative bulk volume through time for just the 14 marker ignimbrites. "Conservative estimates" were calculated by assuming the closest possible source, given local geology. "Best estimates" were calculated by assuming a source at the locations of either modern Mt. Jefferson or modern South Sister (as indicated by field evidence). However, both likely underestimate real volumes, as conservative areal extents were assumed, erosion was not accounted for, and thicknesses were not allowed to increase towards the source. Additionally, over 120 (uncorrelated) airfall tuffs and 130 ignimbrites were not included in the cumulative volume. DRE is not included here. Dashed grey lines indicate ^{40}Ar-^{39}Ar plagioclase ages, which have been treated with Bayesian statistics, with the apriori assumption that stratigraphy be met. Eruption ages of ignimbrites without ^{40}Ar-^{39}Ar data were interpolated.

Initial estimates for some of the larger ignimbrite units suggest volumes ranging up to 10 km^3, with sources near the Three Sisters and Mt. Jefferson regions. Conservative estimates of the cumulative volume for only 14 marker ignimbrites is greater than 80 km^3 (Fig. 1). Furthermore, ^{40}Ar-^{39}Ar dating of plagioclase from 7 different ignimbrites indicate that this large volume of silicic material was erupted in less than 1 million years, between 5.44 ±0.04 Ma and 6.24 ±0.07 Ma (2σ). Using the estimated volumes of only these 14 marker ignimbrites, the Central Oregon Cascades had an average silicic eruption rate of 2.1 km^3/m.y. per km of arc length, more than 3 times the rate calculated for the 10 million years prior and 3 million years following this short period. It is likely that after correlating some of the over 300 tuff samples collected within the Deschutes Fm., this regional eruption rate may approach 10 times that of background levels. This seems to suggest that this early phase of the High Cascades in this region were marked by a relative silicic flare-up event.

Glass compositions of pumice from ignimbrites and select tephra fall units (n=718) range from 54 to 76 wt. %

SiO_2. Single eruptions can contain multiple populations of pumice which, in some cases, span a compositional range of almost 20 wt. % SiO_2. This, and the widespread existence of banded pumice, suggests that many eruptions involved multiple magma types. In particular, two marker ignimbrites which contain banded pumice are characterized by a compositional gap between 62 and 68 wt. % SiO_2, possibly suggesting limited mingling of a mafic magma with one derived from partial crustal melting. Trace element data (e.g. Nb, Ce, Th) demonstrate differing trends between pumice sourced from the Mt. Jefferson area and those sourced from the Three Sisters area, indicating that each source sampled compositionally different crust (i.e. Siletzia terrain in the North) and/or mantle sources.

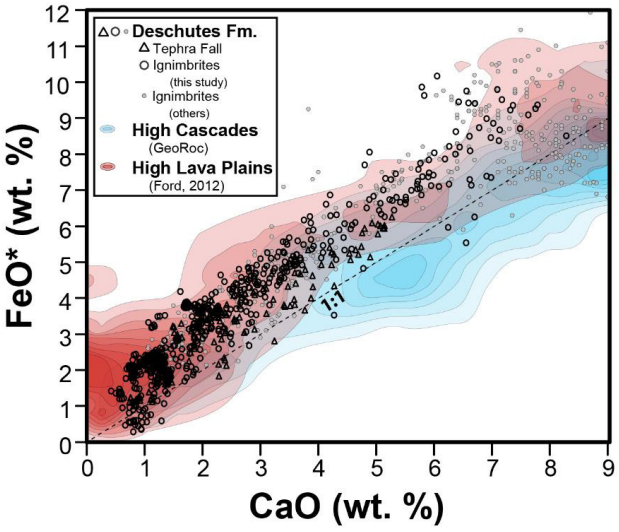

Figure 2. FeO total vs. CaO for the High Cascades (n=2,998), High Lava Plains (n=784), and Deschutes Fm. (n=751, this study). Note that Deschutes Fm. ignimbrites are generally much higher in FeO* for a given CaO [and SiO_2] than Quaternary Cascade products, and instead are more similar to volcanics from the High Lava Plains.

Analyses of pumice glass also indicate that Deschutes Fm. ignimbrites are generally much higher in FeO* for a given CaO or SiO_2 than Quaternary Cascade products, and instead are more similar to volcanics from the High Lava Plains (Fig. 2). This suggests hotter and drier melting conditions during rift-related mantle upwelling and partial melting of mafic crust. We suggest that extension, expressed locally by the Cascade graben, may have contributed to the formation and eruption of large volumes of silicic magma. Furthermore, the eastward shift of magmatic activity to the High Cascades, and subsequent anatexis of previously un-melted crust, could have helped to produce large volumes of silicic magma.

Collaborative Research: From the Slab to the Surface: Origin, Storage, Ascent, and Eruption of Volatile-Bearing Magmas (NSF 1456939 & 1456814)

Diana Roman, Erik Hauri, Terry Plank

On any given day, approximately 15-30 volcanoes worldwide are either in eruption or show strong signs of unrest (e.g., anomalously high rates of seismic activity, ground deformation, or gas emissions). Volcanic activity, including high-altitude eruptions of ash or emission of large volumes of gas, poses a significant hazard to people and property in the United States and worldwide. This is particularly true in Alaska, with over 10,000 passengers a day flying over 35 historically active volcanoes on North America/Asia flight routes. Although significant progress has been made in recent decades in understanding the physical processes occurring in the upper portions of the Earth's crust that lead directly to volcanic activity and associated unrest, there is a fundamental lack of understanding of how these shallow crustal processes link to and are controlled by the large-scale crustal tectonics and deep mantle melting that are ultimately responsible for arc volcanism. Specifically, although it is well understood that the amount of water and other volatiles dissolved in a magma plays a key role in its generation, ascent, and eruption, it is unclear why some arc volcanoes erupt 'wetter' magmas than others. Identifying large scale controls on magma volatile contents is thus critical for accurate forecasting of the frequency, volume, and explosivity of volcanic eruptions.

Beginning in August 2015, we will conduct an integrated geochemical-geophysical study of the Unimak-Cleveland corridor of the Aleutian volcanic arc, which encompasses six volcanoes that have erupted in the past 25 years with a wide range of magmatic water contents. This relatively small corridor also exhibits a range of deep and upper-crustal seismicity, apparent magma storage depths, and depths to the subducting tectonic plate. Our goal is to link two normally disconnected big-picture problems: 1) the deep origin of magmas and volatiles, and 2) the formation and eruption of crustal magma reservoirs, which we propose to do by establishing the depth(s) of crustal magma reservoirs and pre-eruptive volatile contents throughout the corridor. The integrated study components include analysis of volcano- seismic events and magmatic volatile analysis. Existing seismic data catalogs contain ~ 14,000 events, and some samples of volcanic eruption products are already in hand. The existence of two actively erupting volcanoes in the corridor further motivates collection of simultaneous seismic, gas (in collaboration with the USGS Alaska Volcano Observatory) and tephra samples during eruption, that reflect active evolution of the magmatic system.

Cleveland Volcano

Integrating laboratory, geophysical and geological data to understand the Aleutian megathrust from the trench to the base of the seismogenic zone

Demian Saffer, Donna J. Shillington, Geoffrey A. Abers, Anne Bécel, Katie M. Keranen, Jiyao Li, Mladen Nedimović

The largest earthquakes and most powerful tsunamis are generated on subduction zone megathrusts, many of which are associated with sediment-rich trenches. Variations in the in situ conditions and physical properties of the megathrust plate interface are primary controls on great earthquake rupture, the mode of fault slip, and the manner in which slip might reach the trench to produce tsunamis. Our ongoing project is integrating laboratory data from modern oceanic sediment and exhumed metapelites with existing, multi-resolutional geophysical data to improve our understanding of in situ conditions and processes along the plate boundary megathrust from the trench to ~30-40 km depth. Our study focuses on the Alaska subduction zone, the portion of the Alaska/Aleutian Margin Primary Site chosen by the GeoPRISMS community for focused studies of the subduction megathrust, where several existing geophysical datasets and DSDP/IODP cores can be leveraged (Fig. 1). We seek to develop an improved quantitative understanding of the conditions and materials along the megathrust, their relationship to seismicity, and provide a template for similar studies at other margins.

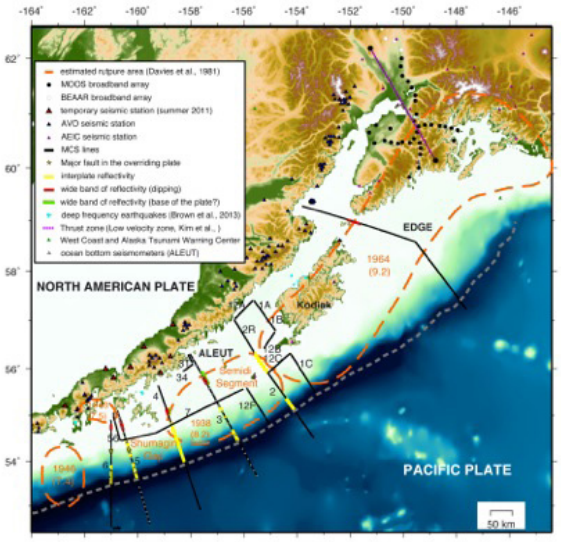

Figure 2. Map showing existing drilling and seismic data along the Alaska subduction zone.

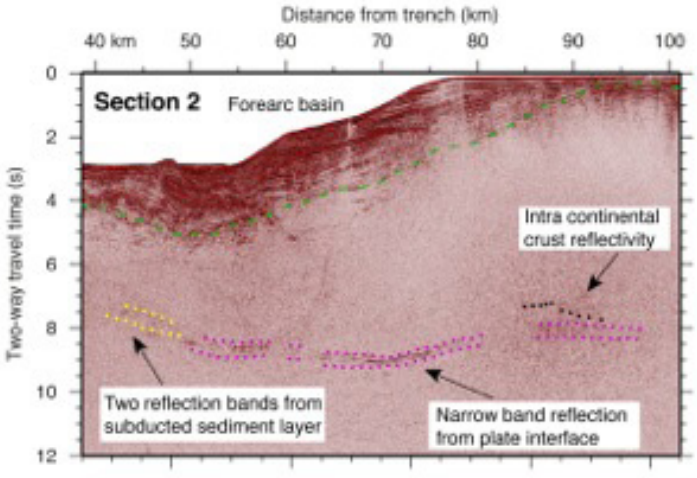

Figure 2. Seismic reflection image from the Semidi segment offshore the Alaska Peninsula within the rupture zone of the 1938 8.2 earthquake, which is characterized by a bright, narrow reflection.

The properties of the megathrust vary with depth in multi-resolutional seismic imaging datasets. In seismic reflection data from the ALEUT dataset, the megathrust is represented by a narrow, bright reflection within the center of past great earthquake ruptures (Fig. 2). Deeper and farther landward, the plate interface transitions to a wide band of multiple reflections, where it appears to intersect the forearc mantle wedge and where abundant seismicity is observed at its updip end and tremor is observed at its downdip end (Li et al., JGR, in review). Synthetic seismograms indicate that the narrow band reflection is best explained by a ~100-250 m thick low-velocity zone (Fig. 2) while the wide band of multiple reflections requires a 3-5 km thick zone

comprising a series of thin layers of variable velocities (Li et al., JGR, in review). Thus, the downdip end of the locked zone and transition to tremor appears to be marked by a broadening of deformation based on seismic reflection data. Receiver functions indicate that the megathrust is associated with a few km wide zone with 20-30% slower Vs than its surroundings and anomalously high Vp/Vs ratios both within and downdip of the main rupture zone of the 1964 earthquake (Fig. 3, Kim et al., 2014).

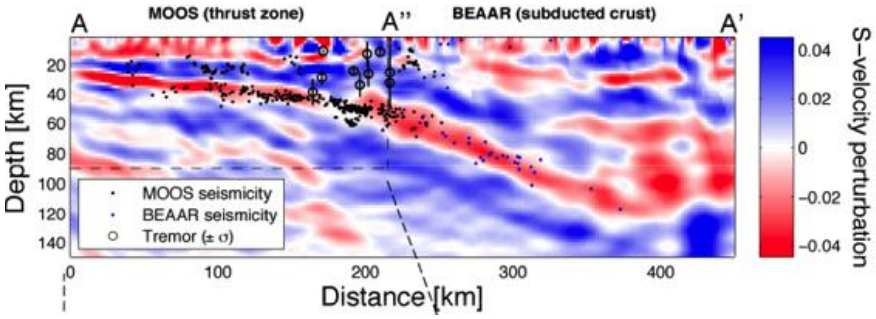

Figure 3. Receiver function image across Alaska subduction zone, showing low velocities along the megathrust.

Low velocity zones, high Vp/Vs and high reflectivity observed in seismic data in Alaska and in other subduction zones have been interpreted to represent very high pore-fluid pressures along different parts of the plate boundary, but could also arise from changes in sediment porosity and lithology with depth, or from anisotropy in elastic properties.

To link the observations from seismic imaging with in situ state, we are using laboratory measurements on samples from the recent IODP cruise off Alaska and from underplated metasediments exhumed from ~12-15 km depth collected from Kodiak Island, to constrain and calibrate relationships between Vp and Vs, porosity and effective stress (Fig. 4). Our initial dataset defines clear relationships between velocity and stress, and indicates substantial (15-20%) anisotropy.

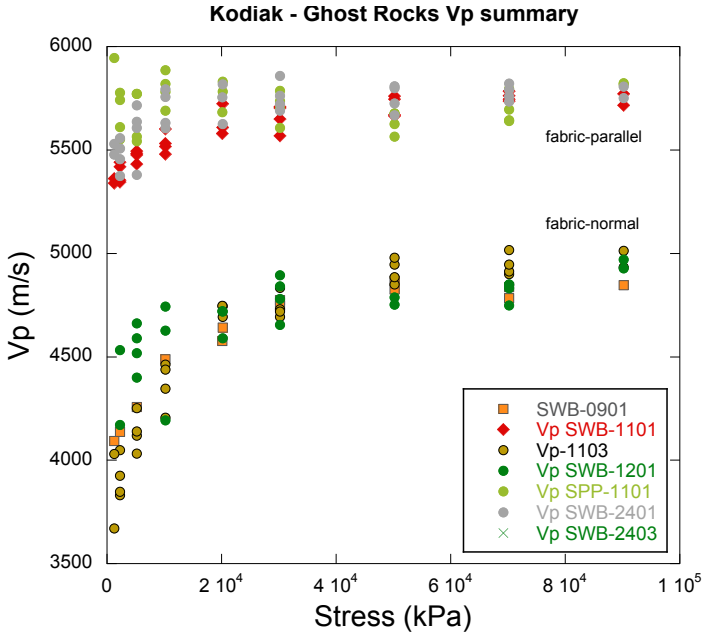

Figure 4. Compilation of Vp-porosity trends showing data from: DSDP sites along the Alaska/Aleutian margin that span porosities from ~70% to ~35%, including sites on the subducting plate (178 & 183) and the shallow accretionary wedge (186)

Our next steps are to: (1) extract more detailed information on the velocity structure of the plate boundary to depths of ~20 km with pre-stack depth migration and amplitude analysis of seismic reflection data and waveform modeling of wide-angle seismic data, and integrate these with the laboratory measurements to quantify in situ porosity and stress conditions, to ultimately determine the underlying cause(s) of bright reflections and low velocity zones along the shallower part of the plate boundary; and (2) link waveform modeling, laboratory measurements on exhumed rocks, and theoretical mineral-based predictions of elastic moduli and seismic wavespeed at greater depths (>~20 km) to assess the contributions of crack geometry, anisotropy, and composition, to better constrain the cause of the kms-thick low velocity zone.

Developing a comprehensive model of subduction and continental accretion at Cascadia

Yang Shen, Haiying Gao

A full-wave ambient noise seismic tomography reveals distinct low-velocity volumes in the upper mantle along the Cascades back-arc, which suggest subduction-driven upwelling, decompression melting, and the 3D small-scale mantle convection beneath the back-arc. The project provided a velocity model for the community through IRIS EMC and training for a female postdoc, Haiying Gao, who recently started a tenure-track faculty position at the University of Massachusetts Amherst in 2013. Gao and Shen also validated the recent shear-wave velocity models in the Pacific Northwest and the United States with full-wave simulation under the support of this project.

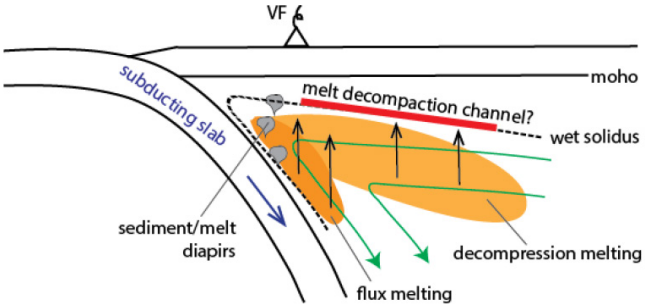

Figure 1. Schematic illustration of possible melt generation and migration processes at general subduction zones, Thin lines with open arrows indicate melt paths, while those with solid arrows represent mantle flow lines. VF stands for the volcanic front. Gao and Shen (EPSL, 2014).

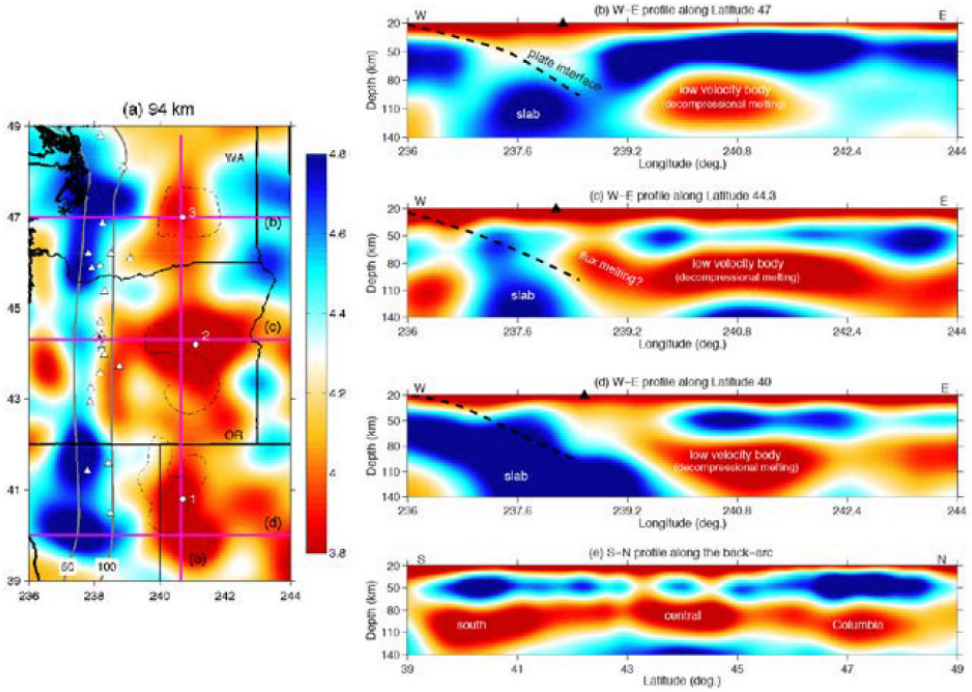

Figure 2. Segmented low-velocity anomalies along the Cascade back-arc. (a) Horizontal slice at depth of 94 km (Vs in km/s). The black dashed lines outline the amplitude of largest negative Sp phase from receiver functions. The magenta lines mark profile locations in (b)-(e), respectively. All the panels share the same color bar. (b-d) W-E profiles across the back-arc anomalies. The triangles mark the volcano centers. The Juan de Fuca plate interface at depths of 20-100 km is projected. (e) S-N profile along the back-arc low-velocity anomalies, which spatially correlate with the three volcano clusters as in (a). Gao and Shen (EPSL, 2014).

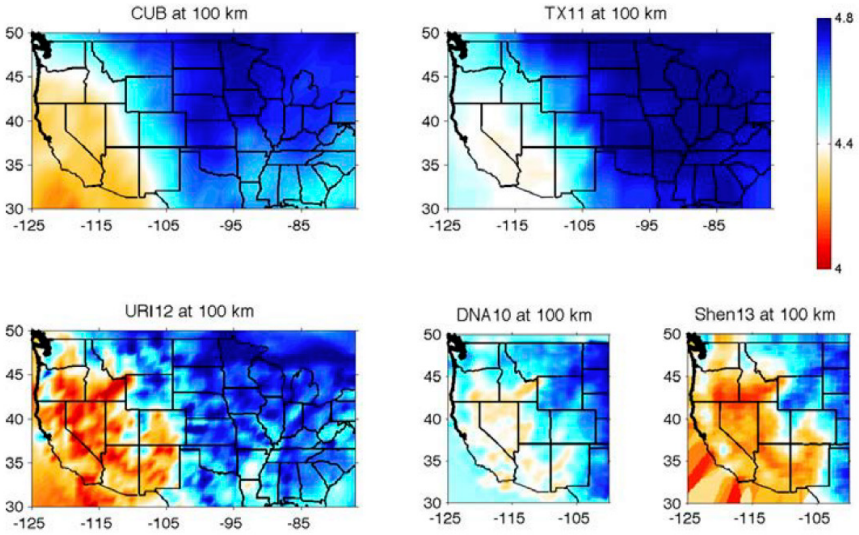

Figure 3. Shear-wave velocity models for model validation at depth of 100 km. CUB, TX11 and URI12 cover the entire US while DNA10 and Shen13 cover the western and central US. Gao and Shen (JGR, 2015).

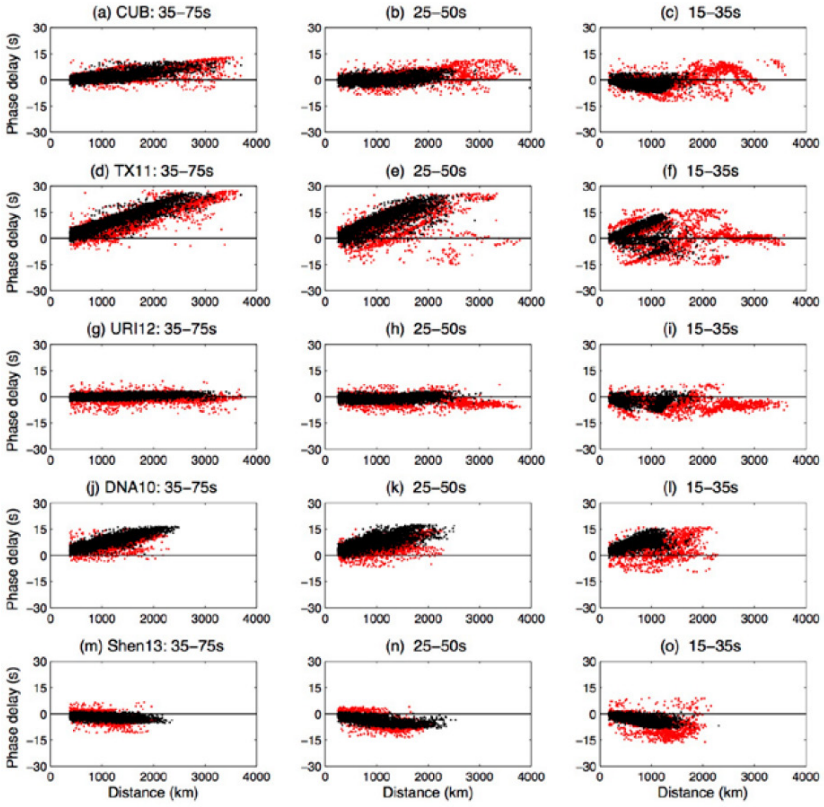

Figure 4. Phase delays versus source-receiver distance filtered at three period bands. Each row represents one model and each column represents one period band. Black and red dots are measurements from ambient noise and regional earthquakes, respectively. A positive linear trend indicates that the synthetics arrive earlier than the observations, which prefers a relatively slower Earth structure. Gao and Shen (JGR, 2015).

References

Gao, H., and Y. Shen (2012), Validation of Shear-wave velocity models of the Pacific Northwest, Bull. Seism. Soc. Am., 102(6), 2611-2621, doi:10.1785/0120110336.

Gao, H., and Y. Shen (2014), Upper mantle structure of the Cascades from full-wave ambient noise tomography: Evidence for 3D mantle upwelling in the back-arc, Earth Planet. Sci. Lett., 309, 222-233, doi:10.1016/j.epsl.2014.01.012.

Gao, H., and Y. Shen (2015), Validation of recent shear wave velocity models in the United States with full-wave simulation, J. Geophys. Res. Solid Earth, 120, 534-358, doi:10.1002/2014JB011369.

Imaging Magma Under mount St. Helens (iMUSH): Earthquake-seismic component

Carl Ulberg, Kayla Crosbie, Ken Creager, Seth Moran, Geoff Abers, John Vidale, Heidi Houston, Roger Denglinger, Alan Levander, Eric Kiser, Brandon Schmandt, Steve Malone

To better understand volcanic activity, it is fundamental to get an accurate representation of magma generation zones and storage regions in the Earth's crust and upper mantle. Illuminating the architecture of the plumbing system beneath volcanoes indicates (1) at which depths and conditions magmas are generated, and (2) the shapes and sizes of pathways and reservoirs along which magma travels towards the surface. Such knowledge will improve predictions on the durations of volcanic crises and on the total volume of erupted material during eruptive episodes. The iMUSH project focuses on Mount St. Helens (WA, USA), whose explosive eruption in 1980 attracted world's attention, and was the first volcano to be thoroughly monitored with modern instruments. Mount St. Helens is active, easily accessible, and has a well recorded past history. iMUSH uses several different methods (active and passive source seismic tomography and scattered wave imaging, magnetotelluric imaging, petrology and geochemistry), involving a large collaborative team, to image the volcano's plumbing system with unprecedented resolution from the subducting plate to the surface. This Nugget describes the earthquake seismic component of the project.

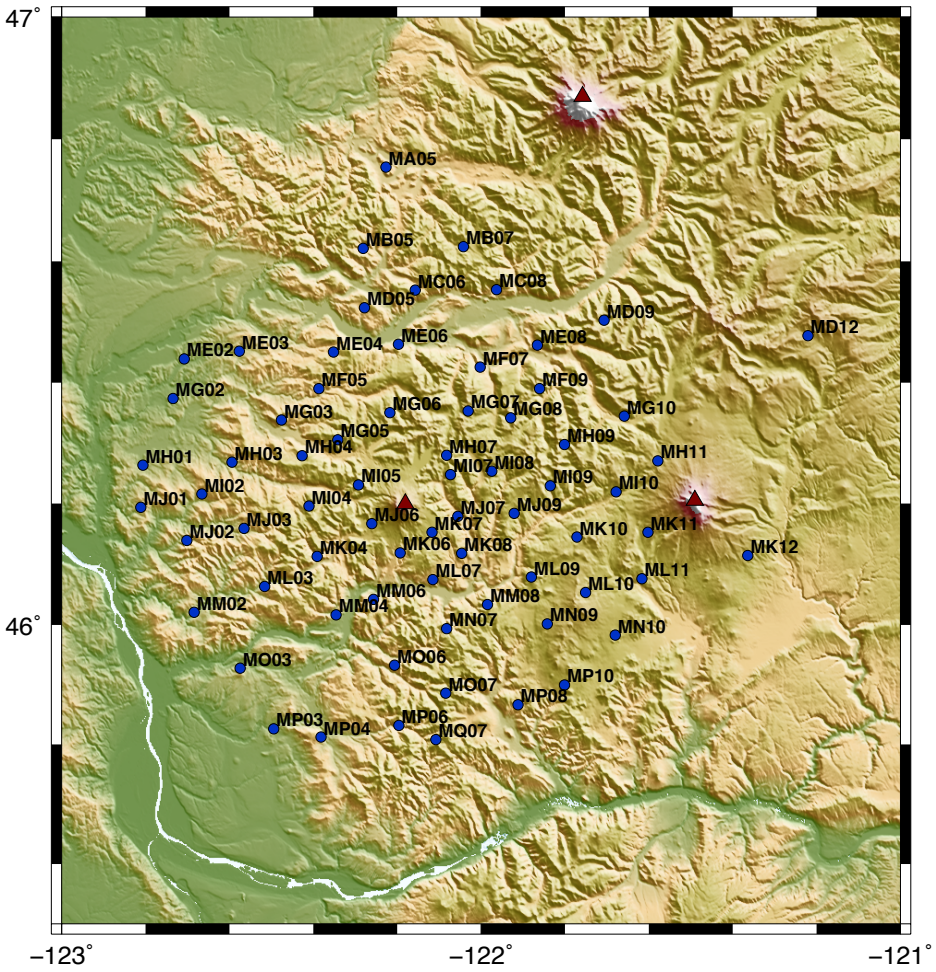

Figure 1. The iMUSH Broadband array. The 70 stations are distributed within 50 km of the summit of Mount St. Helens from the Cascadia foothills to Mount Adams. Triangles show volcanic centers.

In the summer of 2014, seventy broadband seismometers were deployed in a 50 km radius around the summit of the volcano (Fig. 1). These stations will remain for two years to record signals from local earthquakes associated with the volcano, long-period tremor, and teleseismic signals from around the world. Many of the signals will be used for imaging the crust and mantle wedge, with targets including the slab presumed to be subducting beneath the array, the mantle melting region, the Moho and how it is influenced by the ascent of melt from the mantle, and the crustal architecture beneath the volcano. Crustal signals refine our understanding of magma plumbing and crustal differentiation beneath this active arc, and various volcano-related sources will help us understand the deformation associated with active volcanism. This is the largest dense array over a volcano at this scale anywhere in the world, so should play an important role in addressing GeoPRISMS science goals associated with magmatic processes.

As of summer 2015 we have one year of data from nearly all of the stations and are rapidly accumulating a comprehensive set of high-quality P-wave travel-time picks from the 600 local earthquakes recorded to date. This effort will continue through the planned two years of recording. We have also picked the times at these stations from last summers 23 shots that were part of the iMUSH active-source experiment (see Levander nugget). These data sets, along with P-wave picks from the permanent network stations will be inverted for earthquake hypocenter locations and 3-D structure beneath MSH using struct3DP, which calculates travel times by 3-D eikonal-equation solver. We will follow up with inversions from S-wave picks and using double difference tomography applied to cross-correlation-derived differential travel-times of P and S waves from pairs of nearby events recorded at a given station. In parallel, ambient-noise tomography is providing initial estimates of shear-velocity structure of the crust, showing a strong influence of pre-arc basement structure on wave speeds. These data will be integrated with receiver functions to provide structural models of the crust and uppermost mantle of the volcano and its surroundings.

As seismological results emerge and the dataset becomes complete, deeper imaging and higher-resolution imaging are planned. These results will compliment the active source work by providing fully 3-D models and resolution to greater depths, though with lower resolution for the shallow structure, and will be integrated with magnetotelluric imaging to better understand volcanic plumbing and architecture. When completed, the iMUSH dataset and models will provide some of the most thoroughly integrated and highest-resolution images of a volcanic system anywhere, from subducting slab to surface.